IDA

INSTITUTE FOR DEFENSE ANALYSES

Evaluation of the Multi-Sensor Towed Array Detection System *(MTADS)* Performance at Jefferson Proving Ground, January 14-24, 1997

Samuel L. Park
Marc Mander

19990519 050

February 1999

Approved for public release;
distribution unlimited.

IDA Document D-2174
Log: H 98-002023

DTIC QUALITY INSPECTED 4

This work was conducted under contract DASW01 94 C 0054, Task T-AM2-1528, for the Deputy Under Secretary of Defense (Environmental Security). The publication of this IDA document does not indicate endorsement by the Department of Defense, nor should the contents be construed as reflecting the official position of that Agency.

© 1998, 1999 Institute for Defense Analyses, 1801 N. Beauregard Street, Alexandria, Virginia 22311-1772 • (703) 845-2000.

This material may be reproduced by or for the U.S. Government pursuant to the copyright license under the clause at DFARS 252.227-7013 (10/88).

PREFACE

This paper was prepared by the Institute for Defense Analyses (IDA) in partial response to the task entitled "Assessment of Traditional and Emerging Approaches to the Detection and Identification of Surface and Buried Unexploded Ordnance."

CONTENTS

FIGURES

TABLES

SUMMARY

A. BACKGROUND

The Environmental Security Technology Certification Program (ESTCP) sponsored the development of the Multi-sensor Towed Array Detection System (MTADS) at the Naval Research Laboratory (NRL). This document analyzes the results of a test of MTADS at Jefferson Proving Ground (JPG) from 14–24 January 1997.

MTADS is a vehicle-towed sensor with an array of coils that can be used as a magnetometer (MAG) or an electromagnetic induction (EMI) sensor. There were three scenarios in the MTADS test, each roughly 10 acres in size. It took 5 to 8 hours of actual survey time to cover most of the 10 acres, which as a practical matter meant that a day or two was needed to survey each scenario with each sensor configuration (MAG or EMI).

Known baseline ordnance appropriate to the scenario were emplaced at random locations on the site. Table S-1 shows the number of emplaced ordnance in the areas that were surveyed, as well as the number of declarations that the MTADS operators believed were ordnance. The probability of detection, P_D, also shown in Table S-1, comes from the number of those declarations that were correct.

Table S-1. Detection

	Scenario	Number of Baseline Ordnance	Number of Ordnance Declarations	Number of Correct Ordnance Declarations	P_D (%)
1	Aerial Gunnery	47	185	45	95.7
2	Artillery and Mortars	73	216	70	95.9
3	Submunitions and Grenades	86	215	80	93

The number of false alarms (*FA*s) is defined as the number of declarations as ordnance that did not correspond to baseline ordnance. The false-alarm rate is shown in Table S-2.

Table S-2. False Alarm Rates

Scenario	Area Surveyed (Square Meters)	Number of False Alarms	False Alarm Rate (per Hectare)[a]
1 Aerial Gunnery	33,445 (8.265 acres)	140	41.9
2. Artillery and Mortars	39,391 (9.735 acres	146	37.6
3. Submunitions and Grenades	29,729 (7.347 acres)	135	45.4

* A hectare is 10,000 m^2 or 2.47 acres.

The addition of EMI sensor information was crucial for reducing the *FAR*, particularly in scenarios 1 and 3, where it took part in every good detection. In scenario 1 it was not, by itself, responsible for any false alarms.[1] Table S-3 shows the discriminants that were derived in each case and the potential *FAR* reduction.

The obvious implications are that between 25- and 50-percent reduction in false alarms should be achievable with fairly rudimentary discrimination algorithms. An important caveat to this finding is that it is essential to know what kind of scenario one is in. No useful discriminant was found that was good in all three scenarios. Also, it should be emphasized that although Table S-3 accurately shows the *FAR* reduction that would have been achieved in the JPG MTADS test, it is not necessarily indicative of performance in other tests. Specifically, the discriminant thresholds chosen were such as to allow *zero* missed detections on account of the false-alarm mitigation. The real population distribution may have tails that would imply some number of missed detections as the tradeoff for reducing the FAR. Only further tests or a very good understanding of the detection physics can determine this. On the other hand, knowledge of the detection physics could very well allow one to do false alarm mitigation *better* than indicated in Table S-3.

---

1 This assumes that those declarations for which there were both EMI and MAG data were not more difficult (in some sense) than those for which only MAG or only EMI data were available. That is, no essential synergy is assumed between MAG and EMI.

Table S-3. Potential FAR Reduction by Using Linear Discriminants

Scenario	Declaration Type	Proportion of FAs	Discriminant	Possible FAR Reduction	Total FAR Reduction
1	Common and EMI-only	58% (81/140)	RFE_EM	16%	51.4%
	MAG-only	42% (59/140)	Not Applicable	100%	
2	Common	42.5% (62/146)	Function of ZMAG, INCLIN, GOF_EM	60%	25.5%
	MAG-only	45.2 (66/146)	None	0%	
	EMI-only	12.3% (18/146)	None	0%	
3	Common (excluding 3)	30.4% (41/135)	RMAG	41%	44%
	MAG-only	31.9% (49/135)	Not Applicable	100%	
	EMI-only (including 1 common)	36.3 (49/135)	None	0%	
	No Information (excluded from common)	1.5% (2/135)	None	0%	

Legend: ZMAG = fitted depth, magnetometer
INCLIN = fitted inclination
RFE_EM = ferrous radial size, EMI sensor
GOF_EM = goodness of fit, EMI sensor
RMAG = fitted radius, magnetometer

I. INTRODUCTION

In the past several years the Environmental Security Technology Certification Program (ESTCP) has sponsored development of an unexploded ordnance (UXO) detection system mounted on a vehicle. The vehicle systematically traverses a given terrain region and produces data in or nearly in real time that indicate the existence and location of UXO. This system was developed at the Naval Research Laboratory (NRL) and is called the Multi-Sensor Towed Array Detection System (MTADS).

MTADS has been through three previous tests. The first was a technical evaluation (TECHEVAL) to verify system technical characteristics. The second was a demonstration at the Magnetic Test Range (MTR) in Twentynine Palms, California, in December 1996. The third was a commercial demonstration in the third Jefferson Proving Ground test (JPG III).

The test that is the subject of this document was a demonstration of the MTADS at Jefferson Proving Ground (JPG) conducted from 14–24 January 1997. The test was conducted in accordance with the Technology Demonstration Plan (TDP) (Ref. I-1) dated 20 December 1996.

This document assesses the overall detection performance of the MTADS at JPG during this test. Supporting analysis, as well as data providing insight into MTADS operation, is also provided. The structure of this document is straightforward. After an introduction to the MTADS system and the test, an analysis of the data is presented. A final chapter is devoted to conclusions and directions for further study.

A. THE MTADS

The MTADS is an array of sensors on two carts and the low-magnetic-signature vehicle that tows them. The sensor arrays are either of magnetometers or electromagnetic induction (EMI) coils. The magnetometers can also be used as a magnetic gradiometer, a configuration that provides data with much the same information as the magnetometer. Only the magnetometer array was used in the test analyzed in this document.

MTADS is designed to minimize the noise and signal bias caused by the tow vehicle and carts. Good navigation, essential to quality data collection, has been a

principal issue, both in terms of potential remediation protocol (that is, finding the ordnance when digging for it) and in the conduct of tests. The vehicle and sensor positions are determined by a real-time kinematic differential global positioning system (RTK-DGPS), providing location accuracy to within 5 cm. This high location accuracy allows the co-registration and integration of data taken at different times.

MTADS includes a data acquisition system (MTADS-DAQ) and a data analysis system (MTADS-DAS). MTADS-DAQ is software used for collection and saving of magnetometer or EMI data during MTADS operation. MTADS-DAS is a stand-alone suite of programs used for later data analysis. Based on Interactive Data Language (IDL) tools, MTADS–DAS runs on a Unix workstation. It is a menu-driven system that permits easy visualization of the data and allows the user to hand pick anomalies within the sensor data and then determine features or parameters associated with the anomaly. These parameters are used for later remediation of suspected UXO. The parameter set depends on the sensor being towed. For the magnetometer, the parameters are

- Location (Northing and Easting coordinates)
- Depth
- Size
- Magnetic Moment
- Azimuth (of dipole moment)
- Inclination (of dipole moment)
- GoF.

For the EMI, the parameters are

- Location (Northing and Easting coordinates)
- Depth
- Ferrous Size
- Nonferrous Size
- GoF.

B. THE JPG FIELD TEST

From 14–24 January 1997, an NRL team surveyed an area with MTADS. The location was JPG, north of Madison, Indiana (Figure I-1). There are two principal areas at JPG that are used to test means of UXO detection. The "North Site" was the scene of the MTADS test (Figure I-2).

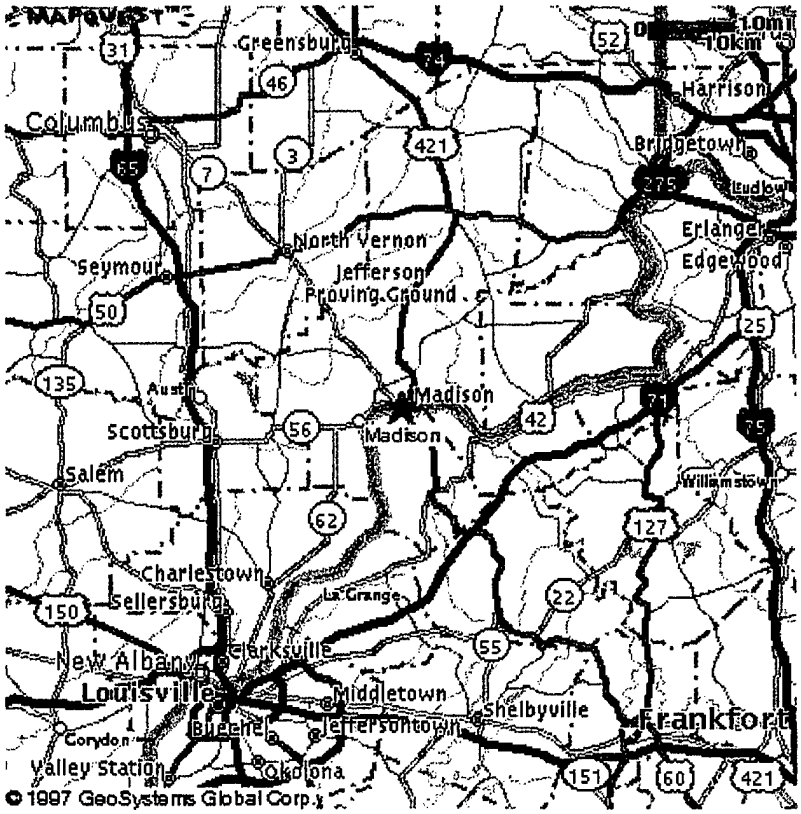

Figure I-1. Jefferson Proving Ground North of Madison, Indiana

The JPG North site has an area of 16 hectares (16,000 m^2), or approximately 40 acres. It is 1,320 ft on a side and is divided into quadrants, each roughly 10 acres. Each quadrant corresponds to a specific scenario and is further divided as evenly as possible into 100-ft (30.48-m) squares. Some "leftover" cells at the southern and western borders of the test site are only 20 ft wide.

Three of the quadrants were used for the MTADS test analyzed in this document. The first scenario entailed detection of ordnance from aerial gunnery (southeast quadrant), the second from artillery and mortars (northwest quadrant), and the third from submunitions and grenades (southwest quadrant).

The NRL team deployed the MTADS vehicle and sensor to the test site, took 1 day to set up, and began to survey the site on 15 January 1997. Table I-1 gives the survey details. They estimated (Ref. I-2) that they would cover about 10 acres per day, assuming a collection rate of 2 m/s. This would imply 1 day per scenario. The information in Table I-1 (from Ref. I-2) indicates that this was attained in terms of hours

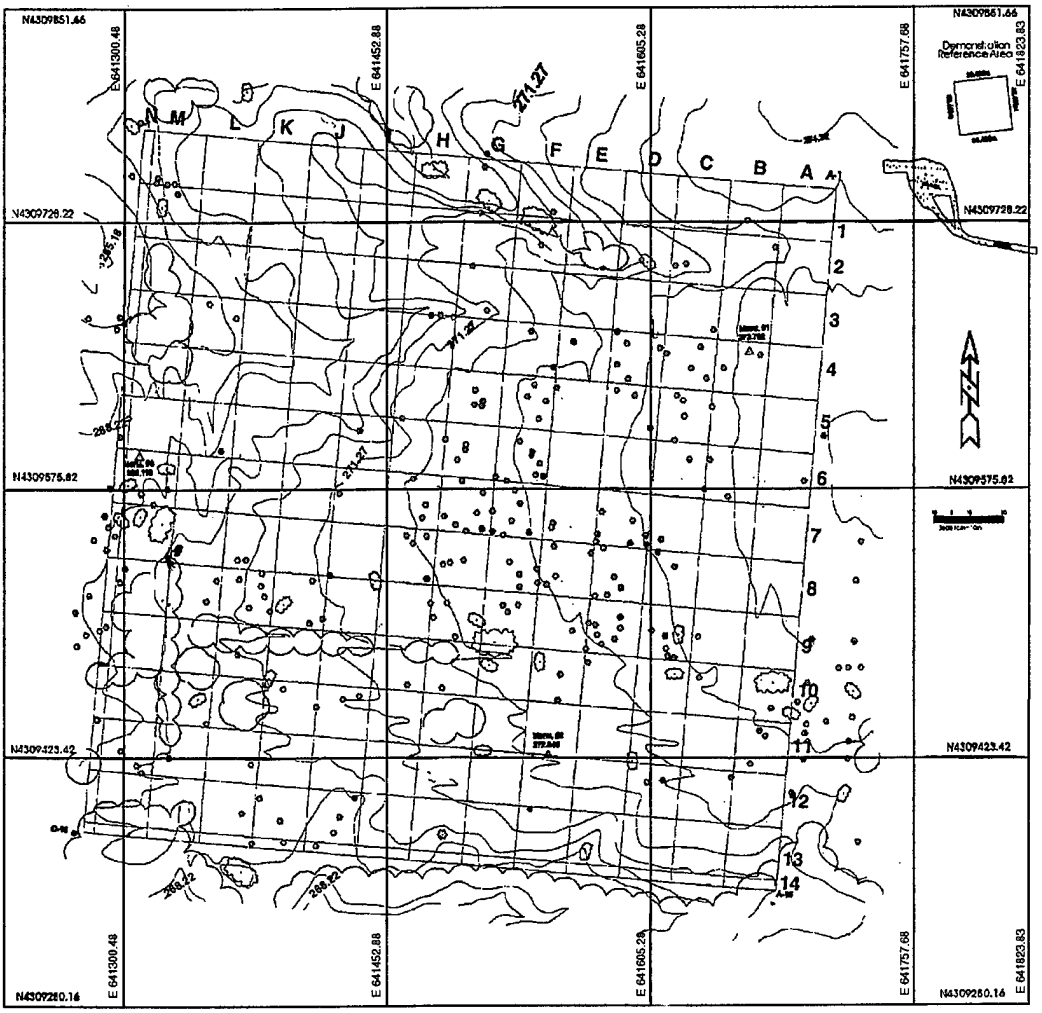

Figure 1-2. North Test Site at Jefferson Proving Ground

Table I-1. Survey Dates and Times. After Ref. I-2.

Scenario	MAG Survey Dates	EMI Survey Dates	MAG Survey Time [Hours]	EMI Survey Time [Hours]
Aerial Gunnery	15–16 January 1997	22 January 1997	5.3	5.8
Artillery and Mortar	16–17 January 1997	17–18 January 1997	5.4	7.8
Grenades and Submunitions	21 January 1997	18–19 January 1997	5.9	7.8

actually spent surveying. The extra time in terms of days (say a factor of two) would need to be incorporated for actual survey planning. Certainly this is also dependent on terrain and weather. The weather in this test was cold (January in Indiana), having periods with wind chills below –20 °F (Ref. I-2). In addition, not all 10 acres in each scenario were actually surveyed. Actual survey coverage is examined more closely later in this section.

NRL personnel used the given characteristics of the scenario to help in the classification of declarations as ordnance or nonordnance. They were specifically told the smallest size of ordnance in each scenario (Ref. I-2, Section 3.1). In addition, NRL appears to have used the scenario type to exclude targets that were too large. This occurred in the last scenario (submunitions and grenades) when a signal apparently like that of a "large bomb" was excluded as "nonordnance."

Only a portion of the test site was actually surveyed. Surveyed grid cells are indicated in Table I-2, based on information in Reference I-2. The corresponding surveyed areas appear in Table I-3. MTADS surveyed 83.5 percent of the approximately 30-acre area. Various reasons account for not surveying a region. For instance, a tree line might have interfered with GPS or the terrain might have been too treacherous. Whatever the cause, only those grid cells specified by NRL as surveyed in Reference I-2 are considered further in this document.

Table I-2. Surveyed Grid Cells. S indicates the cell was surveyed. Red indicates the area for scenario 1, blue for scenario 2, and green for scenario 3. The width of grid cells in the edges labeled N or 14 is 20 ft. Thus, grid cell N14 is 20 ft × 20 ft.

N	M	L	K	J	I	H	G	F	E	D	C	B	A	
S	S	S	S	S	S	S	S							1
S	S	S	S	S	S	S	S							2
S	S	S	S	S	S	S	S							3
S	S	S	S	S	S	S	S							4
S	S	S	S	S	S	S	S							5
S	S	S	S	S	S	S	S							6
S	S	S	S	S	S	S	S							7
S	S	S	S	S	S	S	S	S	S	S	S	S	S	8
S	S	S	S	S	S	S	S	S	S	S	S	S	S	9
S	S	S	S	S	S	S	S	S	S	S	S	S	S	10
S	S	S	S	S	S	S	S	S	S	S	S	S	S	11
S	S	S	S	S	S	S	S	S	S	S	S	S	S	12
S	S	S	S	S	S	S	S	S	S	S	S	S	S	13
S	S	S	S	S	S	S	S	S	S	S	S	S	S	14

Table I-3. Areas of Surveyed Cells

Scenario	Ordnance	Number of Cells		Area [square meters]		Proportion Surveyed [%]
		Total	Surveyed	Total	Surveyed	
1	Aerial Gunnery	36 + 6(.2) = 37.2	35 + 5(.2) = 36	34,560 (8.541 acres)	33,445 (8.265 acres)	96.8
2	Artillery and Mortar	49 + 7(.2) = 50.4	42 + 2(.2) = 42.4	46,823 (11.571 acres)	39,391 (9.735 acres)	84.1
3	Grenades and Submunitions	42 + 13(.2) + (.2)(.2) = 44.64	31 + 5(.2) = 32	29,729 (7.347 acres)	29,729 (7.347 acres)	71.7
All		132.24	110.4	122,855 (30.361 acres)	102,565 (25.347 acres)	83.5

NRL provided three files of UXO declarations to IDA for evaluation, one file for each scenario. Some of the declarations were in cells that were *not* indicated as being surveyed. To complicate matters further, our calculation of which declarations belonged in which cells differed in some instances from that indicated by NRL in the declaration files. That is, the X–Y coordinates in the file did not correspond to the grid cell indicated in the file. Table I-4 shows the disagreements. The grid and object numbers assigned to each declaration by NRL uniquely identify it. Of the 271 declarations in scenario 1, there were 15 differences; of 283 in scenario 2, 17; and of the 242 in scenario 3, 6.

Most of the disagreements were on declarations that were very close to the grid cell boundary, usually within 1 m. Distances from the recorded X–Y positions to the NRL-assigned grid cell are also shown in Table I-4. Four declarations in M2 were more than 9 m from the NRL-assigned cell of N2. These were the largest differences except for object 1 in NRL-assigned cell L10 in scenario 3, for which the X–Y coordinate was actually in cell I10, almost 77 m away.

In only five cases did the different grid cell designation imply a different status of the declaration for the MTADS test. There were three declarations that were completely outside the scenario boundaries: 1/A9/4,[1] 2/G2/2, and 2/G5/2. They are excluded from further analysis. Had they been incorporated, all would have been false alarms.

---

1 Scenario/NRL grid cell assignment/NRL object number (within the grid cell). For instance, 2/H3/3 is object number 3 in NRL-assigned grid cell H3 in scenario 2. Referring to Table I-4, 2/H3/3 is actually in grid cell I3.

Table I-4. Grid Cell Assignment to Declarations: Disagreements Between NRL and IDA. They Are Listed in Order of IDA Grid Cell Assignment.

Scenario	NRL		IDA		
	Grid	Object Number	Grid	Distance to NRL-Assigned Boundary	Comment
1 Aerial Gunnery	A9	4	?9	2 cm	Outside Scenario Boundary
	C8	2	B8	59 cm	
	B11	5	B10	55 cm	
	B10	1	B11	12 cm	
	C11	12	B11	1.0 m	
	C12	14	B12	60 cm	
	E10	6	D10	2 cm	
	E10	7	D10	70 cm	
	D11	6	D12	36 cm	
	D12	12	D13	2 cm	
	D12	13	D13	1.3 m	
	D13	8	D14	3.0 m	
	E13	7	E14	14 cm	
	F9	4	F8	24 cm	
	E13	3	F13	30 cm	
2 Artillery and Mortar	G2	2	F2	10 cm	Outside Scenario Boundary
	G5	2	F5	23 cm	Outside Scenario Boundary
	J2	2	I2	91 cm	
	H3	3	I3	6 cm	
	H3	8	I3	4.4 m	
	H3	9	I3	2.1 m	
	H3	10	I3	5.7 m	
	L2	11	K2	2.5 m	
	L2	12	K2	3.3 m	
	L4	2	K4	92 cm	
	L4	6	K4	3.4 m	
	L4	7	L5	1 cm	
	L1	6	M1	5 cm	
	N2	1	M2	18.5 m	Large Distance to Boundary
	N2	2	M2	16.9 m	Large Distance to Boundary
	N2	3	M2	29.2 m	Large Distance to Boundary
	N2	4	M2	9.6 m	Large Distance to Boundary
3 Submunitions and Grenades	H11	4	H12	46 cm	
	I13	5	H13	3.2 m	
	L10	1	I10	76.8 m	Changed to a Surveyed Cell
	K11	4	J11	4.4 m	Changed to a Surveyed Cell
	L12	6	K12	37 cm	
	L13	1	L12	32 cm	

There were two declarations (3/L10/1 and 3/K11/4) in scenario 3 that were changed from NRL-assigned grid cells that would have corresponded to unsurveyed areas, to grid cells that were counted as surveyed. These declarations are included in our analysis.

The remainder of the miscategorization documented in Table I-4 merely shifted declarations from one surveyed cell to another surveyed cell, hence they are included in the analysis.

Table I-5 shows the cells that were not surveyed,[2] along with the number of declarations in the cells. Thus, of the 271 declarations in scenario 1, 5 were excluded, leaving 266 for further analysis. Of the 283 in scenario 2, 23 were excluded, leaving 260. In scenario 3, 19 were excluded from 242, leaving 223. We used 749 declarations from all three scenarios in our analysis.

The totals of the targets that NRL declared as ordnance or nonordnance in each scenario are given in Table I-6. For ease of comparison to the information provided by NRL in Reference I-2, NRL's numbers are also given in this table, in the "Original Cell Assignments" column. The differences are wholly a consequence of the grid cell assignment differences given in Table I-5. From this point forward, only the numbers from the correct cell assignment are used.

In addition, one of the declarations in scenario 2 is removed because it refers to a "grouped target." A grouped target is a pair of closely spaced, or "grouped," ordnance. It is further explained in the discussion of the baseline items in the next chapter.

Two types of MTADS sensors were used, pulsed EMI and magnetic field measurement (MAG). Most of the time both sensors would detect the supposed ordnance, a common detection (COM); however, at other times, only one sensor made the detection. The breakdown by sensor for scenarios 1, 2, 3, and all scenarios is given in Figures I-3 to I-6, respectively.

---

2 Reference I-2 specifies the cells that were not surveyed.

Table I-5. Declarations in Grid Cells That Were Not Surveyed

Scenario	Grid Cell	NRL Number of Declarations in the Cell	IDA Number of Declarations in the Cell	Comments
1	A13	2	2	
	A14	2	2	
	2 cm East of cell A9	0	1	Outside Scenario Boundary
	Scenario 1 Total	4	5	
2	F2	0	1	Outside Scenario Boundary
	F5	0	1	Outside Scenario Boundary
	G1	5	5	
	H1	5	5	
	M6	7	7	
	M7	3	3	
	N7	1	1	
	Scenario 2 Total	21	23	
3	K11	4	3	One was actually in J11
	L10	2	1	One was actually in I10
	L12	5	6	
	L13	3	2	
	M13	5	5	
	N13	2	2	
	Scenario 3 Total	21	19	

Table I-6. Target Declarations as Ordnance or Nonordnance

Scenario	Declared Target Type	Corrected Cell Assignments		Original Cell Assignments	
		Number Surveyed	Number Unsurveyed	Number Surveyed	Number Unsurveyed
1 Aerial Gunnery	Ordnance	185	4	186	3
	Non-ordnance	81	1	81	1
2 Artillery and Mortar	Ordnance	217 (216)*	13	218	12
	Non-ordnance	43	10	44	9
3 Submunitions and Grenades	Ordnance	215	19	213	21
	Non-ordnance	7	0	7	0

* The number in parentheses excludes a declaration on a grouped target. See next chapter for further explanation.

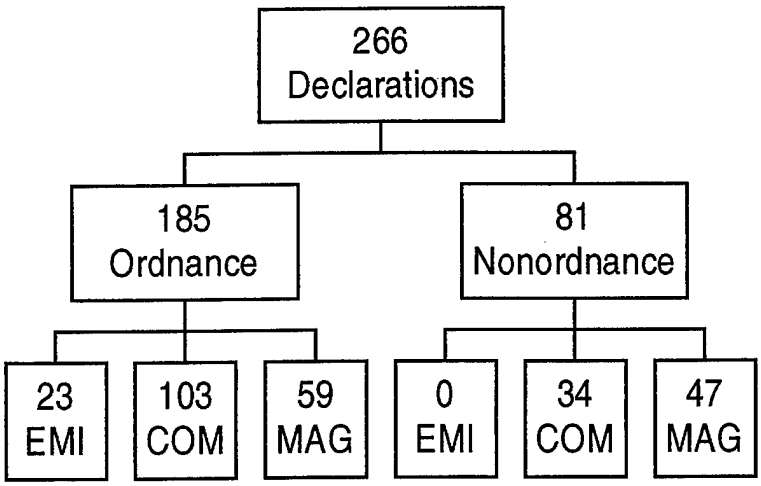

Figure I-3. Declarations by Sensor Type for Scenario 1—Aerial Gunnery

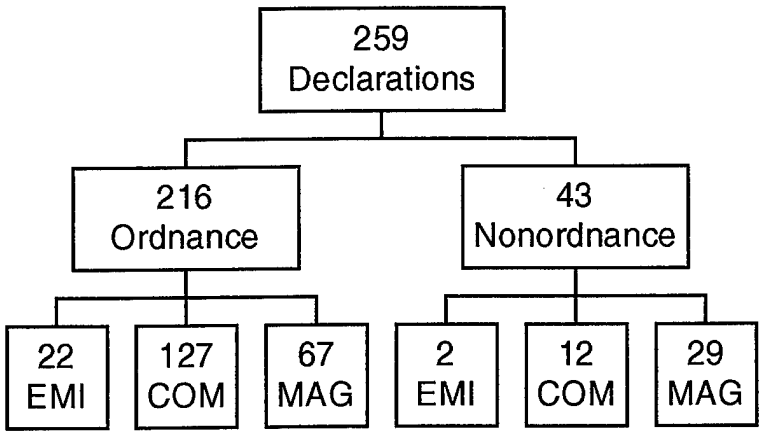

Figure I-4. Declarations by Sensor Type for Scenario 2—Artillery and Mortar

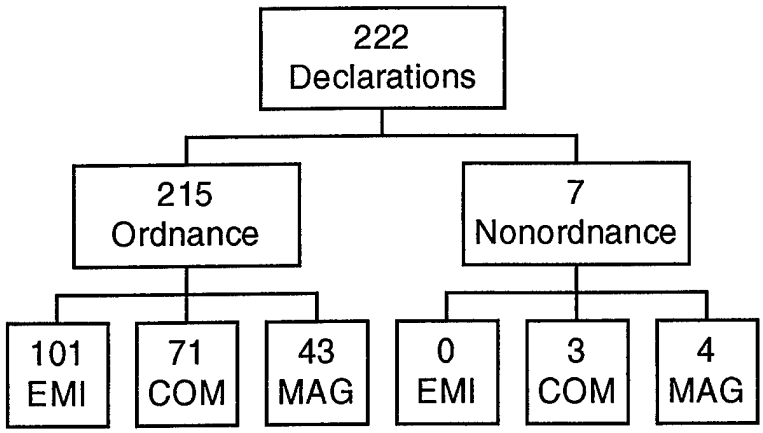

Figure I-5. Declarations by Sensor Type for Scenario 3—Submunitions and Grenades

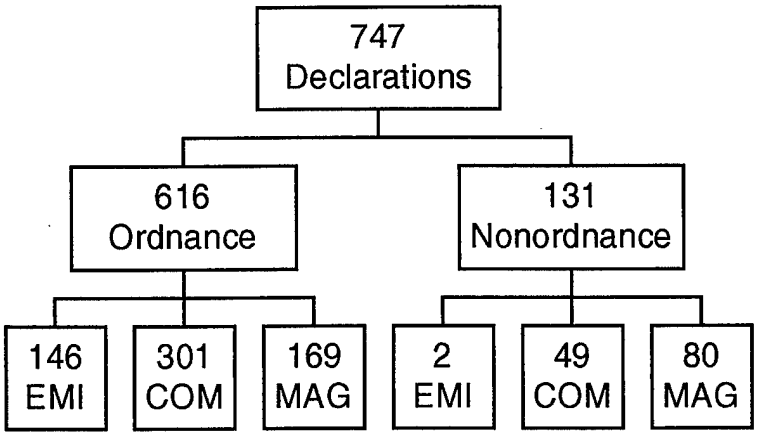

Figure I-6. Declarations by Sensor Type for All Scenarios

C. TEST DATA

All the test data were provided by NRL in the form of three spreadsheets. These data, as specified in Ref. I-2 and described in this chapter, are used in our analysis.

II. ANALYSIS OF NRL DECLARATIONS

This chapter presents a detailed analysis of the MTADS detections. The analysis is predicated on NRL's declaration of each detection as ordnance or nonordnance, as outlined in Chapter I. The analysis is presented in the following order:

- Description of the known baseline items
- Performance, including probability of detection and false-alarm rates
- Sensor performance characteristics, including location accuracy and correlation among sensors (EMI and MAG).

A. THE BASELINE

Baseline items are those items that were purposefully placed in the ground at the North Test Site at JPG. This baseline includes both ordnance and nonordnance items. In the following analysis, the MTADS performance is evaluated against the baseline items. There is no guarantee that items other than the baseline items are not in the ground; indeed, it is expected that there are such items. With this in mind, this analysis, strictly speaking, is an exercise in setting performance bounds. Specifically, performance is evaluated only with respect to the *known* baseline items, given in Table II-1. The density of UXO is conveniently expressed in terms of number per hectare. (A hectare is 10,000 m^2, or about 2.5 acres.)

Table II-1. Number of Baseline Items in the Surveyed Areas

Scenario	Number of UXO			Density of UXO (per hectare)		
	Ordnance	Nonordnance	Total	Ordnance	Nonordnance	Total
1	47	78	125	14.1	23.3	37.4
2	75 (73)*	50	125 (123)*	19.1 (18.5)*	12.7	32 (31)*
3	86	38	124	28.9	12.8	41.7
All	208 (206)*	166	374 (372)*	20.3 (20.1)*	16.2	36.5 (36.3)*

* Two ordnance were within R_{crit} of each other and were excluded for that reason.

One pair of ordnance in scenario 2 was within the critical radius, R_{crit}, of 1 m. R_{crit} is the nominal resolution of the sensors and can be thought of as defining a detection

"opportunity." That is, each sensor has the opportunity to detect an ordnance item for every subsequent area of 1 m^2 that is surveyed.

There is some ambiguity attached to detection of ordnance closer than R_{crit} to another ordnance item. Should a detection of one be considered a detection of the other, that is, *two* detections? Or, should it be considered a single detection of a pair, that is, *one* detection? Rather than attempting a definitive resolution, we avoided this issue by excluding all grouped ordnance (see Table II-2) from the analysis. This is consistent with the recent analysis of the MTADS performance at Twentynine Palms, California (Ref. II-1).

Table II-2. Grouped Ordnance (from scenario 2)

Type Ordnance #1	Type Ordnance #2	Surface Distance Between Ordnance (m)	Depth of Ordnance #1 (m)	Depth of Ordnance #2 (m)
81-mm mortar (illumination case)	8-in. projectile	0.77	0.23	0.61

B. GENERAL PERFORMANCE RESULTS

We compared the MTADS data sets from the three scenarios to the items in the baseline. To match a baseline item (ordnance or nonordnance) to a declaration, the distance in the plane of the Earth's surface, the two-dimensional radial distance, r, derived from the relative northing and easting offsets, must be within the critical radius, R_{crit}, of the center of the emplaced item. If the declaration is classified by NRL as ordnance, $R_{crit} \geq r$, and the item in the baseline is ordnance, it is a detection. If $r > R_{crit}$ or the baseline item is nonordnance, the declaration is a false alarm. (See Figure II-1.)

1. Probabilities of Detection and *FAR*s

Detection probabilities (P_Ds) and false-alarm rates (*FAR*s) were determined for the three scenarios, individually and in aggregate. Table II-3 gives the P_Ds. Table II-4 gives the *FAR*s. An R_{crit} of 1.0 m is used throughout. The results here combine the sensors such that if any detection by any sensor (MAG or EMI) is within R_{crit}, it is considered a detection, hereafter referred to as an "overall" detection.

More stringent requirements are examined in detail later. For the moment, the effect of greater stringency may be usefully gauged by requiring that *both* sensors achieve a satisfactory detection. This P_D is given in the last column of Table II-3.

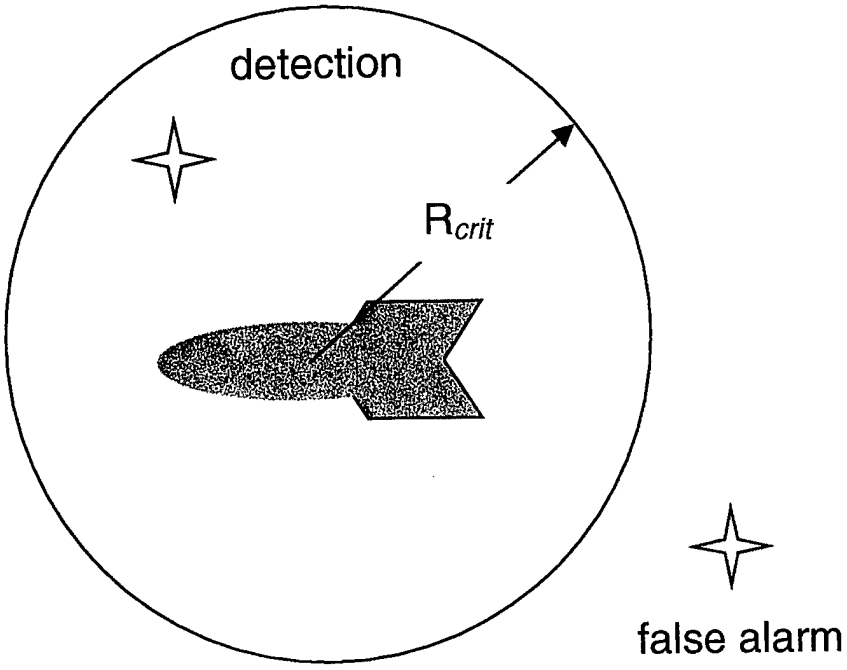

Figure II-1. Detection and False-Alarm Dependence on R_{crit}. Detection of the ordnance item is dependent on the relative location of the declaration, marked with a four-pointed star, and the center of volume of the item. If the item is ordnance and the declaration is within the critical radius, R_{crit}, the ordnance is detected. If the declaration is nonordnance, not in the baseline, or outside R_{crit}, it is a false-alarm.

Table II-3. MTADS Overall Detection Probability at Jefferson Proving Ground

Scenario	Number of Ordnance	Number Detected By			Overall Number Detected	Overall P_D [%]	Restrictive P_D (both sensors required)
		EMI Only	MAG Only	Both MAG and EMI			
1	47	15	0	30	45	95.7	63.8
2	73	5	1	64	70	95.9	87.7
3	86	54	0	26	80	93.0	30.2
All	206	74	1	120	195	94.7	58.3

We also studied more restrictive subsets of declarations: (1) declarations that had at least one magnetometer location datum (a MAG declaration), and (2) declarations that had at least one EMI location datum (an EMI declaration). These subsets focus on the relative contribution of MAG versus EMI.

Table II-4. MTADS Overall False-Alarm Rates at Jefferson Proving Ground

Scenario	Declaration Not in Baseline	Nonordnance Baseline Items Declared Ordnance—Detection by:			Total Number of False Alarms	*FAR* (per hectare)	P_{fa}
		EMI only	MAG only	Both MAG and EMI			
1	81	0	3	56	140	41.9	1.32×10^{-2}
2	100	9	0	37	146	37.6	1.18×10^{-2}
3	110	8	3	14	135	45.4	1.43×10^{-2}
All	291	17	6	107	421	41.1	1.29×10^{-2}

We also studied detections and false alarms of declarations that were either exclusively MAG or exclusively EMI. It turns out that the main issues as far as P_D go are already apparent in the (nonexclusive) MAG and (nonexclusive) EMI presentations given next. On the other hand, the mutually exclusive MAG-EMI data well illustrate trends in *FAR*. Therefore, it is presented in the corresponding section, section 3 below.

a. EMI Declarations

EMI declarations include those with only EMI ordnance coordinates and those with both EMI and MAG ordnance coordinates. Tables II-5 and II-6 summarize this cut of the data, relevant to P_D and *FAR*, respectively. Most prominent is the P_D for scenarios 1 and 3 (colored cells in Table II-5). It is the same as the P_D for both sensors combined (compare to Table II-3). Even more impressively, the *FAR* decreased significantly, as shown by comparing the colored cells in Table II-6 to the corresponding data in Table II-4. In these scenarios it would have been better not to have used the magnetometer at all.

Table II-5. MTADS Detection Probabilities for the EMI Sensor

Scenario	Number of Ordnance	Number Detected By			Overall Number Detected	Overall P_D [%]	Restrictive P_D (both sensors required)
		EMI Only	MAG Only	Both MAG and EMI			
1	47	15	0	30	45	95.7	63.8
2	73	5	0	64	69	94.5	87.7
3	86	54	0	26	80	93.0	30.2
All	206	74	0	120	194	94.2	58.3

Table II-6. MTADS *FAR*s for the EMI Sensor

Scenario	Declaration Not in Baseline	Nonordnance Baseline Items Declared Ordnance—Detection by:			Total Number of False Alarms	*FAR* [per hectare]	P_{fa}
		EMI only	MAG only	Both MAG and EMI			
1	22	0	3	56	81	24.2	7.6×10^{-3}
2	34	9	0	37	80	20.3	6.4×10^{-3}
3	68	8	2	14	92	31.0	9.7×10^{-3}
All	124	17	5	107	253	24.7	10^{-3}

b. MAG Declarations

MAG declarations include declarations with only MAG ordnance coordinates and those with both EMI and MAG ordnance coordinates. Tables II-7 and II-8 summarize this cut of the data, relevant to P_D and *FAR*, respectively.

c. False Alarms for Declarations Not Common to Magnetometer and EMI

False alarms are examined several ways in this document. In this section, an analysis is done in terms of declarations made exclusively by one or the other sensor.

Table II-7. MTADS Detection Probabilities for the MAG Sensor

Scenario	Number of Ordnance	Number Detected By			Overall Number Detected	Overall P_D [%]	Restrictive P_D (both sensors required)
		EMI Only	MAG Only	Both MAG and EMI			
1	47	2	0	30	32	68.1	63.8
2	73	1	1	64	66	90.4	87.7
3	86	1	0	26	27	31.4	30.2
All	206	4	1	120	125	60.7	58.3

Table II-8. MTADS *FAR*s for the MAG Sensor

Scenario	Declaration Not in Baseline	Nonordnance Baseline Items Declared Ordnance – Detection by:			Total Number of False Alarms	*FAR* [per hectare]	P_{fa}
		EMI only	MAG only	Both MAG and EMI			
1	71	0	3	56	130	38.9	1.22×10^{-2}
2	89	2	0	37	128	32.5	1.02×10^{-2}
3	70	0	3	14	77	25.9	8.1×10^{-3}
All	230	2	6	107	345	33.6	1.06×10^{-2}

Subtle issues attend the analysis of false alarms. These are mostly a consequence of reasonably defining an "opportunity," the denominator in P_{fa}.

$$P_{fa} = \frac{\#\, false\ alarms}{\#\, opportunities} \quad . \tag{II-1}$$

As done in Reference II-1, a resolution may be reached by convention, in this case defining a nominal opportunity in terms of a circular area around a declaration with radius R_{crit}. The total number of opportunities is then

$$\#opportunities = \frac{Area_{surveyed}}{\pi R_{crit}^2} \quad . \tag{II-2}$$

For a high density of false alarms, the overlap of the areas associated with each false alarm can be significant. Correcting for the overlap yields a definition of P_{fa} in terms of "the area of the false-alarm declarations," A_{fa}, and the total surveyed area:

$$P_{fa} = \frac{A_{fa}}{Area_{surveyed}} \tag{II-3}$$

In the present case of low P_{fa}, the overlaps are negligible, so

$$A_{fa} = \#\, false\ alarms \times \pi R_{crit}^2 \quad , \tag{II-4}$$

which implies

$$P_{fa} = FAR \times \pi R_{crit}^2 \tag{II-5}$$

where

$$FAR = \frac{\#\, false\ alarms}{Area_{surveyed}} \quad . \tag{II-6}$$

This limiting case is used here, but strictly speaking, the P_{fa} so calculated should be regarded as a surrogate for the true P_{fa}.

The false alarms due exclusively to one sensor are given in Tables II-9 and II-10, for EMI-exclusive declarations and MAG-exclusive declarations, respectively. The EMI does better on false alarms except for scenario 3, where the *FAR*s are comparable (16.2 per hectare for EMI and 14.5 per hectare for MAG). However, the difference in their contribution to P_D is dramatic. The contribution is called ΔP_D here because it is in addition to the detections that EMI and MAG had in common.

ΔP_D for each sensor is defined as

$$\Delta P_D \text{ for EMI(MAG)} \equiv \frac{\#\text{ of EMI(MAG) declarations that result in a declaration}}{\#\text{ of baseline ordnance}} \quad .$$

Thus, using EMI as an example,

ΔP_D(EMI) from Table II-9 + ΔP_D(MAG) from Table II-7 = Overall P_D from Table II-3.

Or, numerically, for Scenario 1,

$$\frac{13}{47} \text{ from Table II-9} + \frac{32}{47} \text{ from Table II-7} = \frac{45}{47} \text{ from Table II-3} \quad .$$

Similarly, ΔFAR for each sensor is defined as

$$\Delta FAR \text{ for EMI(MAG)} \equiv \frac{\#\text{EMI(MAG)-only declarations that result in a false alarm}}{\text{area surveyed}} \quad ,$$

so that, using EMI as an example,

$$\Delta FAR\text{(EMI)} + FAR\text{(EMI)} = \text{overall FAR} \quad .$$

Referring to Scenario 1 and Tables II-9, II-8, and II-4, as an example, gives

$$3.0 + 38.9 = 41.9 \quad ,$$

as it should.

ΔP_D hovers around 1 percent for MAG, but reaches over 60 percent for EMI.

Table II-9. Detections and False Alarms for EMI-Exclusive Declarations

Scenario	Number Detected	ΔP_D [%]	Not In Baseline	Not Ordnance	Total False Alarms	ΔFAR [per hectare]	ΔP_{fa}
1	13	28	10	0	10	3.0	9.4×10^{-3}
2	4	5.5	11	7	18	4.6	1.44×10^{-3}
3	53	62	40	8	48	16.2	5.1×10^{-3}
All	70	34	61	15	76	7.4	2.3×10^{-3}

Table II-10. Detections and False Alarms for MAG-Exclusive Declarations

Scenario	Number Detected	ΔP_D [%]	Not In Baseline	Not Ordnance	Total False Alarms	ΔFAR [per hectare]	ΔP_{fa}
1	0	0	59	0	59	17.6	5.5×10^{-3}
2	1	1.4	66	0	66	16.8	5.3×10^{-3}
3	0	0	42	1	43	14.5	4.5×10^{-3}
All	1	0.5	167	1	168	16.4	10^{-3}

d. Introduction to the Baseline Partitions and the Declaration Partitions

There are two complementary ways to look at detection effectiveness: as a partition of the baseline items or as a partition of the declarations. Partitioning the baseline ordnance items into detected and undetected classes gives the P_D measure of effectiveness (MOE). Partitioning the number of declarations of ordnance into those that are correct and those that are erroneous yields the P_{fa} MOE. These partitions are a systematic display of the data as (inverted) classification trees, sometimes called dendrograms or dendritics, but referred to here simply as trees.

Different kinds of analyses of this data could also be done. One could view the MOE as a chain of conditional probabilities, and examine the chain to explore where the problem of producing better MOEs lies. One could also ask whether other classification trees might be more informative about the MOE. CART (Classification and Regression Trees) is a well-developed statistical method for building and using such trees. Neither of these methods is further pursued here. The conditional probabilities are evident in the trees themselves, and are conventionally taken as the probability to detect (given a target) and the probability to classify (given a detection). CART and other classification techniques may prove informative but are beyond the scope of the present study.

2. Scenario 1

The analysis of scenario 1, aerial gunnery, is presented in two parts. The first section presents partitions of the important data sets and gives the essential results of the test. The last section explores false-alarm mitigation using linear statistical discrimination.

a. Partitions of the Baseline and the Declaration Set

Figure II-2 shows the partition of the 125 baseline items in scenario 1. The baseline is the relevant set for determining P_D. Specifically, the 47 ordnance in the baseline constituted the detection opportunities. There were 46 "detections"[1] in one of the three categories of declarations: EMI, MAG, or both (COM). There was *no* declaration by MAG alone that corresponded to an actual detection. By contrast, EMI made a third (15/46) of the detections by itself.

In a similar manner, Figures II-4 and II-6 give the P_D-relevant information by sensor.

Figure II-3 shows the partition of the 266 declarations relevant for determination of the *FAR*. Specifically, the 185 items declared as likely ordnance each can end up being a false alarm. Of the 104 "detections" in the baseline, 15 were by EMI alone, 3 solely by MAG, and 86 by both sensors. The number of false alarms was the sum of those "detections" of nonordnance and the "detection" of items not in the baseline. That is, there were 140 false alarms, the components of which are shown colored in Figure II-3. EMI by itself did not contribute any false alarms arising from baseline nonordnance. There were, however, 10 nonbaseline items detected only by EMI that were false alarms (see Table II-11).

Figures II-5 and II-7 give the false alarm (FA)-relevant information by sensor.

---

[1] Quotes distinguish "detection" of some object in the baseline, be it ordnance or nonordnance, as opposed to detection without quotes, which refers (in most of this document and in UXO work generally) to detection of only baseline ordnance and does not include "detection" of nonordnance.

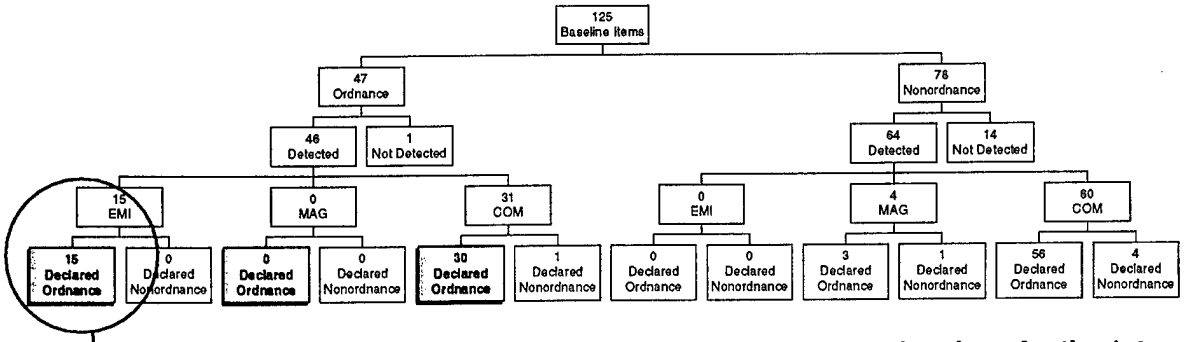

Figure II-2. Partition of the Baseline for the P_D MOE: All Sensor Declarations for the 1st Scenario, Aerial Gunnery. The yellow boxes (with shadow and bold type) contain the declarations that contribute to P_D. The EMI, MAG, and COM boxes indicate the number of *declarations* by EMI alone, MAG alone, and by both MAG and EMI (that is, common declarations).

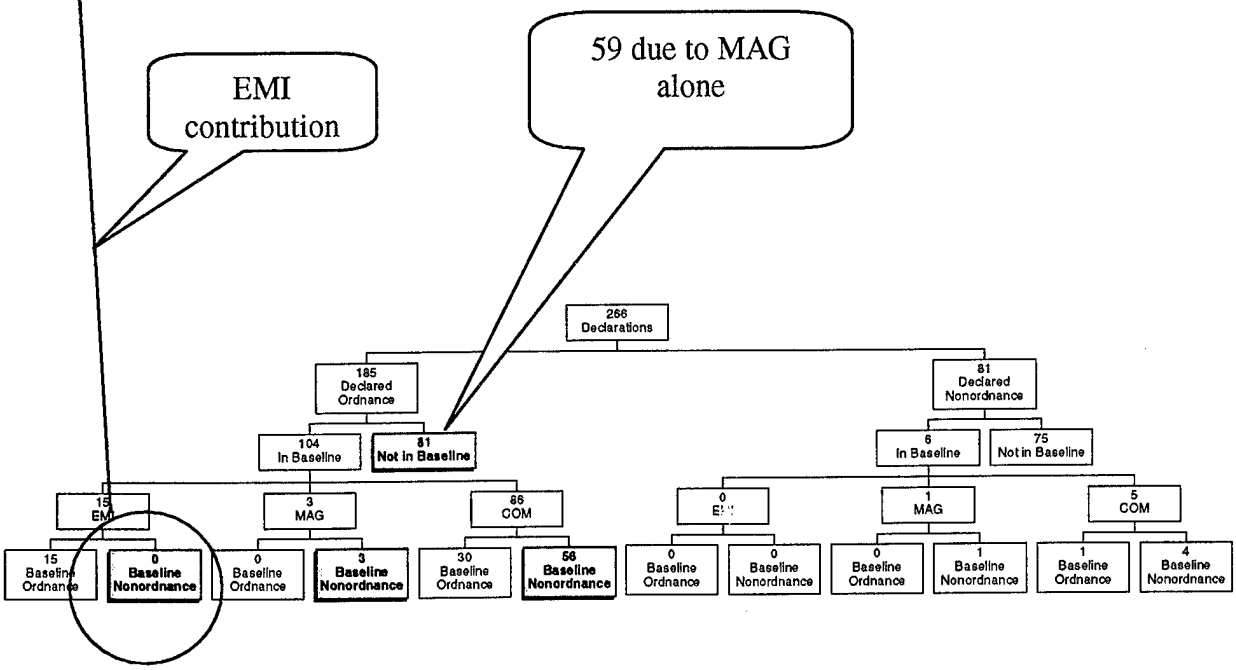

Figure II-3. Partition of the Declarations for the *FAR* MOE: All Sensor Declarations for the 1st Scenario, Aerial Gunnery. The yellow boxes (with shadow and bold type) contain the declarations that contribute to the *FAR*. The P_{fa} is calculated assuming that an opportunity occurs for every circular area with radius of R_{crit}. A 1-m R_{crit} is used. The EMI, MAG, and COM boxes indicate the number of *detections* achieved by EMI alone, MAG alone, and by both MAG and EMI (that is, common detections).

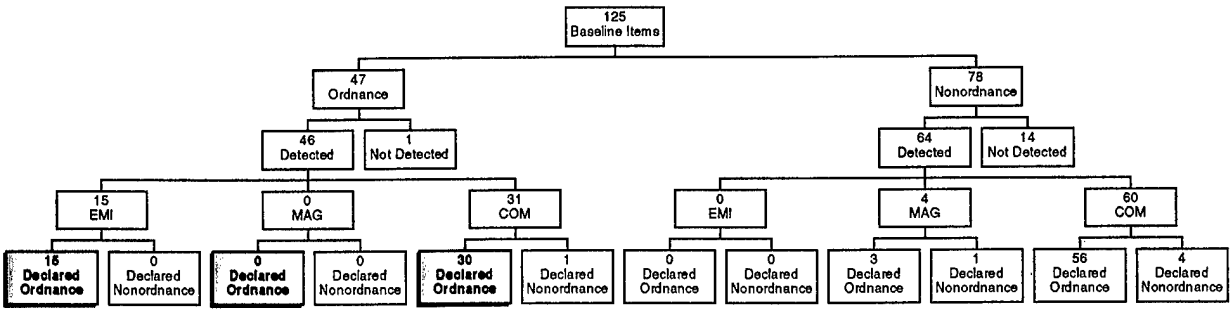

Figure II-4. Partition of the Baseline for the P_D MOE: EMI Declarations for the 1st Scenario, Aerial Gunnery. The yellow boxes (with shadow and bold type) contain the declarations that contribute to. The EMI, MAG, and COM boxes indicate the number of declarations by EMI alone, MAG alone, and by both MAG and EMI (that is, common declarations).

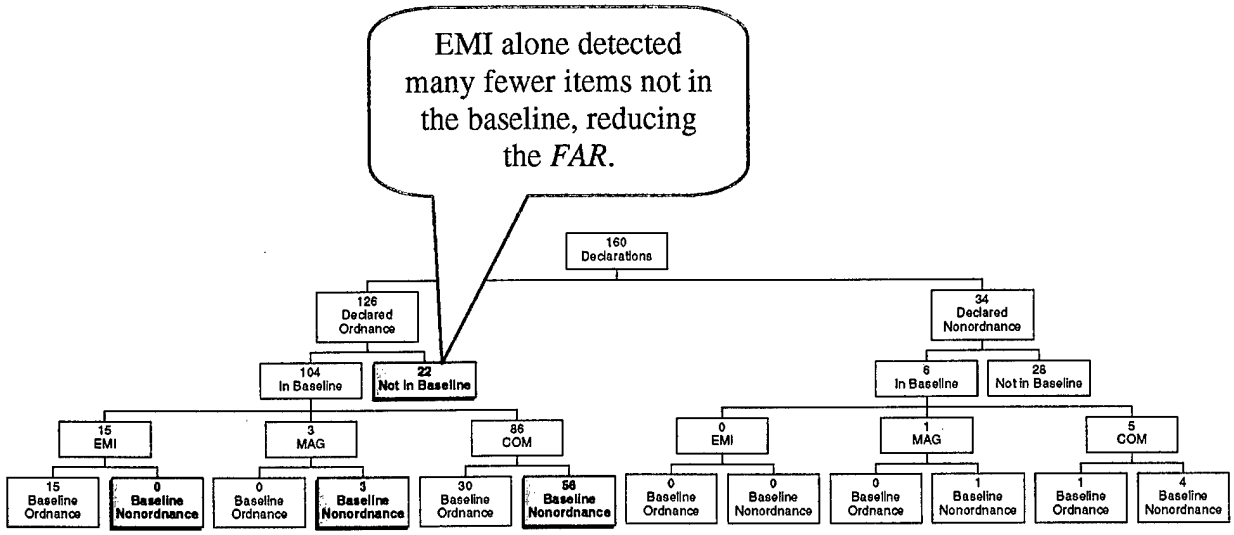

Figure II-5. Partition of the Declarations for the *FAR* MOE: EMI Declarations for the 1st Scenario, Aerial Gunnery. The yellow boxes (with shadow and bold type) contain the declarations that contribute to the *FAR*. The P_{fa} is calculated assuming that an opportunity occurs for every circular area with radius of R_{crit}. A 1-m R_{crit} is used. The EMI, MAG, and COM boxes indicate the number of *detections* achieved by EMI alone, MAG alone, and by both MAG and EMI (that is, common detections).

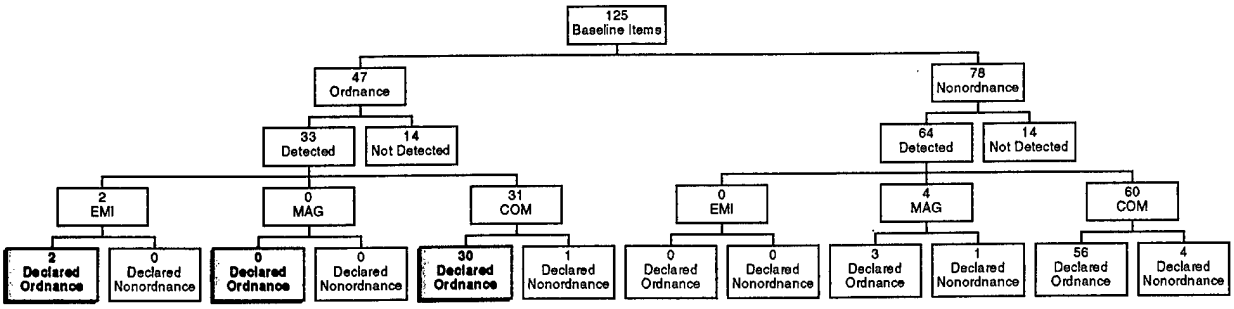

Figure II-6. Partition of the Baseline for the P_D MOE: MAG Declarations for the 1st Scenario, Aerial Gunnery. The yellow boxes (with shadow and bold type) contain the declarations that contribute to P_D. The EMI, MAG, and COM boxes indicate the number of declarations by EMI alone, MAG alone, and by both MAG and EMI (that is, common declarations).

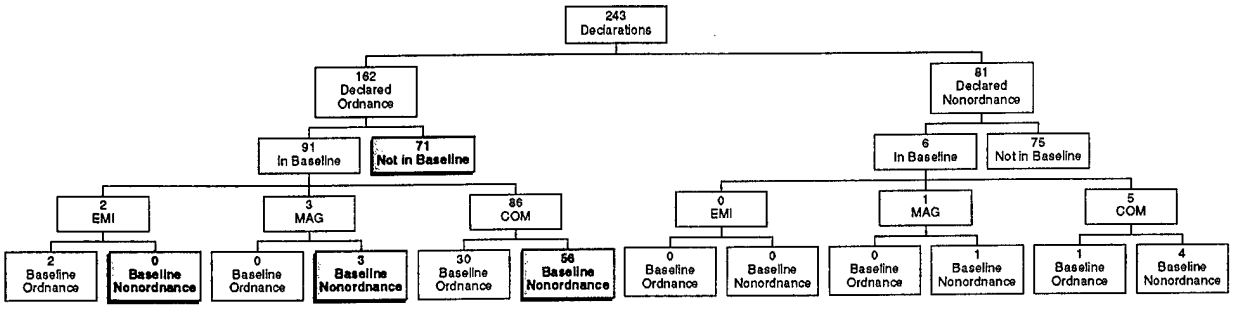

Figure II-7. Partition of the Declarations for the *FAR* MOE: MAG Declarations for the 1st Scenario, Aerial Gunnery. The yellow boxes (with shadow and bold type) contain the declarations that contribute to the *FAR*. The P_{fa} is calculated assuming that an opportunity occurs for every circular area with radius of R_{crit}. A 1-m R_{crit} is used. The EMI, MAG, and COM boxes indicate the number of detections achieved by EMI alone, MAG alone, and by both MAG and EMI (that is, common detections).

Table II-11 shows how the nonbaseline declarations break down. All information in Table II-11 can be derived from the trees. For example, the 12 common declarations for nonbaseline items that appears in the ordnance declarations in Table II-11 can be derived from the tree information, as follows.

1. Add the 22 EMI ordnance declarations not in the baseline (Figure II-5) to the 71 MAG ordnance declarations not in the baseline (Figure II-7).
2. Take the total, 93, and subtract the 81 ordnance declarations by all sensors (Figure II-3).
3. The difference, 12, appears as the number of common declarations in Table II-11.

The other data in Table II-11 can be similarly deduced: they are displayed here for clarity.

Table II-11. Sensor Relation to "Detected" Object Type for Scenario 1

	Actual Object Type	Declaration Sensor			Total
		MAG	Common	EMI	
Declared as Ordnance	Non-baseline	59	12	10	81
	Non-ordnance	0	59	0	59
	Ordnance	0	32	13	45
	Total Declared Ordnance	59	103	23	185
Declared as Non-Ordnance	Non-baseline	47	28	0	75
	Non-ordnance	0	5	0	5
	Ordnance	0	1	0	1
	Total Declared Ordnance	47	34	0	81

b. False-Alarm Mitigation: Correlation and Discriminant Analysis

In this section, the issue of discriminating FAs from detections for the purpose of reducing the *FAR* is explored.

The method of analysis is straightforward classical linear discrimination, as described in Reference II-2 (Chapter 3) or Reference 2 (Chapter 11). In particular, the adoption of Fisher's linear discriminant (Ref. II-2, p. 93) enables a simple maximization of the ratio of the between-group variance to the within-group variance, a reasonable goal even in the absence of multivariate normality. On the other hand, if multivariate normality obtains,[2] Fisher's rule follows from classical decision theory (Ref. II-2, Section 11.3). Here, the groups are MTADS' ordnance declarations that correspond to ordnance, called "Detections," and such declarations that do not, called "False Alarms."

We conducted discriminant analyses on four batches of data. The first three correspond to the individual scenarios; the fourth batch is an aggregation of all three scenarios. It was analyzed first with the hope of identifying a discriminant that is robust across scenarios. None was found. Failing that, this linear discriminant analysis was used to see if the scenario could be identified solely by using the data. This also was not

---

2 For the linear discriminant, it is also necessary to assume equal covariance matrices.

possible at this level of examination. More sophisticated techniques could be brought to bear, but this is not within the scope of this document.

The variables (in statistical parlance "factors") that we considered are those to which the MTADS operator might conceivably have access. For the MTADS magnetometer these are fitted depth (ZMAG), fitted radius (RMAG), magnetic moment (MAGMOM), fitted inclination (INCLIN), fitted azimuthal angle (AZIM), and the GoF (GOF_MAG). For the MTADS EMI detection they are fitted depth (ZEM), ferrous radial size (RFE_EM), nonferrous radial size (RAL_EM), and GoF (GOF_EM). The aim here is to examine variables that could be used to mitigate FAs. When a case does not have a required variable, it is omitted from the analysis altogether. The inclusion of variables, such as the GoF, which are currently the result of a rather elaborate fitting process, is justified by anticipating that a more expeditious method of producing them, or close surrogates, could be achieved. Whether this is in fact possible or practical is an issue for further study.

An initial survey of the data aggregated from all scenarios gives the variable correlations shown in Table II-12. There were 298 declarations with all data available.

Table II-12. Correlation Matrix for All Scenarios.
298 declarations had all data available.

	ZMAG	ZEM	RMAG	RFE_EM	RAL_EM	MAGMOM	INCLIN	AZIM	GOF_MAG
ZMAG	1								
ZEM	0.724	1							
RMAG	0.71	0.584	1						
RFE_EM	0.687	0.831	0.777	1					
RAL_EM	0.682	0.807	0.774	0.989	1				
MAGMOM	0.529	0.432	0.834	0.633	0.667	1			
INCLIN	0.176	0.071	–0.149	0.04	0.038	–0.093	1		
AZIM	–0.061	–0.056	0.022	0.039	0.036	–0.053	–0.16	1	
GOF_MAG	0.136	0.187	0.362	0.302	0.266	0.194	–0.177	0.051	1
GOF_EM	0.192	0.207	0.371	0.451	0.362	0.198	0.04	0.073	0.347

The largest correlations are for (RFE_EM, RAL_EM) with correlation 0.989 and (RMAG, MAGMOM) with correlation 0.834. Scatterplots of these pairs (Figures II-8 and II-9, respectively) show that the variables are completely dependent. Thus, only one of each pair is used in the following analysis. The variable of each pair that is kept has a

"more even" distribution of hits. From the histogram in Figure II-9, it is clear that RMAG is preferred, the distribution of MAGMOM being much more peaked and skewed.

Like consideration of Figure II-8 indicates a preference for RFE_EM, though it is not so pronounced. This is because the relation of RFE_EM to RAL_EM is nearly linear. Were the relation completely linear, either variable would be equally acceptable.

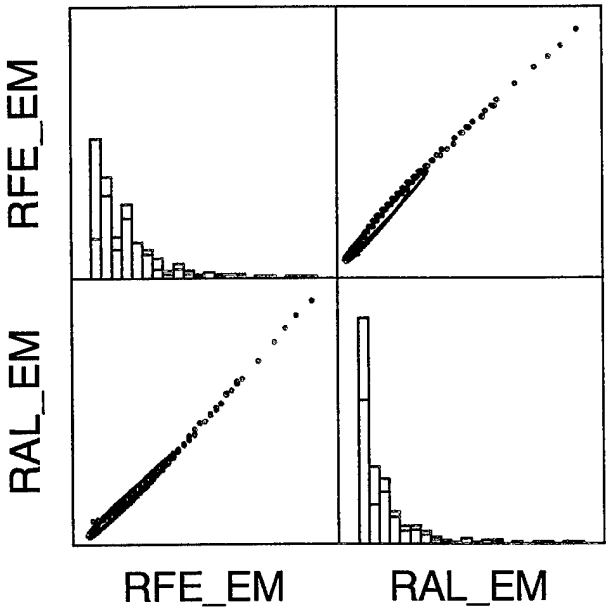

Figure II-8. Correlation of EMI Ferrous and Nonferrous Radii.
Combined data with 50-percent ellipses are shown.

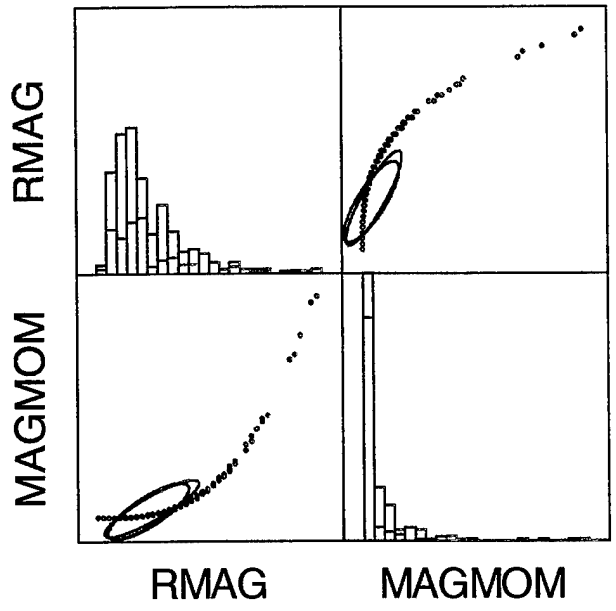

Figure II-9. Correlation of Fitted Magnetometer Radius and Magnetic Moment.
Combined data with 50-percent ellipses are shown.

b. Discriminant Analysis

In Scenario 1, the MTADS operators decided that 185 of the 266 declarations were ordnance. These ordnance declarations are shown in scatterplots: Figure II-10 for magnetometer variables, Figure II-11 for EMI variables, and Figure II-12 for the cross of magnetometer and EMI variables. Table II-13 shows correlation of the variables in scenario 1.

Table II-13. Correlation of Scenario 1 Variables. 103 Declarations for Which all Data Was Available

	ZMAG	ZEM	RMAG	RFE_EM	INCLIN	AZIM	GOF_MAG	GOF_EM
ZMAG	1							
ZEM	0.724	1						
RMAG	0.696	0.522	1					
RFE_EM	0.712	0.807	0.73	1				
INCLIN	0.32	0.272	-0.082	0.237	1			
AZIM	-0.166	-0.14	-0.124	-0.076	-0.046	1		
GOF_MAG	0.322	0.162	0.447	0.271	0.271	-0.051	1	
GOF_EM	0.223	-0.009	0.363	0.282	0.282	0.014	0.309	1

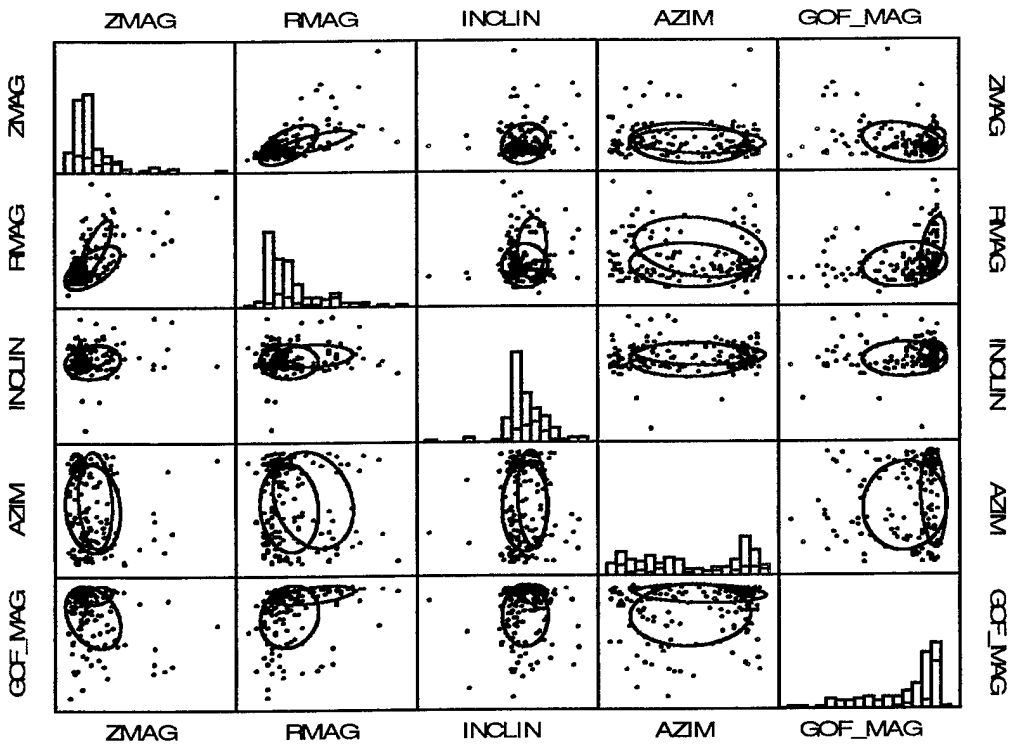

Figure II-10. Scenario 1 Correlation of Magnetometer Variables
Blue indicates false alarms. Red indicates detections.
50-percent ellipses are shown.

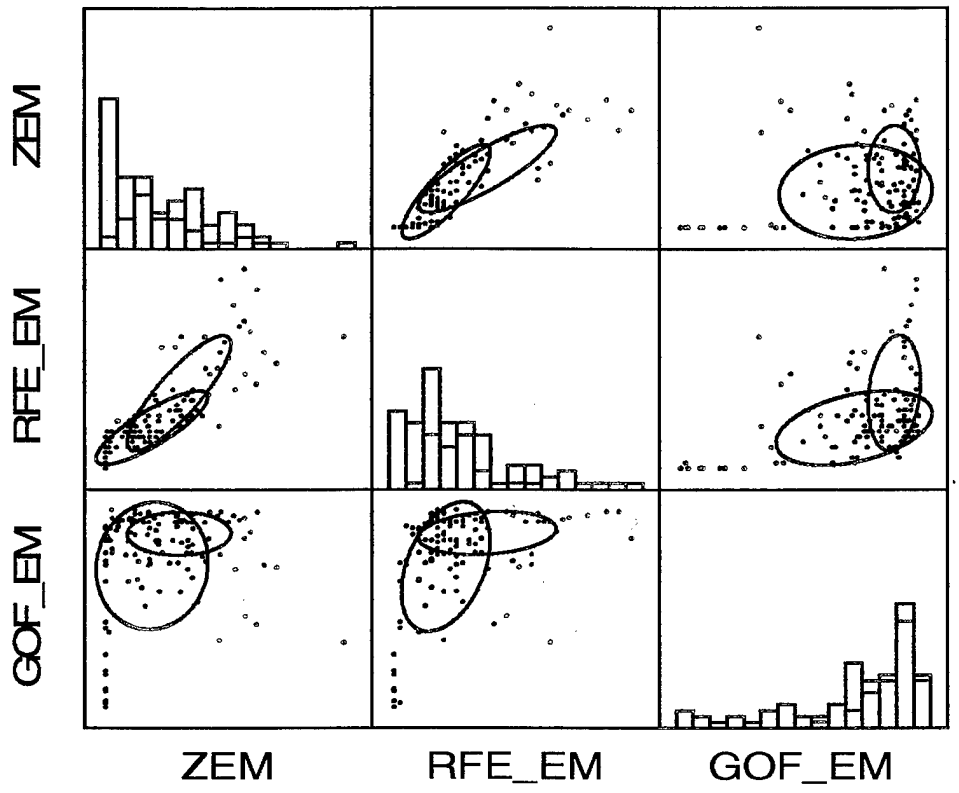

Figure II-11. Scenario 1 Correlation of EMI Variables.
Blue indicates false alarms. Red indicates detections.
50-percent ellipses are shown.

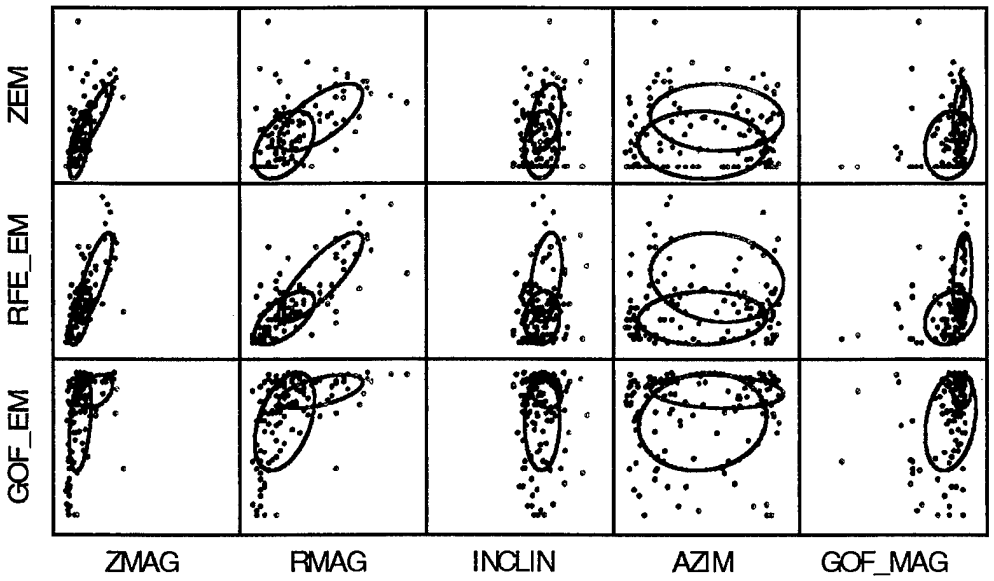

Figure II-12. Scenario 1 Cross-Correlation: EMI vs. MAG.
Blue indicates false alarms. Red indicates detections.
50-percent ellipses are shown

Figures II-13 and II-14 show the histograms of the detections and false alarms with the scale of the independent variable indicated. The bins are not at the same positions or of the same width as those in the previous figures, so the histogram bar heights will not coincide, in general.

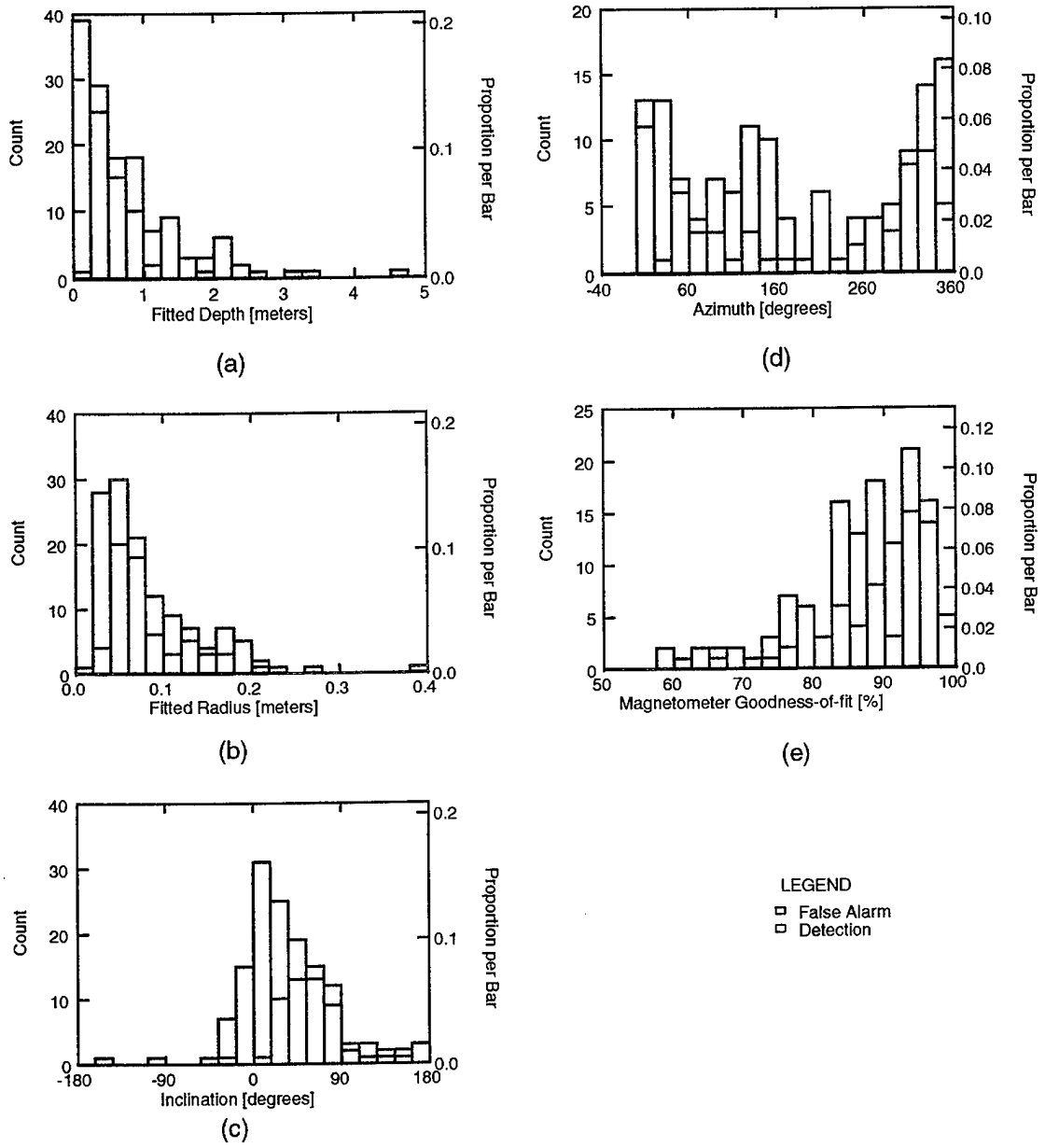

Figure II-13. Histograms of Detections and False Alarms for the Magnetometer Variables for Scenario 1. (a) Depth, (b) Radial size, (c) Inclination, (d) Azimuthal angle, (e) GoF.

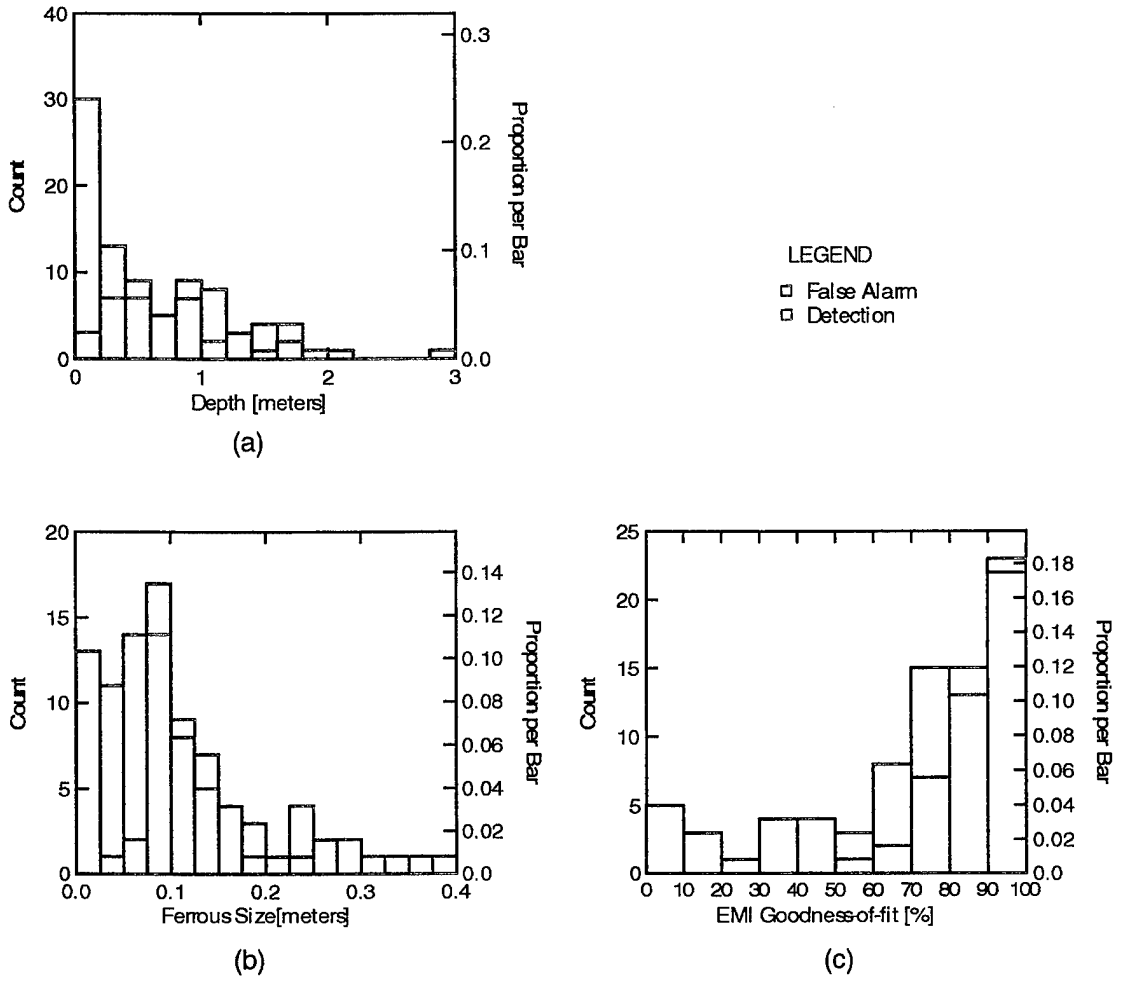

Figure II-14. Histograms of Detections and False Alarms for the EMI Variables for Scenario 1. (a) Depth, (b) Ferrous Size, (c) GoF.

The discriminant analysis proceeds from consideration of all the independent variables, both MAG and EMI, and uses backward elimination to select the statistically significant variables. An F test[3] is used, with the criteria for variable elimination being a tail probability of 0.15. This procedure gives only RFE_EM as statistically significant for scenario 1.

Thus, the best one can do, according to this analysis, is to mitigate false alarms by setting a threshold on RFE_EM. The RFE_EM histogram is given in Figure II-14(b). It is not greatly encouraging. Of the 81 false alarms, only 13 can be mitigated by using a ferrous size threshold of 0.025 m. The prescription would be to classify all objects with

---

3 An F test uses the ratio of sample variances as a test statistic. Under the assumption that the underlying variance is normally distributed, the F statistic is distributed in accordance with a known function, the F distribution. In this case, the F statistic is the ratio of the between-group and within-group variances.

EMI ferrous size less than 0.025 m as nonordnance in this scenario. The false alarms are thereby reduced from 81 to 68, a reduction of 16 percent.

The RFE_EM discriminant was derived by using only the separation of the means of the distributions themselves as the goal. More robust discriminants are likely available. For instance, inspect the GOF_EM vs. RFE_EM plot in Figure II-11. The lower left region more clearly separates the false alarms from the detections, as indicated by the 50-percent ellipses. But by just using the separation of detection and false alarm means as a criterion, the EMI GoF does not make the cut. It is easy to get possible *FAR* reductions of 25 percent or more by using statistically insignificant variables in this way. A quadratic boundary (instead of a linear one) also helps.

We avoided using variables that are not statistically significant in this work, principally because we feel it amounts to overfitting the data. The point here is that a physical model or more exhaustive testing could well result in discriminants (such as GOF_EM) that could achieve *greater FA* mitigation. The procedure adopted here, because it is conservative in its assumptions, likely understates the FA mitigation that could actually be achieved.

Last, it should be noted that RFE_EM is only available for declarations that have an EMI contribution and thus is not a usable discriminant for MAG-only declarations. There were 140 FAs for Scenario 1. RFE_EM was available for only 81 of those. Therefore, the true reduction of false alarms would seem to be only

$$\frac{81}{140}(0.16)=9.3\% \quad . \tag{II-7}$$

However, as noted in the scenario 1 performance results section, *all* the MAG-only declarations were false alarms. This suggests mitigating false alarms in this type of scenario by a two-step process.

1. Disregard all declarations for which only magnetometer performance is available,
2. For the remaining declarations, EMI information is available. Apply the RFE_EM discriminant here, reducing FAs, by an additional 16 percent.

Thus, a better estimate of FA mitigation may be

$$\frac{81}{140}(0.16)+\frac{59}{140}=51.4\% \quad . \tag{II-8}$$

3. Scenario 2

We present our analysis of scenario 2, artillery and mortar, in two parts. First, we partition the important data sets to give the essential results of the test. Second, we explore false-alarm mitigation using linear statistical discrimination.

a. Partitions of the Baseline Set and the Declaration Set

Figure II-15 shows the partition of the 123 scenario 2 baseline items. The 73 ordnance are relevant for determining P_D. Similarly, Figures II-17 and II-19 give the P_D- relevant information by sensor.

Figure II-16 shows the partition of the 259 scenario 2 declarations. The 216 declared as ordnance are relevant for detecting the FAs.

Figures II-18 and II-20 give the FA-relevant information by sensor.

Table II-14 shows the explicit relation of the declaration type to the "detected" object (nonbaseline means the object type was not known).

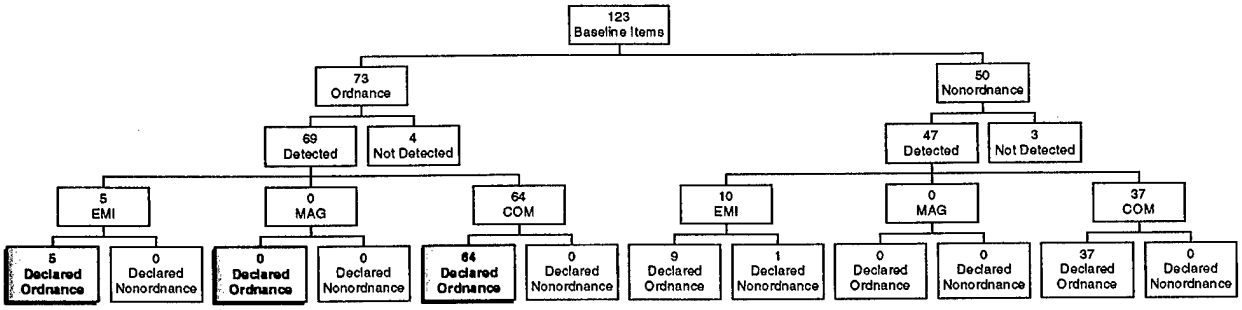

Figure II-15. Partition of the Baseline for the P_D MOE: All Sensor Declarations for the 2nd Scenario, Artillery and Mortar. The yellow boxes (with shadow and bold type) contain the declarations that contribute to P_D. The EMI, MAG, and COM boxes indicate the number of declarations by EMI alone, MAG alone, and by both MAG and EMI (that is, common declarations).

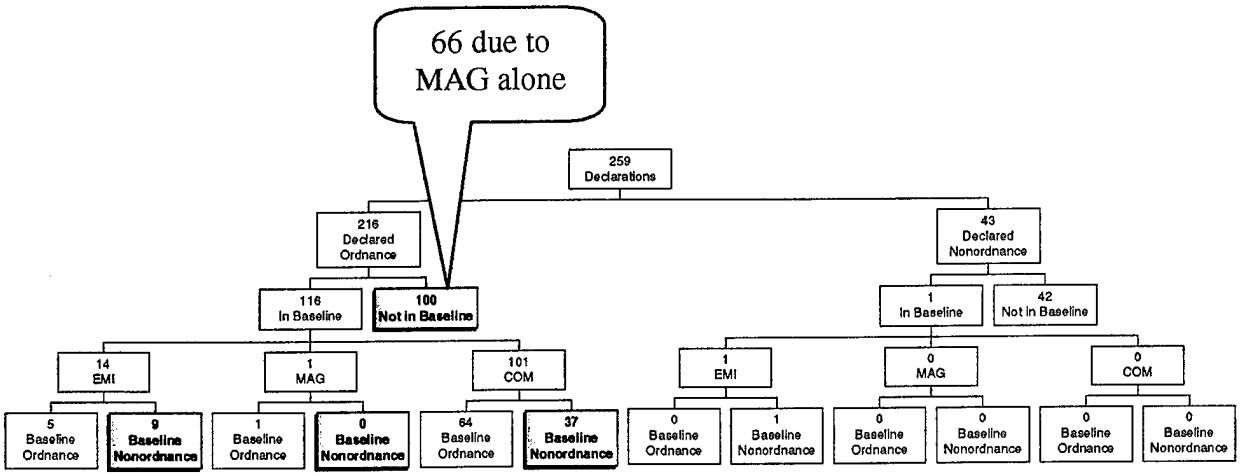

Figure II-16. Partition of the Declarations for the *FAR* MOE: All Sensor Declarations for the 2nd Scenario, Artillery and Mortar. The yellow boxes (with shadow and bold type) contain the declarations that contribute to the *FAR*. The P_{fa} is calculated assuming that an opportunity occurs for every circular area with radius of R_{crit}. A 1-m R_{crit} is used. The EMI, MAG, and COM boxes indicate the number of "detections" achieved by EMI alone, MAG alone, and by both MAG and EMI (that is, common detections).

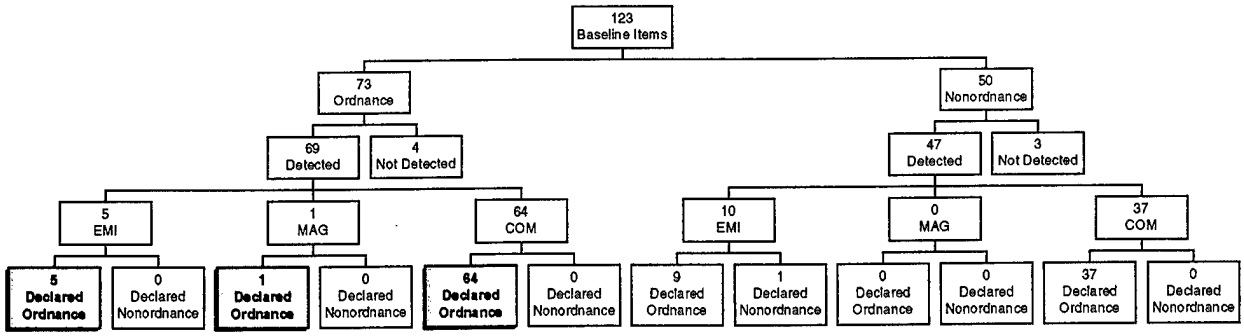

Figure II-17. Partition of the Baseline for the P_D MOE: EMI Declarations for the 2nd Scenario, Artillery and Mortar. The yellow boxes (with shadow and bold type) contain the declarations that contribute to P_D. The EMI, MAG, and COM boxes indicate the number of declarations by EMI alone, MAG alone, and by both MAG and EMI (that is, common declarations).

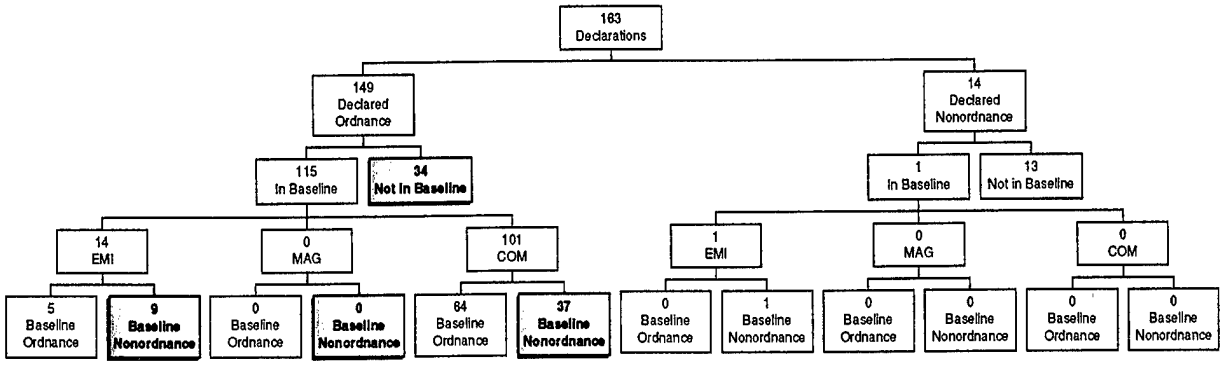

Figure II-18. Partition of the Declarations for the *FAR* MOE: EMI Declarations for the 2nd Scenario, Artillery and Mortar. The yellow boxes (with shadow and bold type) contain the declarations that contribute to the *FAR*. The P_{fa} is calculated assuming that an opportunity occurs for every circular area with radius of R_{crit}. A 1-m R_{crit} is used. The EMI, MAG, and COM boxes indicate the number of "detections" achieved by EMI alone, MAG alone, and by both MAG and EMI (that is, common detections).

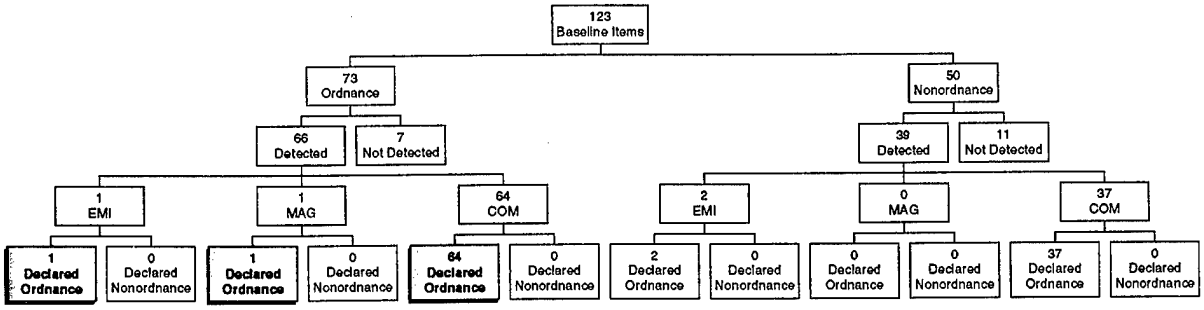

Figure II-19. Partition of the Baseline for the P_D MOE: MAG Declarations for the 2nd Scenario, Artillery and Mortar. The yellow boxes (with shadow and bold type) contain the declarations that contribute to P_D. The EMI, MAG, and COM boxes indicate the number of declarations by EMI alone, MAG alone, and by both MAG and EMI (that is, common declarations).

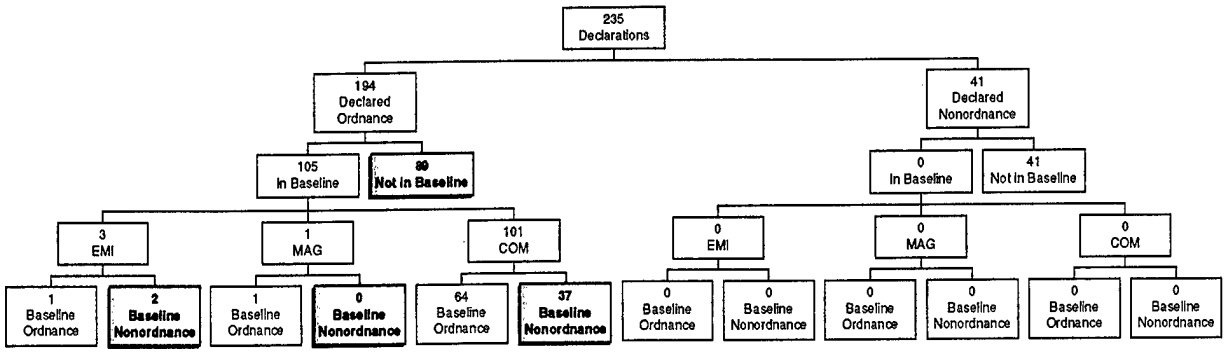

Figure II-20. Partition of the Declarations for the *FAR* MOE: MAG Declarations for the 2nd Scenario, Artillery and Mortar. The yellow boxes (with shadow and bold type) contain the declarations that contribute to the *FAR*. The P_{fa} is calculated assuming that an opportunity occurs for every circular area with radius of R_{crit}. A 1-m R_{crit} is used. The EMI, MAG, and COM boxes indicate the number of "detections" achieved by EMI alone, MAG alone, and by both MAG and EMI (that is, common detections).

Table II-14. Sensor Relation to "Detected" Object Type for Scenario 2 Ordnance Declaration

	Declaration Sensor				Total
	"Detected" Object Type	MAG	Common	EMI	
Declared as Ordnance	Nonbaseline	66	23	11	100
	Nonordnance	0	39	7	46
	Ordnance	1	65	4	70
	Total Declared Ordnance	67	127	22	216
Declared as Nonordnance	Nonbaseline	29	12	1	42
	Nonordnance	0	0	1	0
	Ordnance	0	0	0	0
	Total Declared Nonordnance	29	12	2	43

b. False-Alarm Mitigation: Correlation and Discriminant Analysis

As for scenario 1, this section puts forward a simple discriminant analysis for the MTADS declarations that the NRL analysts believed were ordnance. The aim is to identify promising means of reducing the *FAR*. Again, we use Fisher's linear discriminant.

As before, the redundant variables, magnetic moment (correlated with radius) and nonferrous size (correlated with ferrous size), are eliminated from the analysis. Table II-15 shows an initial survey of the correlations. Table II-15 is constructed from the 127 observations for which all variables were available. Figure II-21 shows scatterplots of the

MAG variables; Figure II-22, the EMI variables; and Figure II-23, the EMI versus the magnetometer variable. Figures II-24 and II-25 give histograms of the variables to provide a readable scale.[4]

Table II-15. Correlation of Scenario 2 Variables. 103 Declarations for Which all Data Were Available

	ZMAG	ZEM	RMAG	RFE_EM	INCLIN	AZIM	GOF_MAG	GOF_EM
ZMAG	1							
ZEM	0.605	1						
RMAG	0.572	0.38	1					
RFE_EM	0.461	0.777	0.631	1				
INCLIN	0.272	0.029	-0.112	-0.034	1			
AZIM	-0.104	-0.098	0.074	0.077	-0.242	1		
GOF_MAG	-0.323	-0.206	0.198	0.139	-0.361	0.181	1	
GOF_EM	-0.085	0.014	0.224	0.448	0.044	0.001	0.33	1

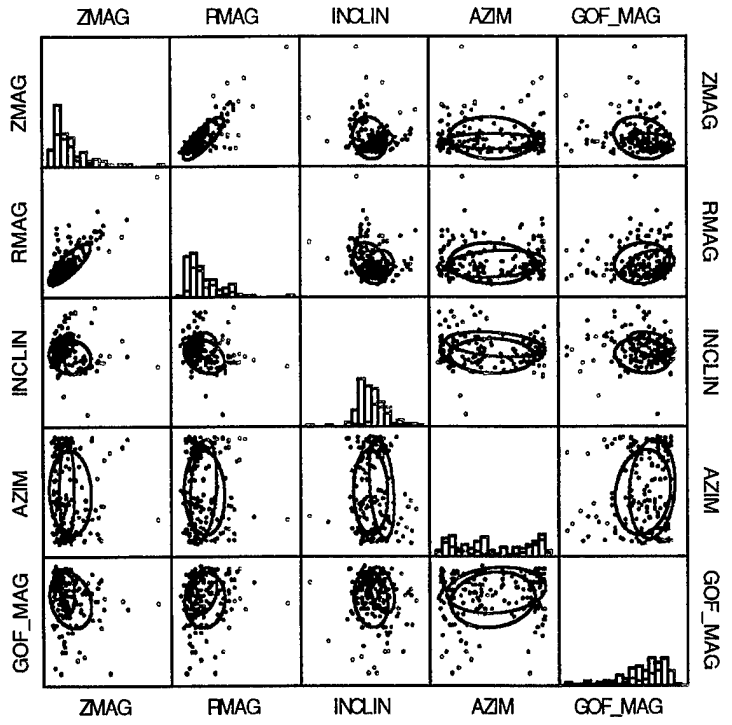

Figure II-21. Scenario 2 Correlation of Magnetometer Variables. Blue indicates false alarms. Red indicates detections. 50-percent ellipses are shown.

4 The bins are not exactly the same as for the scatterplots, giving some height variations relative to the columns shown in Figures II-16 through II-17.

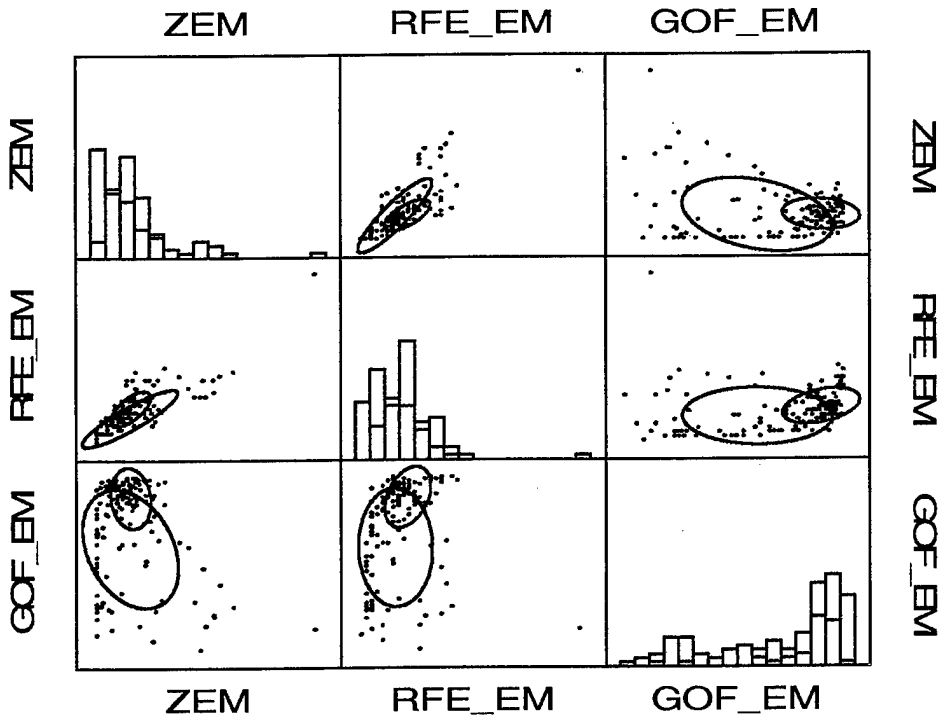

Figure II-22. Scenario 2 Correlation of EMI Variables. Blue = False Alarms. Red = Detections. 50-percent ellipses are shown.

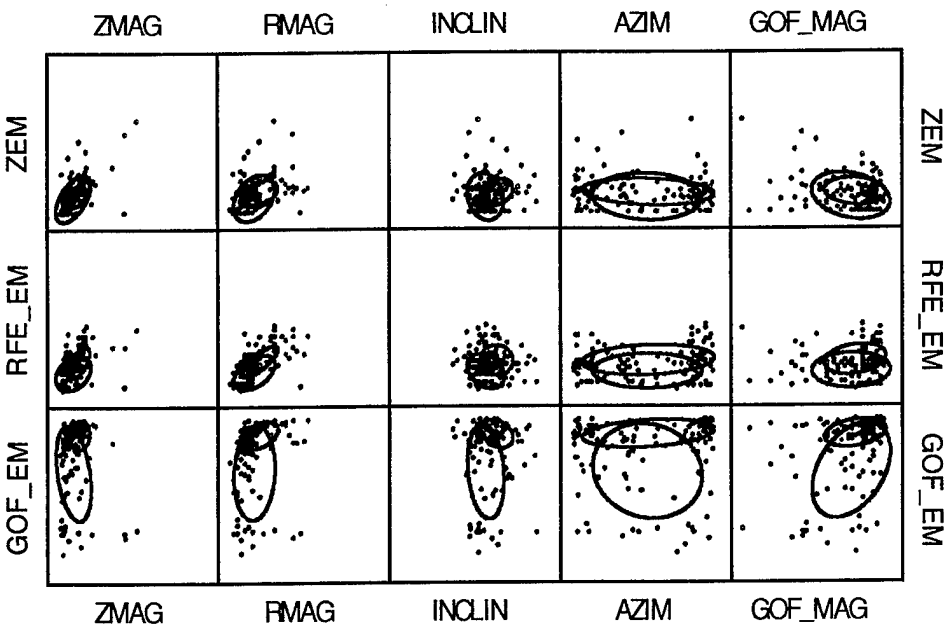

Figure II-23. Scenario 2 Correlation of EMI Variables with Magnetometer Variables. Red = Detections. Blue = False Alarms. 50-percent ellipses are shown.

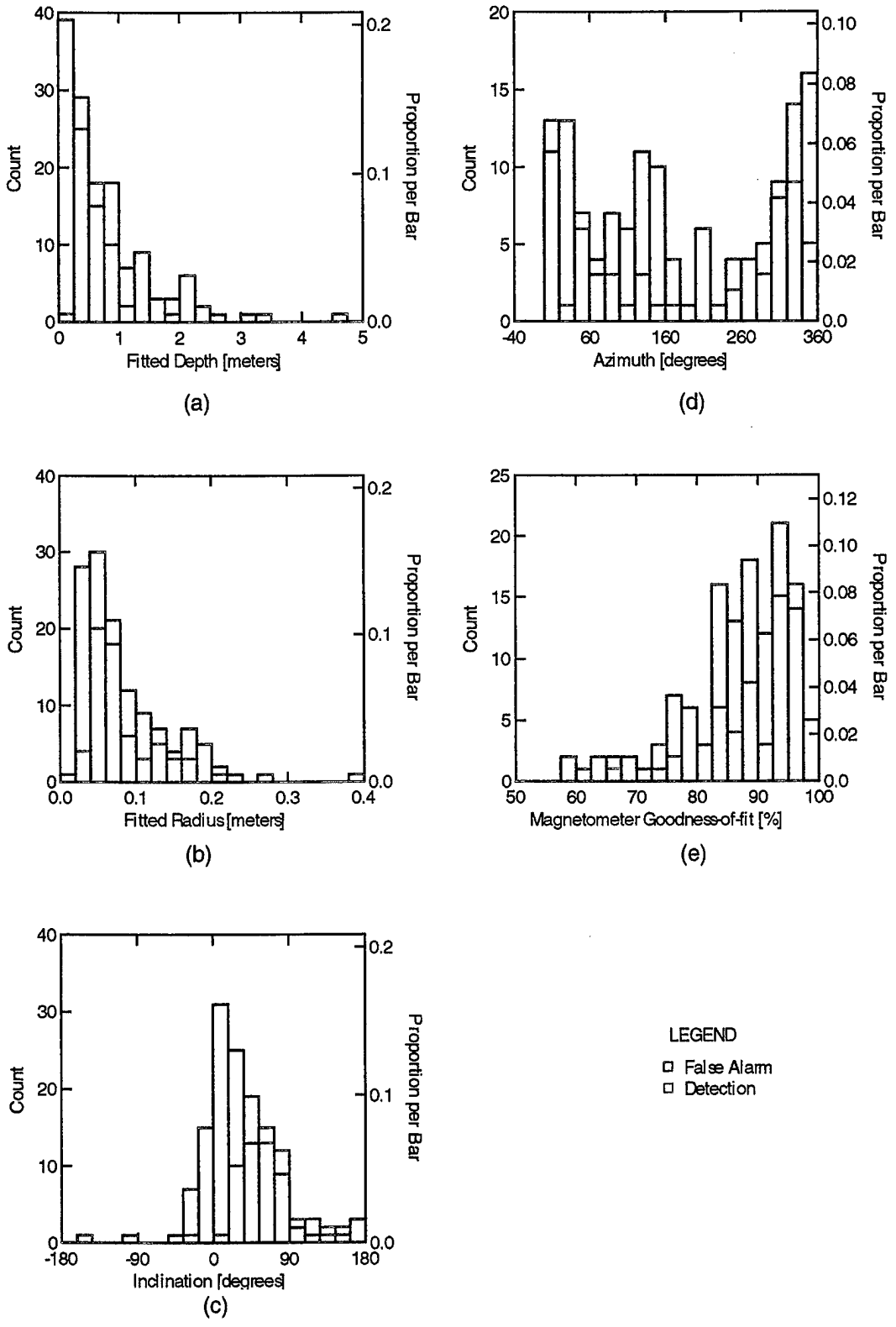

Figure II-24. Scenario 2 MAG Histograms

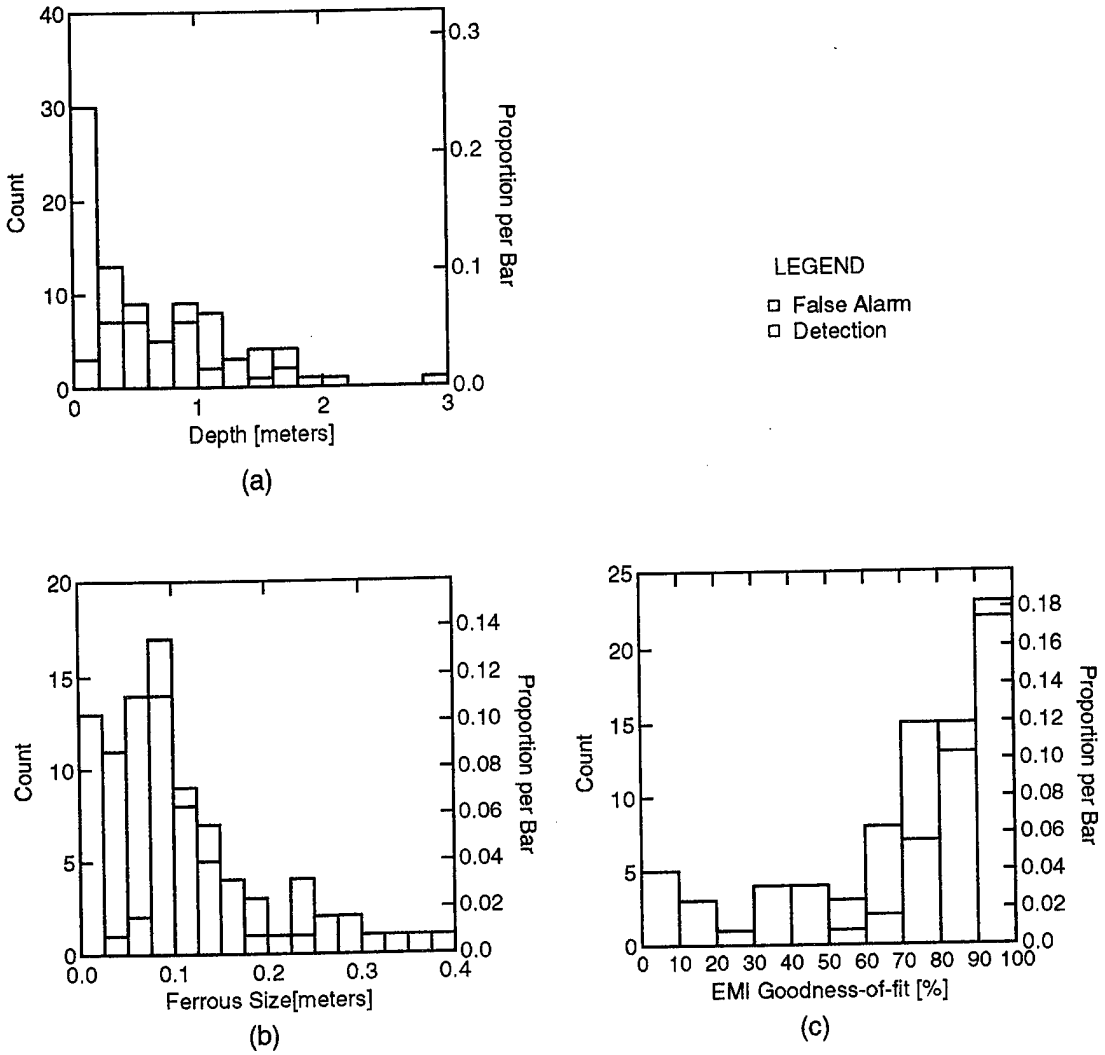

Figure II-25. Scenario 2 EMI Histograms

The discriminant analysis produces a linear combination of the statistically significant variables. It is defined as

$$\text{Factor} = -5.254 + 1.111\ \text{ZMAG} + 0.015\ \text{INCLIN} + 0.051\ \text{GOF\_EM} \quad . \qquad \text{(II-9)}$$

Figure II-26 is a histogram of detections and false alarms. Of the 62 false alarms for which all the variables were available, 37 could have been eliminated by adopting Factor = –0.50 as a threshold and regarding all declarations below this as nonordnance. This scheme could reduce this set of FAs by 60 percent (37/62).

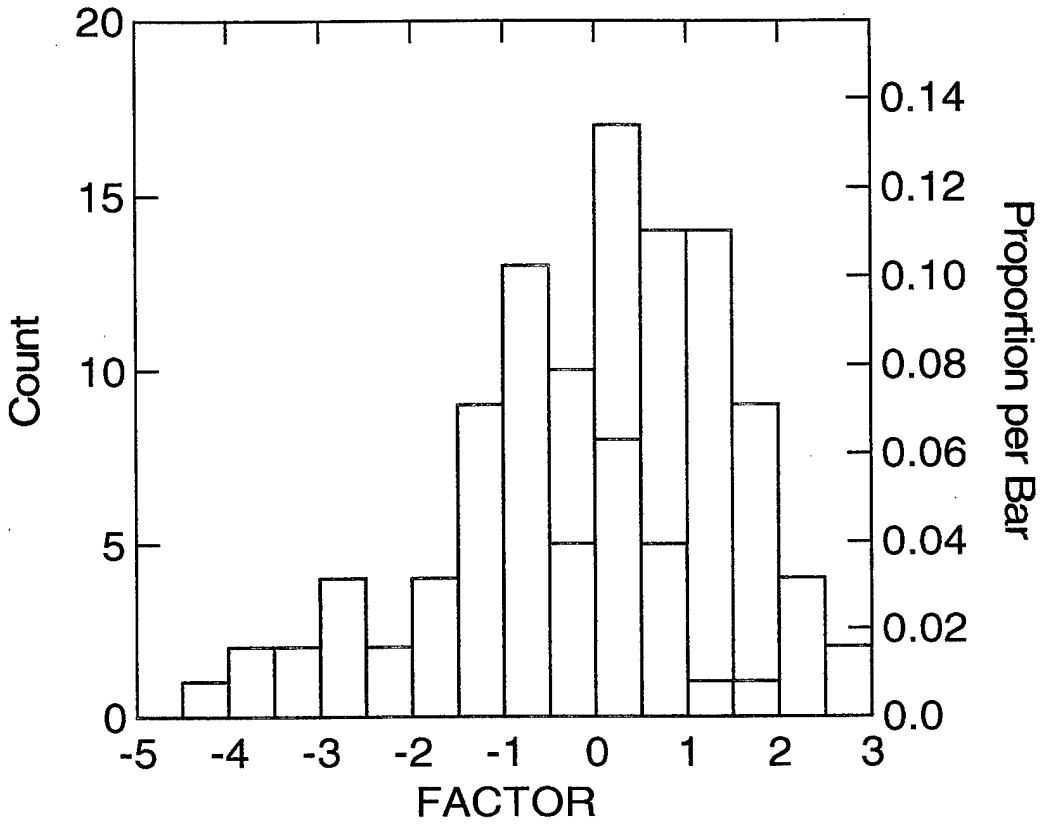

Figure II-26. Scenario 2 Discriminant for Common Declarations.
Factor is defined in Eq. II-9.

Figure II-27 provides another illustration of the interplay of these variables. The declarations of ordnance that were fitted to be deeper, with more negative inclination, and a poorer EMI GoF were more likely to be false alarms. These are the blue squares in Figure II-27; they tend to be in the octant that is lower and toward the viewer. The threshold on Factor corresponds to a plane in Figure II-27 (not shown) that best separates the false alarms from the detections.

This reduction is only applicable for those FAs for which both EMI (its GoF) and MAG (inclination and fitted depth) information is available. A separate discriminant analysis follows for those cases in which only EMI or only MAG data are obtained.

For MAG-only, there were 67 declarations, 66 of which were false alarms. With only one detection the statistics are too poor to find a good discriminant in this case.

Thus, the best estimate of achievable *FAR* reduction is

$$\frac{1}{146}(62\times 60\% + 66\times 0\% + 18\times 0\%) = 25.5\% \quad . \qquad \text{(II-10)}$$

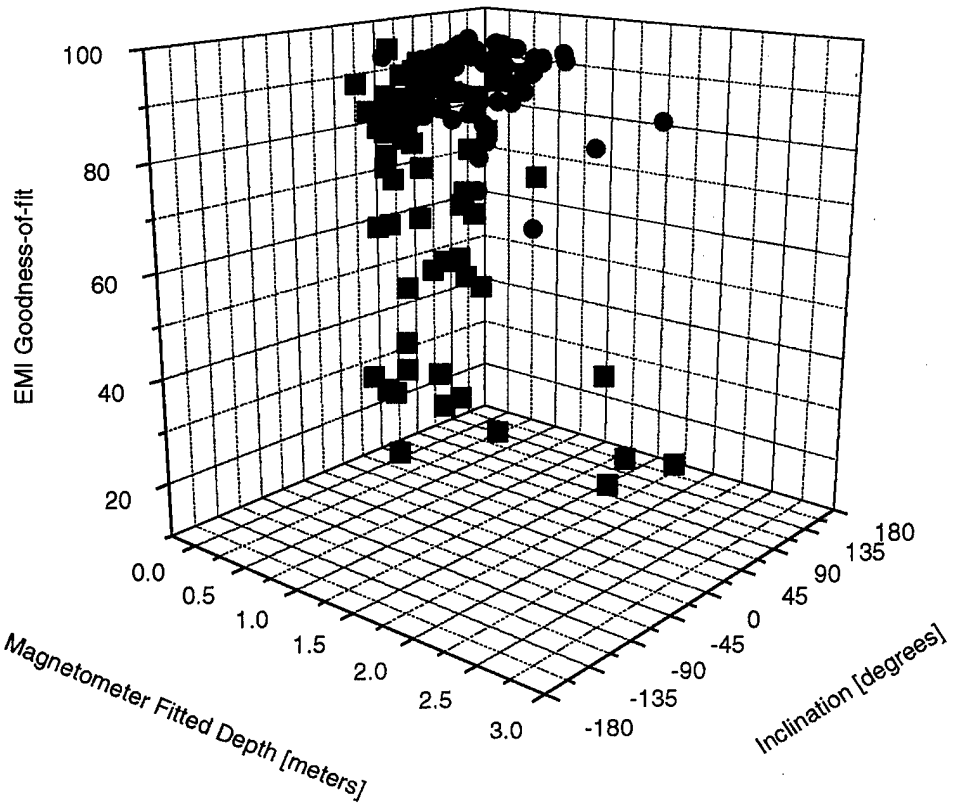

Figure II-27. Dependence of Detections and False Alarms on Variables in the Discriminant for Declarations Common to the Magnetometer and EMI for Scenario 2.
Blue Cubes = False Alarms. Red Spheres = Detections.

The weights derive from the 62 common, 66 MAG-only, and the 18 EMI-only false alarms.

3. Scenario 3

We present our analysis of scenario 3, submunitions and grenades, in two parts. First, we partition the important data sets to give the essential results of the test. Second, we explore false-alarm mitigation using linear statistical discrimination.

a. Partitions of the Baseline Set and the Declaration Set

Figure II-28 shows the partition of the 124 scenario 3 baseline items. The 86 ordnance are relevant for determining P_D. Similarly, Figures II-30 and II-32 give the P_D-relevant information by sensor. Figure II-29 shows the partition of the 222 scenario 3 declarations. The 215 declared ordnance are relevant for determining the FAs. Similarly, Figures II-31 and II-33 give the FA-relevant information by sensor.

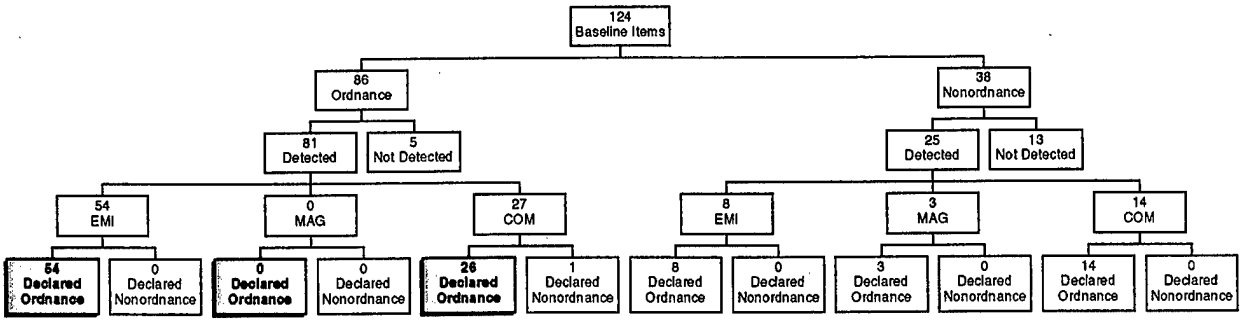

Figure II-28. Partition of the Baseline for the P_D MOE: All Sensor Declarations for the 3rd Scenario, Submunitions and Grenades. The yellow boxes (with shadow and bold type) contain the declarations that contribute to P_D. The EMI, MAG, and COM boxes indicate the number of *declarations* by EMI alone, MAG alone, and by both MAG and EMI (that is, common declarations).

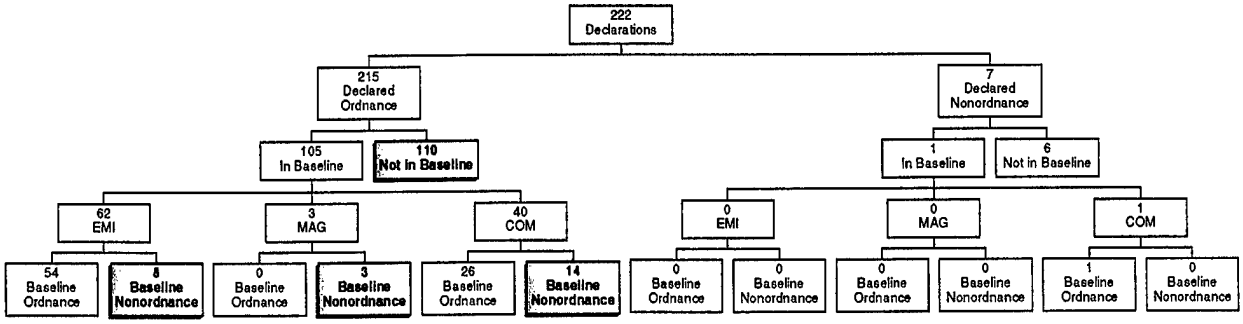

Figure II-29. Partition of the Declarations for the *FAR* MOE: All Sensor Declarations for the 3rd Scenario, Submunitions and Grenades. The yellow boxes (with shadow and bold type) contain the declarations that contribute to the *FAR*. The P_{fa} is calculated assuming that an opportunity occurs for every circular area with radius of R_{crit}. A 1-m R_{crit} is used. The EMI, MAG, and COM boxes indicate the number of "detections" achieved by EMI alone, MAG alone, and by both MAG and EMI (that is, common detections).

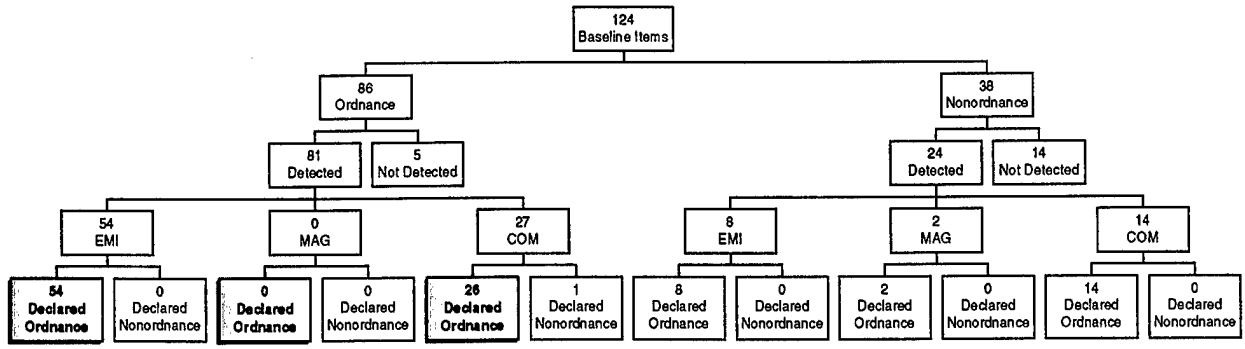

Figure II-30. Partition of the Baseline for the P_D MOE: EMI Declarations for the 3rd Scenario, Submunitions and Grenades. The yellow boxes (with shadow and bold type) contain the declarations that contribute to P_D. of declarations by EMI alone, MAG alone, and by both MAG and EMI (that is, common declarations).

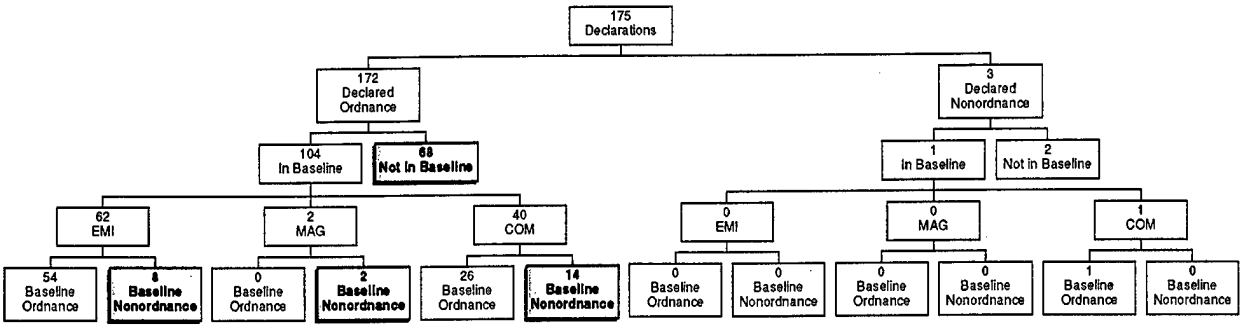

Figure II-31. Partition of the Declarations for the *FAR* MOE: EMI Declarations for the 3rd Scenario, Submunitions and Grenades. The yellow boxes (with shadow and bold type) contain the declarations that contribute to the *FAR*. The P_{fa} is calculated assuming that an opportunity occurs for every circular area with radius of R_{crit}. A 1-m R_{crit} is used. The EMI, MAG, and COM boxes indicate the number of "detections" achieved by EMI alone, MAG alone, and by both MAG and EMI (that is, common detections).

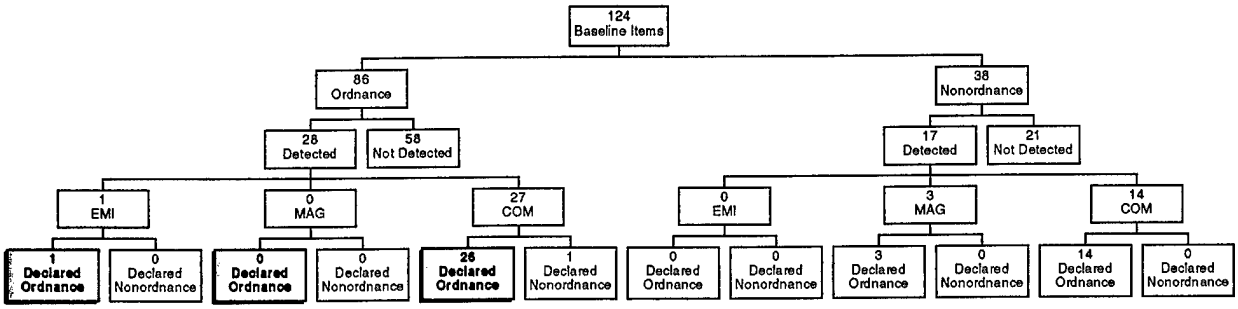

Figure II-32. Partition of the Baseline for the P_D MOE: MAG Declarations for the 3rd Scenario, Submunitions and Grenades. The yellow boxes (with shadow and bold type) contain the declarations that contribute to P_D. The EMI, MAG, and COM boxes indicate the number of *declarations* by EMI alone, MAG alone, and by both MAG and EMI (that is, common declarations).

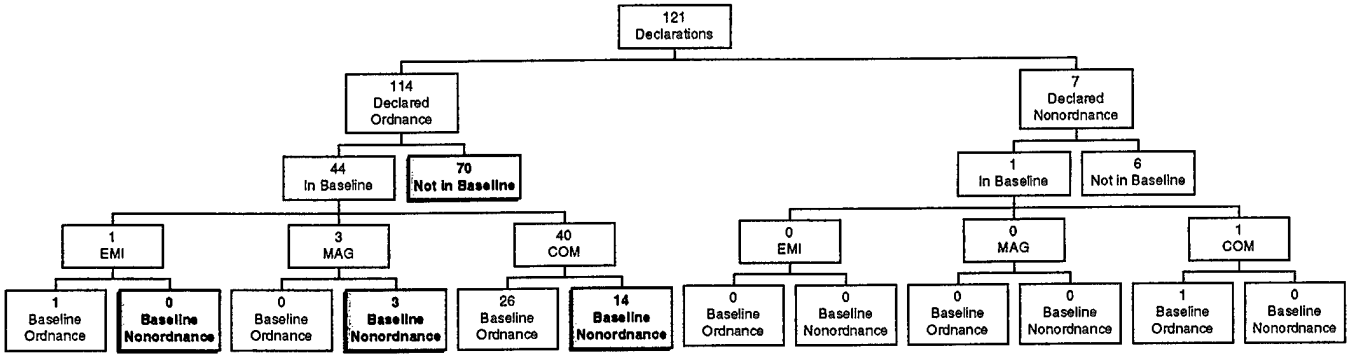

Figure II-33. Partition of the Declarations for the *FAR* MOE: MAG Declarations for the 3rd Scenario, Submunitions and Grenades. The yellow boxes (with shadow and bold type) contain the declarations that contribute to the *FAR*. The P_{fa} is calculated assuming that an opportunity occurs for every circular area with radius of R_{crit}. A 1-m R_{crit} is used. The EMI, MAG, and COM boxes indicate the number of **detections** achieved by EMI alone, MAG alone, and by both MAG and EMI (that is, common detections).

Table II-16 shows the relation of declaration type to the "detected" object (nonbaseline means the object, if there was one, was not known).

Table II-16. Sensor Relation to "Detected" Object Type for Scenario 3 Ordnance Declarations[a]

		Declaration Sensor			Total
	"Detected" Object Type	MAG	Common	EMI	
Declared as Ordnance	Nonbaseline	42	28 (25)[a]	40	110 (107)[a]
	Nonordnance	1	16	8	25
	Ordnance	0	27	53	80
	Total Declared Ordnance	43	71 (68)[a]	101	215
Declared as NonOrdnance	Nonbaseline	4	2	0	6
	Nonordnance	0	1	0	1
	Ordnance	0	0	0	0
	Total Declared Ordnance	4	3	0	7

[a] Two of these declarations, 3/K12/1 and 3/L9/3 had only EMI and MAG data for the Easting and Northing coordinates, but no data for any other variables (RMAG, RFE_EM, etc.) A third declaration, 3/H13/2, had only EMI variables information in addition to the Easting and Northing Coordinates.

b. False Alarm Mitigation: Correlation and Discriminant Analysis

This section constitutes a discriminant analysis for scenario 3, similar to that already given for scenario 1 and 2. Two variables are not examined because they are highly correlated (that is, redundant) with others: magnetic moment (correlated with radius) and nonferrous size (correlated with ferrous size). Table II-17, an initial survey of the correlations, is constructed from the 68 observations for which all variables were available.[1] Scatterplots are shown in Figures II-28 through II-30, for MAG, EMI, and EMI versus MAG, respectively. The scale and detail are more easily apprehended on separate histograms, shown in Figures II-31 and II-32.[2]

---

1 Except for *x–y* position, variables were not available for the two declarations with NRL cell assignments and object numbers K12 #1 and L9 #3. For the H13 #2 declaration, EMI variables were available, although magnetometer ones were not. These three delcarations added to the 68 noted in the text above gave the 71 total common declarations for scenario 3, as noted earlier in this document.

2 The bin widths and locations of the histogram in Figure II-31 and II-32 do not coincide with those in Figures II-28 through II-30. This produces a small difference in the column heights.

Table II-17. Correlation of Scenario 3 Variables. All information was available for 68 declarations.

	ZMAG	ZEM	RMAG	RFE_EM	INCLIN	AZIM	GOF_MAG	GOF_EM
ZMAG	1							
ZEM	0.413	1						
RMAG	0.433	0.439	1					
RFE_EM	0.19	0.788	0.482	1				
INCLIN	-0.014	-0.102	-0.479	-0.067	1			
AZIM	0.065	-0.046	0.064	0.04	-0.166	1		
GPF_MAG	-0.029	0.187	0.35	0.195	-0.147	-0.0706	1	
GOF_EM	-0.049	0.292	0.227	0.736	0.047	0.139	0.166	1

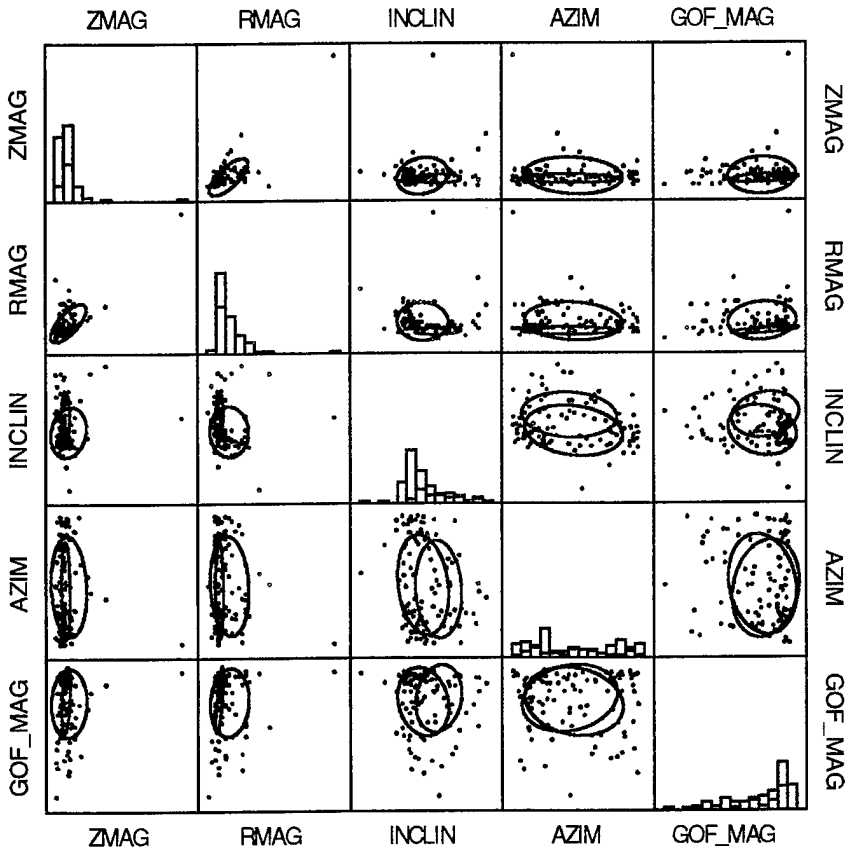

Figure II-28. Scenario 3 Correlation of Magnetometer Variables.
Blue indicates False Alarms. Red indicates Detections
50-percent ellipses are shown.

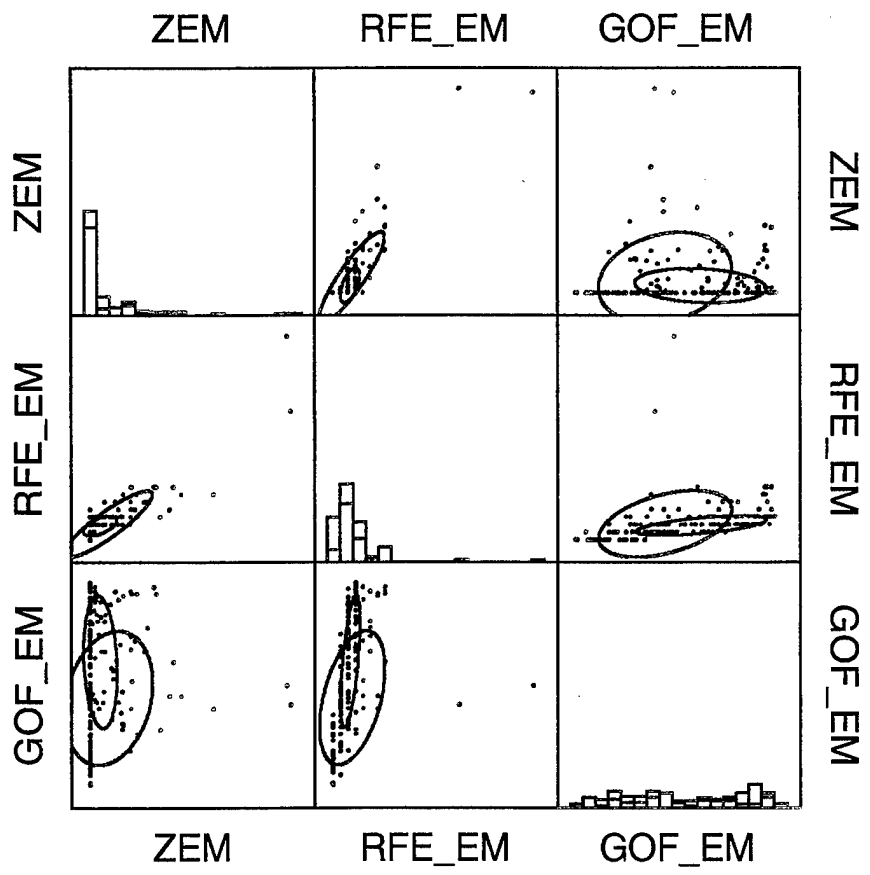

Figure II-29. Scenario 3 Correlation of EMI Variables.
Blue = False Alarms. Red = Detections.
50-percent ellipses are shown.

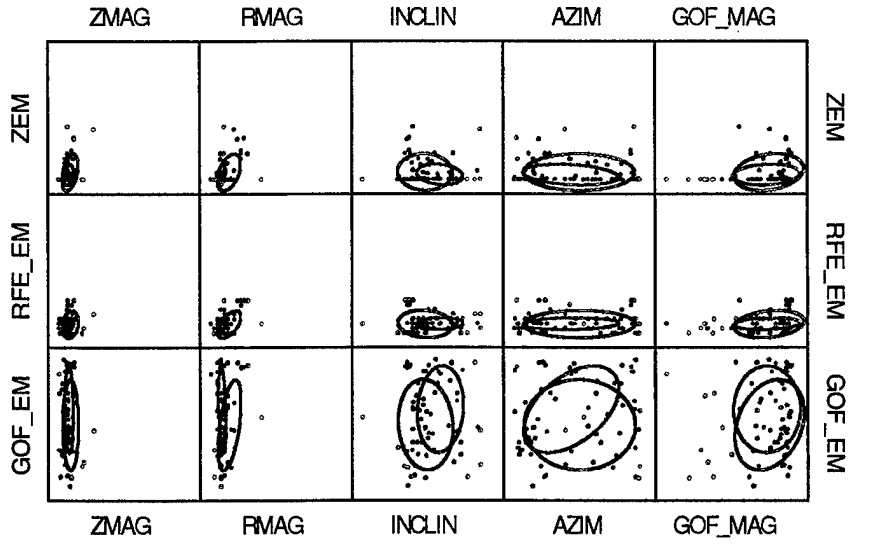

Figure II-30. Scenario 3 Correlation of EMI Variables with Magnetometer Variables.
Red = Detections. Blue = False Alarms. 50-percent ellipses are shown.

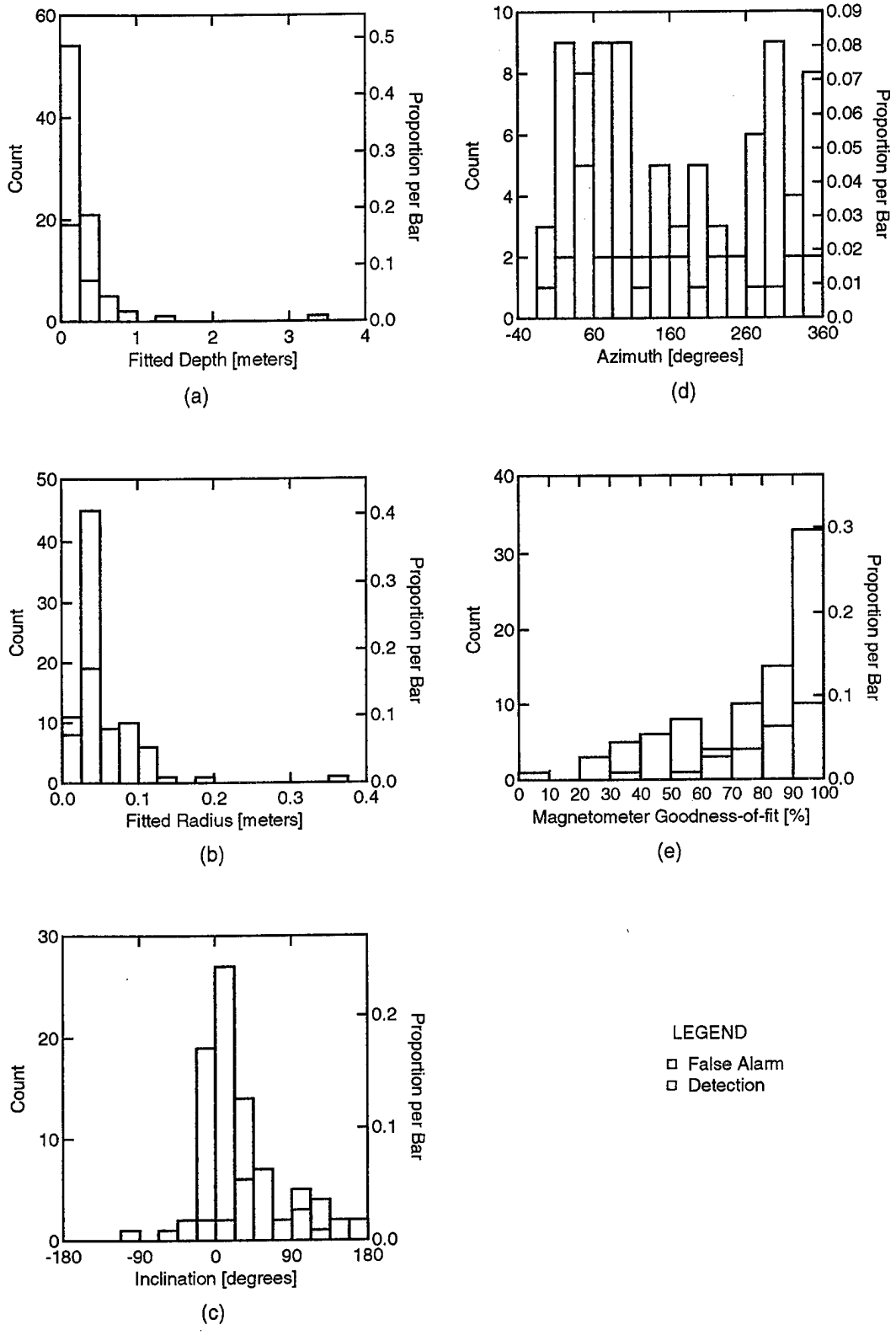

Figure II-31. Scenario 3 MAG Histograms

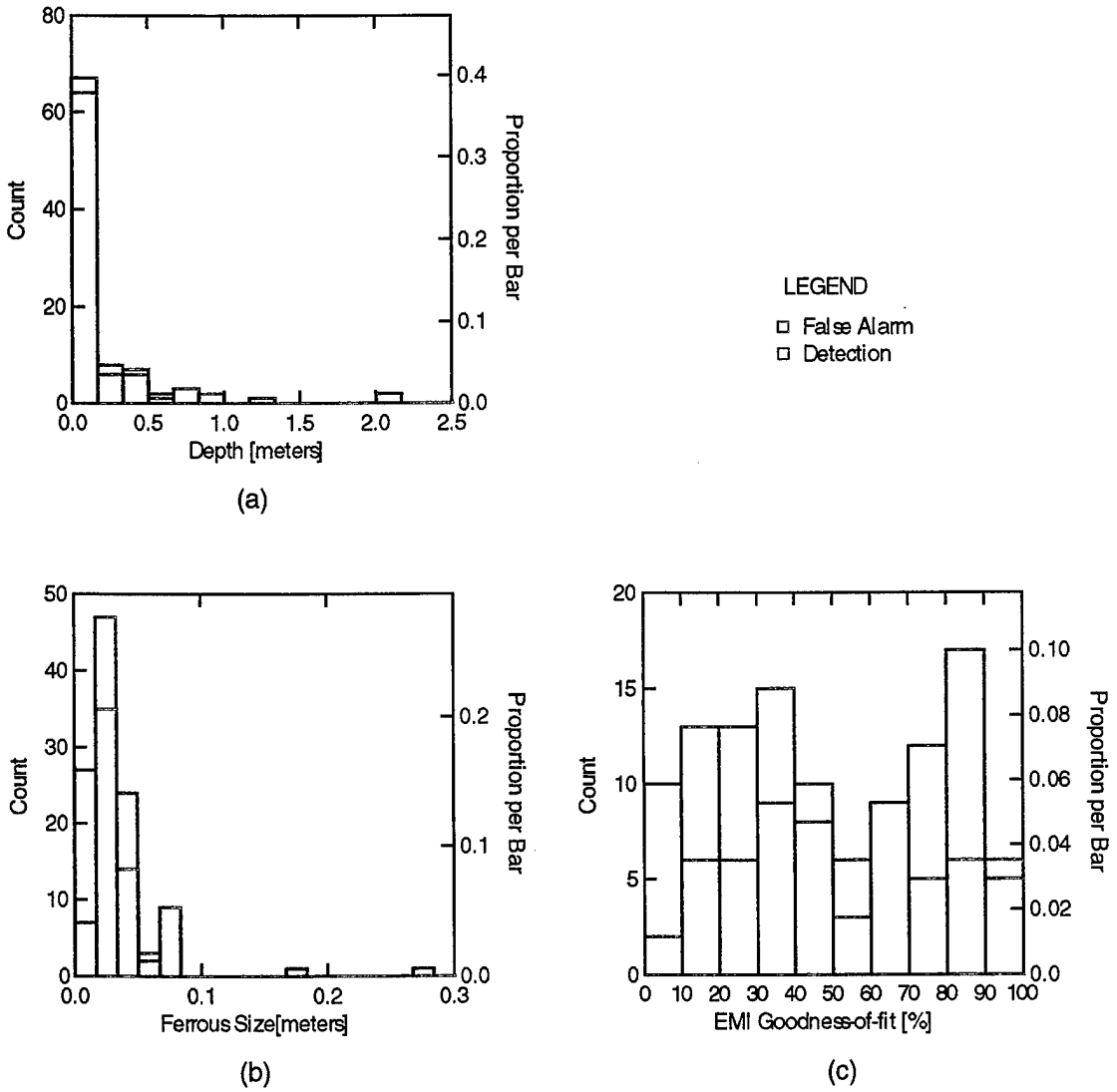

Figure II-32. Scenario 3 EMI Histograms

Statistical analysis produced the following linear discriminant:

$$\text{Factor} = 0.512 - 43.691\ \text{RMAG} + 0.025\ \text{GOF\_EM}\ . \qquad \text{(II-11)}$$

Figure II-30 shows a histogram of detections and false alarms as a function of this discriminant. Using a threshold of −1 would have given a *FAR* reduction of 32 percent (13/41) for the 41 false alarms for which all information was available. Figure II-34 shows the interplay of the magnetometer-determined radius of ordnance (RMAG) and the EMI GoF (GOF_EM). The main contribution is from the magnetometer radius. Indeed, a threshold on RMAG of just above 0.05 meters reduces the *FAR* by 41 percent. Further investigation of these declarations (EMI GoF = 16 percent for NRL declaration K9 #7 and EMI GoF = 0 percent for NRL declaration K9 #8) is merited, but is deferred to future

work. Without understanding these points better, we must conclude that RMAG alone is the better discriminant. A histogram for RMAG is shown in Figure II-35.

Two declarations at larger radii (0.18 m and 0.37 m) in Figure II-31(b) do not appear in Figures II-33, II-34, and II-35 because they were from magnetometer-only declarations: no EMI GoF was available for them. Incorporating the additional 43 declarations with only RMAG data (that is, without EMI GoF data) gives a 33-percent (28/84) *FAR* reduction, as shown in Figure II-36.

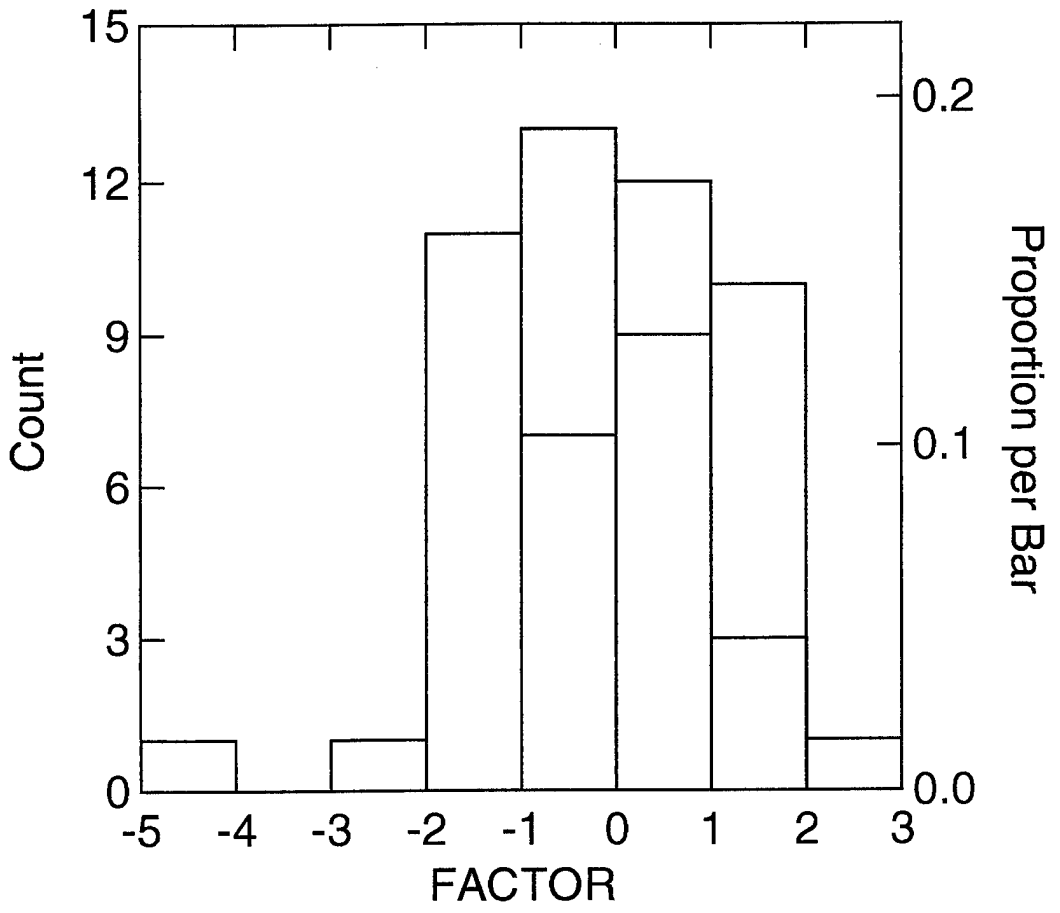

Figure II-33. Scenario 3 Discriminant for Common Declarations.
Factor is defined in Eq. II-11.

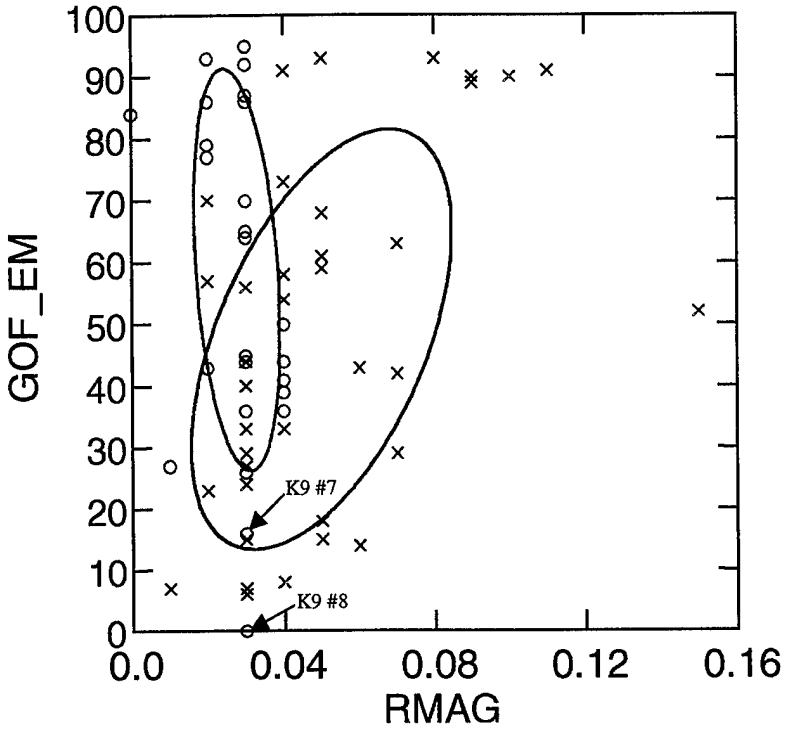

Figure II-34. Scenario 3 Detections and False Alarms as a Function of RMAG and EMI GoF. EMI GoF outliers are labeled by their NRL-assigned cell and object numbers. Red = Detection. Blue Crosses = False Alarms. 50-percent ellipses are shown.

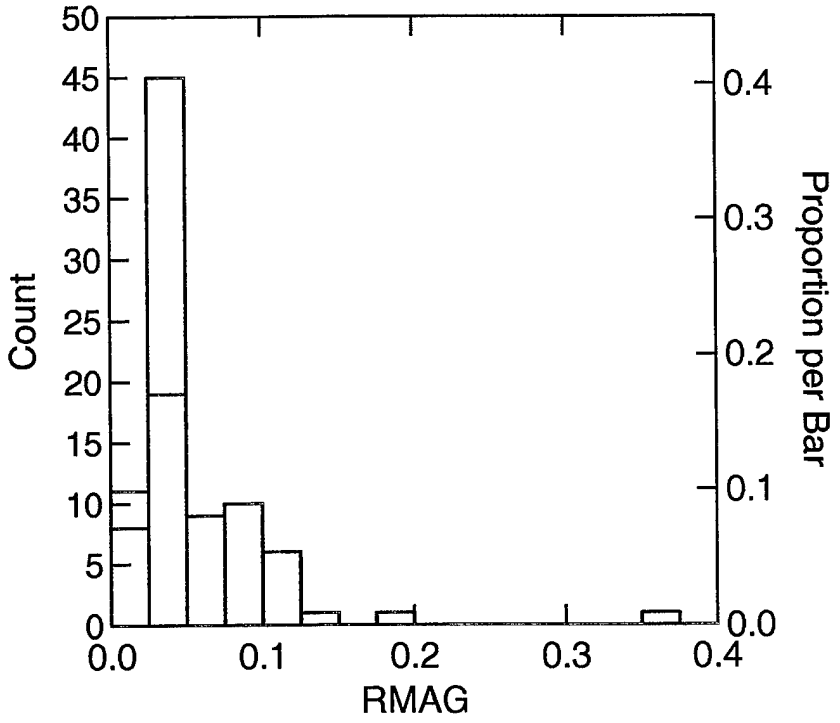

Figure 35. Scenario 3 Detections and False Alarms as a Function of RMAG For These Detections

There is one further interesting item to note regarding the use of the magnetometer-fitted radius as a criterion for mitigating false alarms: one of the missed detections had a large fitted radius. Of the 222 declarations in the third scenario, only 7 were declared nonordnance by NRL. One of those was the MTADS declaration in NRL–assigned cell L9 and number 1 (within the cell). This declaration, by both MAG and EMI, was actually a 155-mm projectile, the only 155-mm projectile in this scenario. This 155-mm projectile arguably may not fit within the ordnance class of submunitions and grenades that the operators were led to expect. The other three 155 projectiles were all in the second scenario, artillery and mortar.

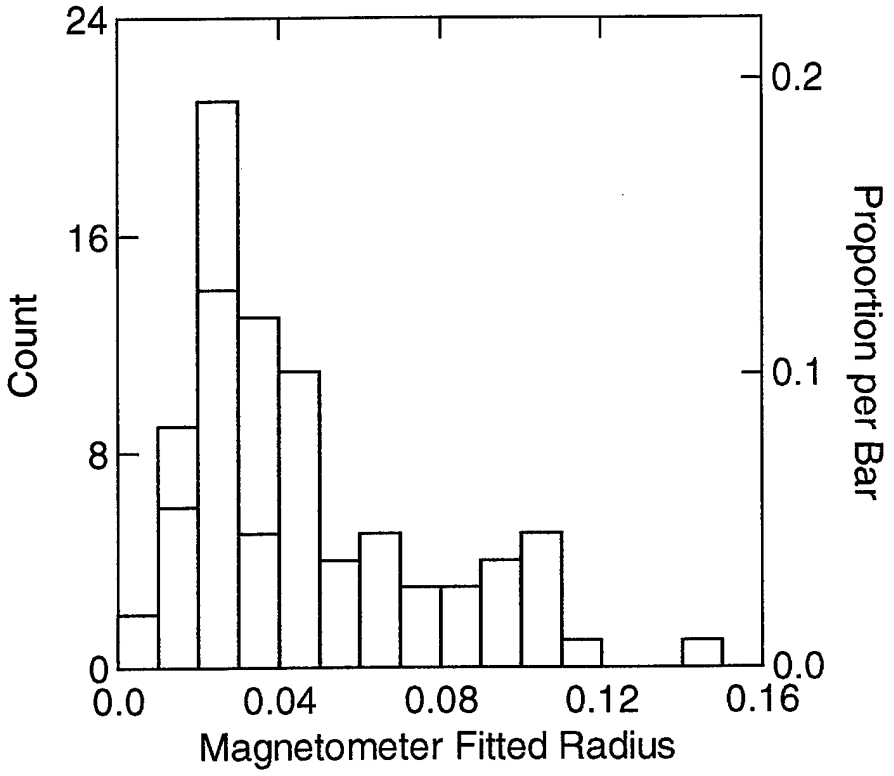

Figure II-36. Scenario 3 Ordnance Radius from the Magnetometer Fit.
This is a histogram of those declarations as ordnance for which there was also EMI data. Red indicates detections. Blue indicates false alarms.

Returning to the subject of FAs, one can make further progress by following the same path as in scenario 1. For the common declarations, a nominal 41-percent *FAR* reduction was derived by using a threshold on RMAG. For the declarations which had only MAG data (that is, for which no EMI data were available), *all* the declarations were false alarms. A possible mitigation strategy is then to simply discount all declarations (in this scenario) for which one has only MAG data.

Doing so leaves the declarations with only EMI data. There are 101 such declarations with x–y (Easting-Northing) coordinates supplied from only the EMI. There is one more declaration that has x–y coordinates from both MAG and EMI, but has fit results for only EMI. That declaration, 3/H13/2, is also incorporated in this discriminant. The statistically significant discriminant turns out to be the EMI goodness-of-fit (GOF_EM). A histogram (Figure II-37) shows that no significant *FAR* reduction can be expected in this case.

Thus, the truest estimate of *FAR* reduction is

$$\frac{1}{135}(41\times 41\% + 2\times 0\% + 49\times 0\%. + 43\times 100\%) = 44.3\% \quad . \qquad \text{(II-12)}$$

The weights in this expression arise from 41 (of 44) common false alarms for which EMI and MAG variables are available, 2 for which no variables are available, 49 which have only EMI variables available (48 EMI declarations plus 1 common declaration), and 43 which have only MAG information available.

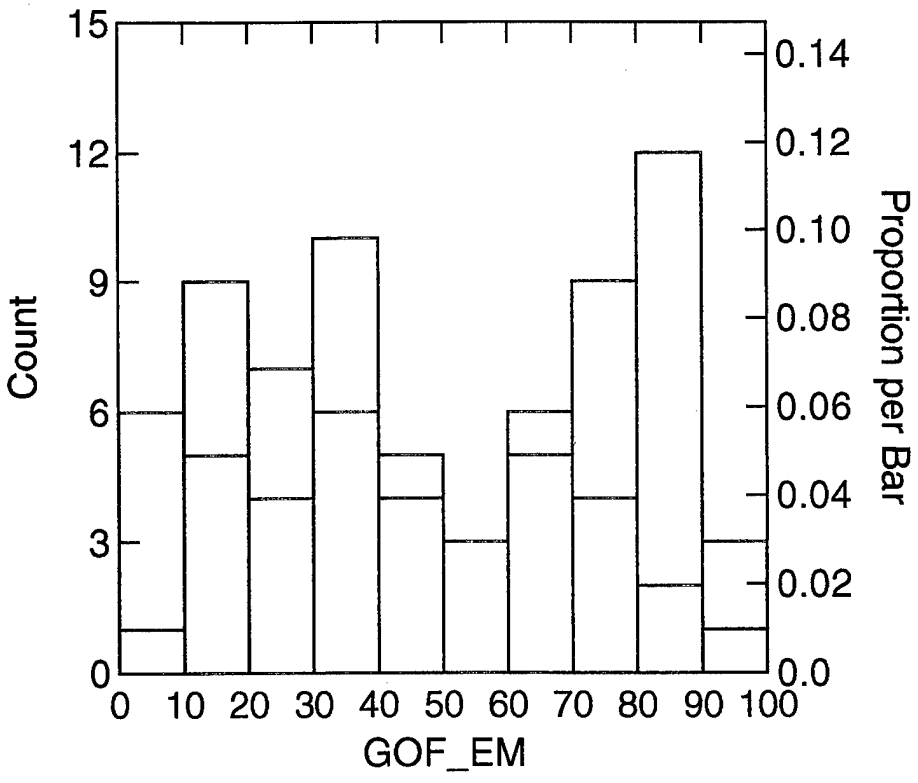

Figure II-37. Scenario 3 EMI GoF for the EMI-only Declarations.
Red indicates detections. Blue indicates false alarms.

C. SENSOR PERFORMANCE

In this section, the MTADS location performance for detected ordnance is characterized by evaluating the detection parameters and determining trends. Using the critical radius of 1 m, as before, 121 of the 206 ordnance items were detected by the magnetometer, while 194 of 206 were detected by EMI. These detected ordnance are examined in greater detail in this section.

1. Performance Dependence on Critical Radius

P_D, FAR, and P_{fa} all depend on R_{crit}. The dependence of P_D is clearest. As the area awarded to each detection is increased, P_D increases. Were the distribution of ordnance random with respect to the declarations, P_D would scale as the square of R_{crit} for low density of ordnance. This is not true because the coordinates of declarations and ordnance are highly correlated, which is of course the whole point in using a sensor such as MTADS and not just drawing guesses from a hat. Rather, declarations are either "close" to ordnance, say within a meter, or are "far" from ordnance, in which case some other physical aspect of the site is causing the UXO-like signal. That is, there is unaccounted-for clutter, not "noise" per se.

Figure II-38 shows the dependence of P_D on R_{crit} for the EMI declarations. Figure II-39 shows the P_D dependence for the MAG declarations. The EMI has generally higher P_D especially for larger R_{crit}. Table II-18 gives the mean and standard deviation of the radial location accuracy and the depth accuracy (signed and absolute value). The EMI system exhibits the best location accuracy, but also shows the largest depth error.

2. Radial Location Accuracy

For each sensor declaration that matched an emplaced ordnance item, the coordinates of the MTADS fit are recorded. The radial location error is computed: radial location error = fit location – actual location of detected ordnance.

a. Electromagnetic Induction

For the EMI, the mean radial location accuracy was 0.53 m with a standard deviation of 0.15 m (see Table II-18). Figure II-40 shows the distribution of EMI radial error.

Table II-18. Detection Location Error and Depth Error for 1-m Critical Radius

Scenario	Sensor	Radial		Depth		Magnitude Depth	
		Error (m)	Standard Deviation (m)	Error (m)	Standard Deviation (m)	Error (m)	Standard Deviation (m)
1	Magnet-ometer	0.43	0.15	0.28	0.14	0.28	0.14
	EMI	0.48	0.16	0.16	0.24	0.24	0.17
2	Magnet-ometer	0.48	0.16	0.22	0.17	0.22	0.16
	EMI	0.48	0.11	0.14	0.20	0.19	0.16
3	Magnet-ometer	0.62	0.12	0.09	0.08	0.11	0.06
	EMI	0.59	0.16	–0.06	0.13	0.12	0.07
All	Magneto meter	0.50	0.16	0.21	0.16	0.21	0.15
	EMI	0.53	0.15	0.07	0.21	0.17	0.14

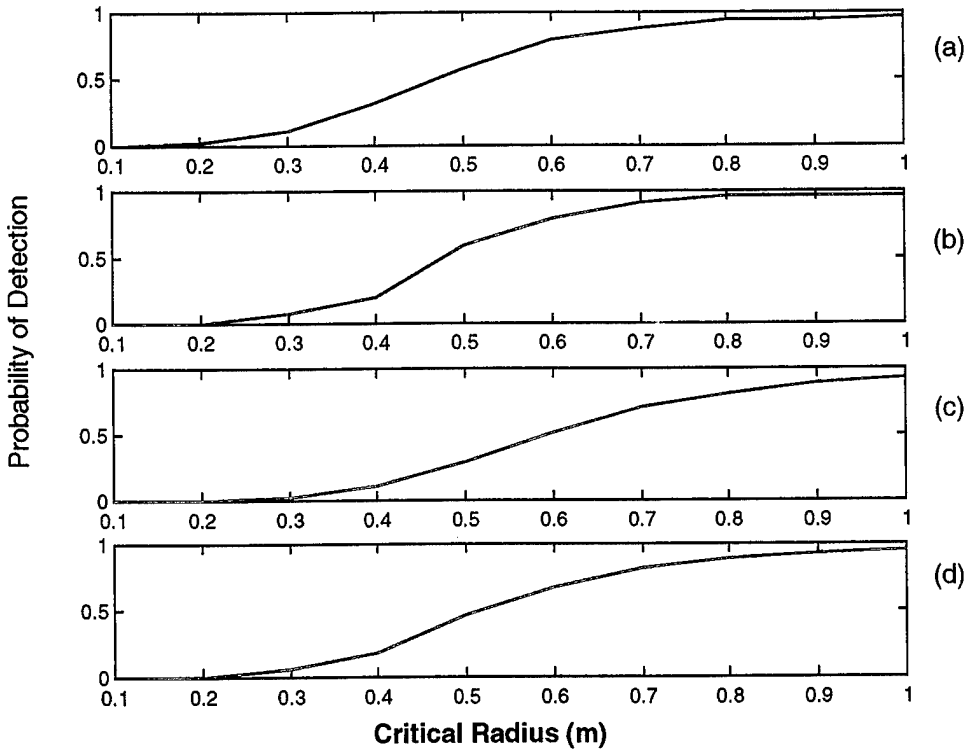

Figure II-38. EMI Detection Performance vs. Critical Radius.
(a) Scenario 1, Aerial Gunnery, (b) Scenario 2, Artillery and Mortar, (c) Scenario 3, Submunitions and Grenades, (d) All Scenarios.

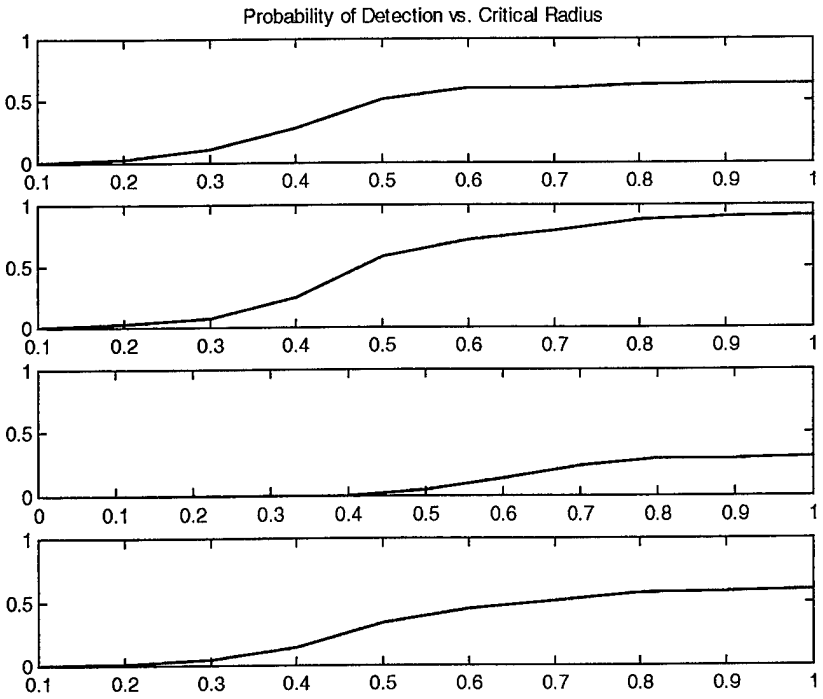

Figure II-39. MAG Detection Performance vs. Critical Radius.
(a) Scenario 1, Aerial Gunnery, (b) Scenario 2, Artillery and Mortar, (c) Scenario 3, Submunitions and Grenades, (d) All Scenarios.

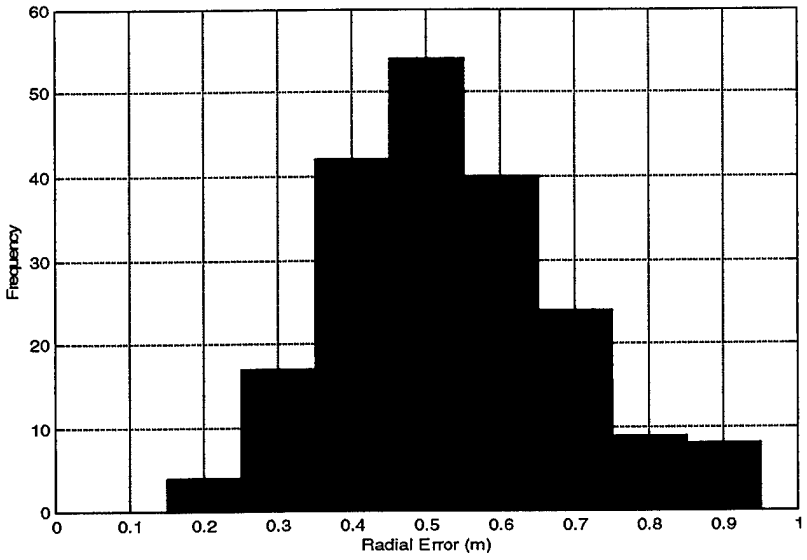

Figure II-40. EMI Radial Error for Detected Ordnance

Figure II-41 shows a small dependence of GoF on radial error. The correlation coefficient is –0.28, indicating a slight tendency for smaller radial error to be associated with better GoF, which is what we expect.

b. Magnetometer

For the magnetometer, the mean radial location accuracy was 0.50 m with a standard deviation of 0.16 m (see Table II-18). Figure II-42 shows the distribution of MAG radial error. Figure II-43 shows some dependence of magnetic moment on radial error. The correlation coefficient of the logarithm of the magnetic moment (that is, as plotted) with the radial error is –0.227. There is a slight tendency for larger magnetic moments to be associated with smaller radial errors. Figure II-44 shows GoF as a function of radial error. The negative correlation coefficient is –0.16, indicating a very slight tendency for large GoFs to be associated with small radial errors. Figure II-45 shows GoF as a function of magnetic moment. The correlation coefficient of 0.27 indicates a slight tendency of larger magnetic moments to be associated with better fits.

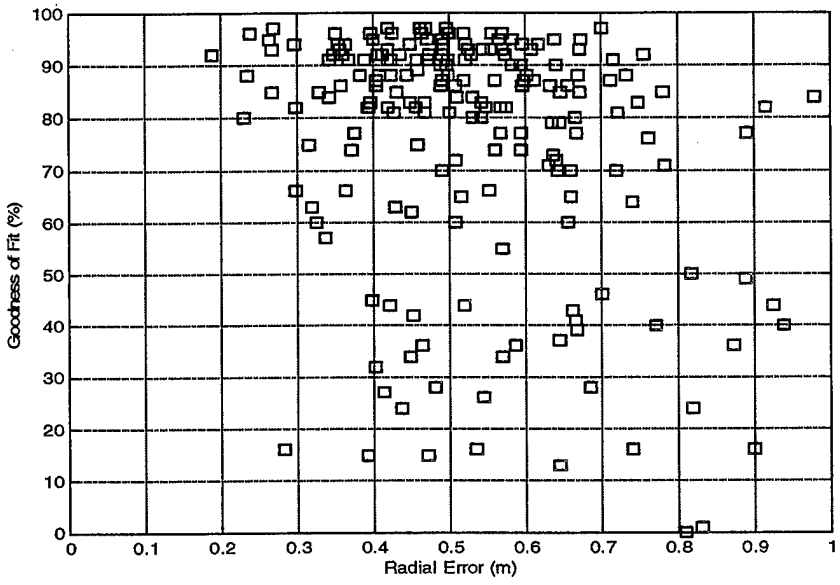

Figure II-41. EMI GoF vs. Radial Error

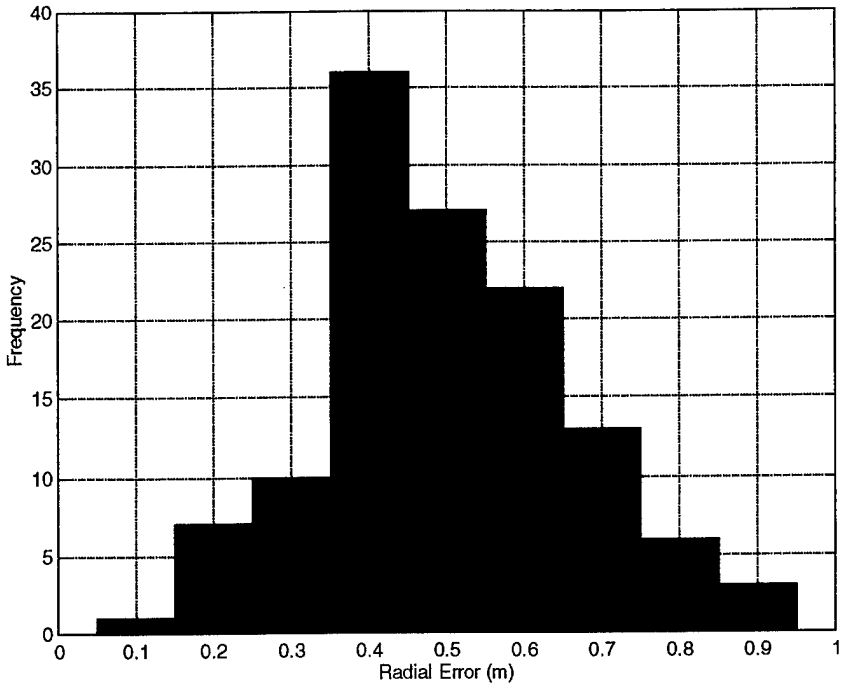

Figure II-42. Magnetic Moment vs. Magnetometer Radial Error

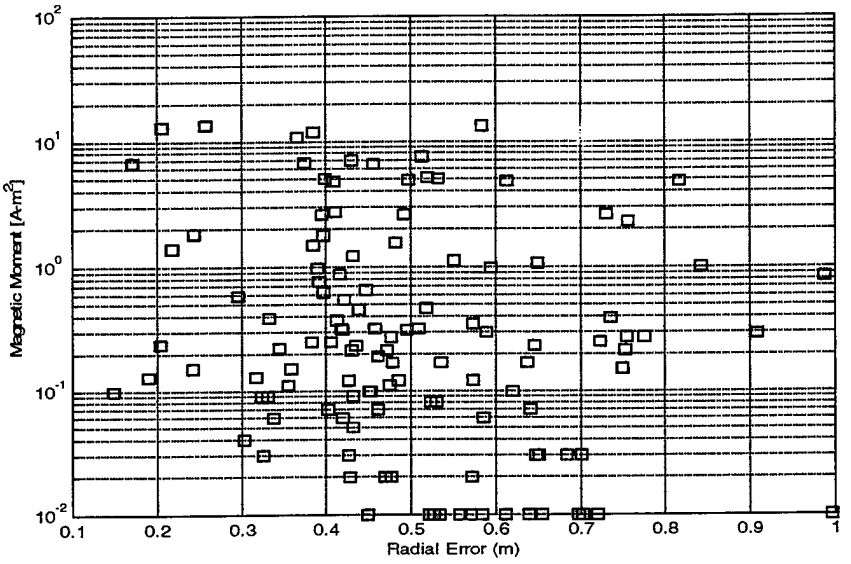

Figure II-43. Magnetometer Magnetic Moment vs. Radial Error

3. Depth Accuracy

For each sensor declaration that matched an emplaced target within the 1-m critical radius, the fitted depth and depth error (depth error = fitted depth – actual depth of the emplaced target) were calculated.

a. Electromagnetic Induction

For the EMI, the depth and depth error are poorly correlated with the other parameters. Figure II-46 shows the depth error of detected ordnance. The average depth error was 7 cm with a standard deviation of 0.21 m, indicating an insignificant bias, or tendency of EMI to indicate a deeper depth than actual. The mean of the absolute value of the depth error was 0.17 m, with a standard deviation of 0.14 m. Figure II-47 shows the GoF as a function of depth. The correlation coefficient of 0.35 indicates some tendency of larger GoFs to go with deeper depths. Figure II-48 shows the radial error as a function of depth, indicating some negative correlation (correlation coefficient of –0.26).

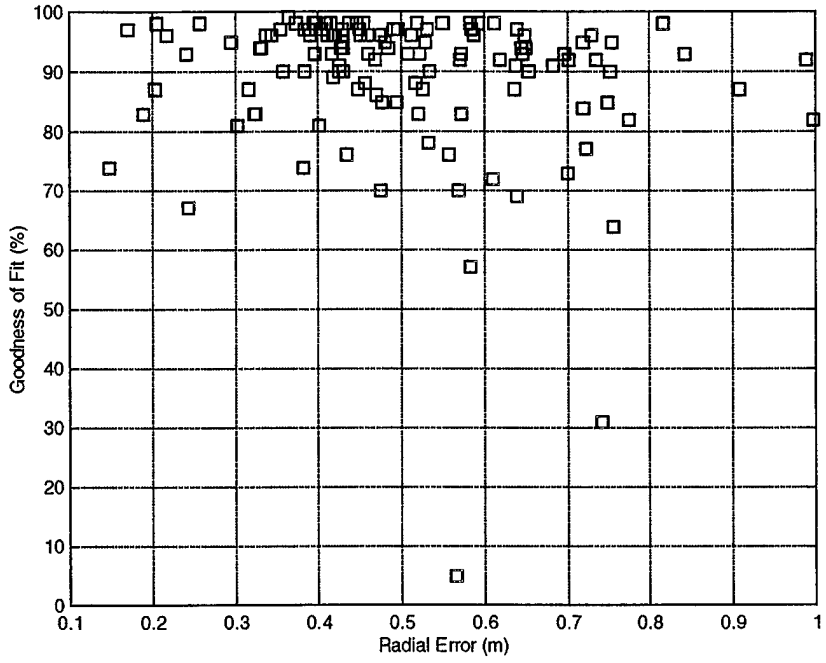

Figure II-44. Magnetometer GoF vs. Radial Error

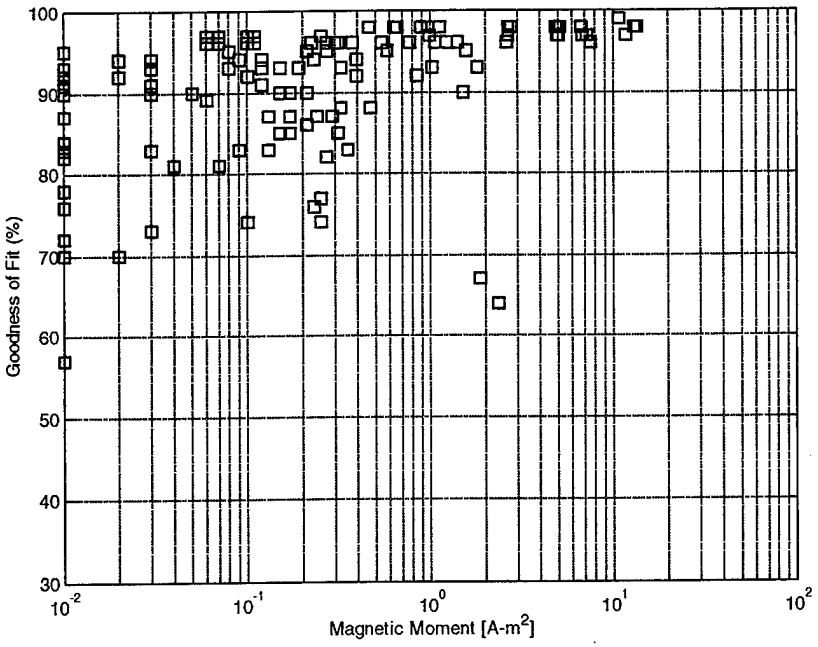

Figure II-45. Magnetometer GoF vs. Magnetic Moment

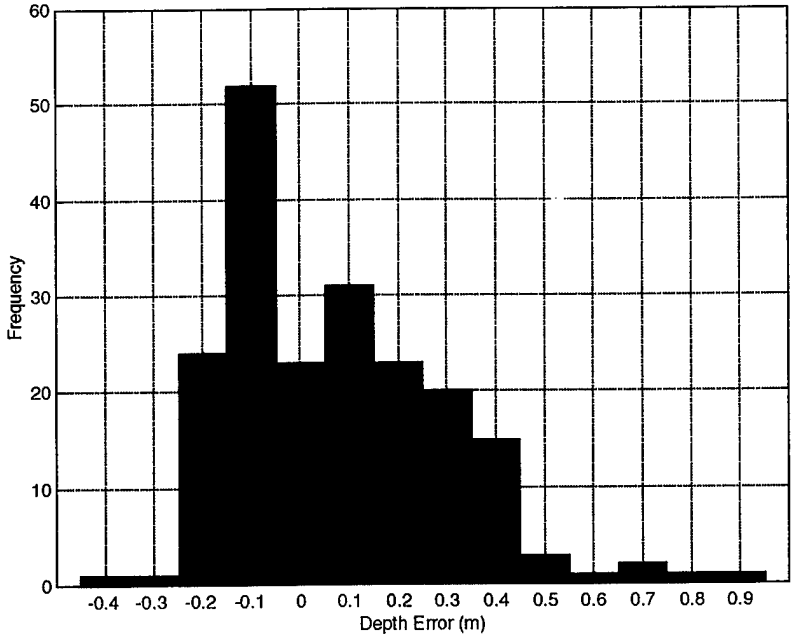

Figure II-46. EMI Depth Error

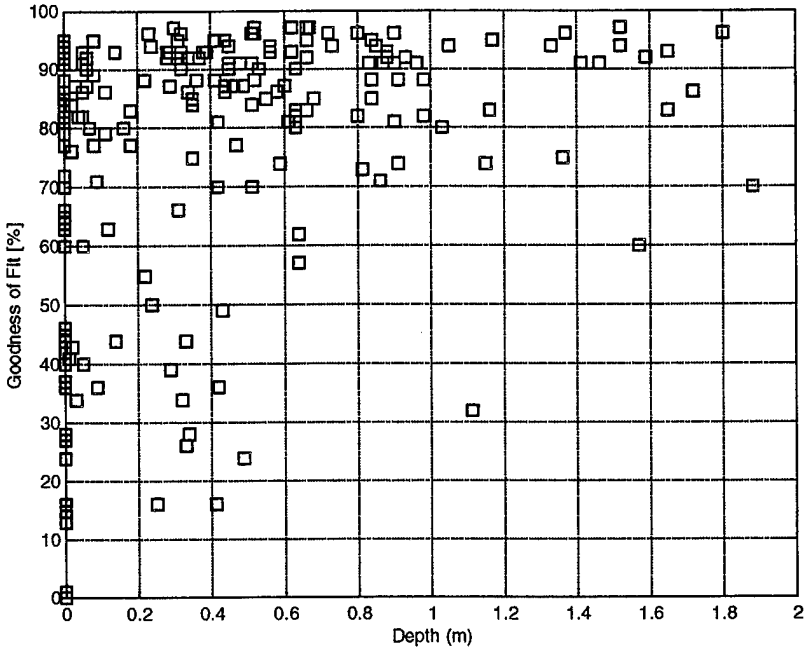

Figure II-47. EMI GoF vs. Depth

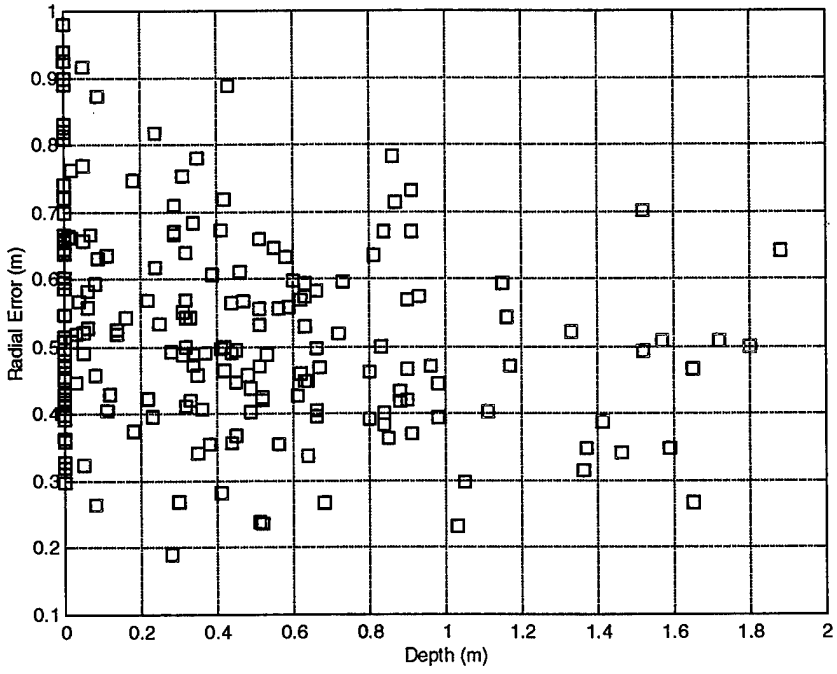

Figure II-48. EMI Radial Error vs. Depth

b. Magnetometer

The average magnetometer depth error was 0.21 m with a standard deviation of 0.16 m. These values were the same as the mean and standard deviation of the absolute value of the depth accuracy because so few points were negative. This indicates a significant tendency for the magnetometer to overestimate the depth (by 21 cm). The median depth error was 17 cm. Figure II-49 shows the magnetometer's distribution of depth error. Figure II-50 shows the dependence of depth error on magnetic moment, with correlation coefficient 0.54. Figure II-51 shows the relationship of depth to magnetic moment, clearly indicating (correlation coefficient of 0.72) that the smaller magnetic moment detections occur at shallower depths, as we would expect. Figure II-52 shows the GoF dependence on depth, with correlation coefficient 0.30. Figure II-53 shows the magnetometer radial error as a function of depth, with correlation coefficient –0.21.

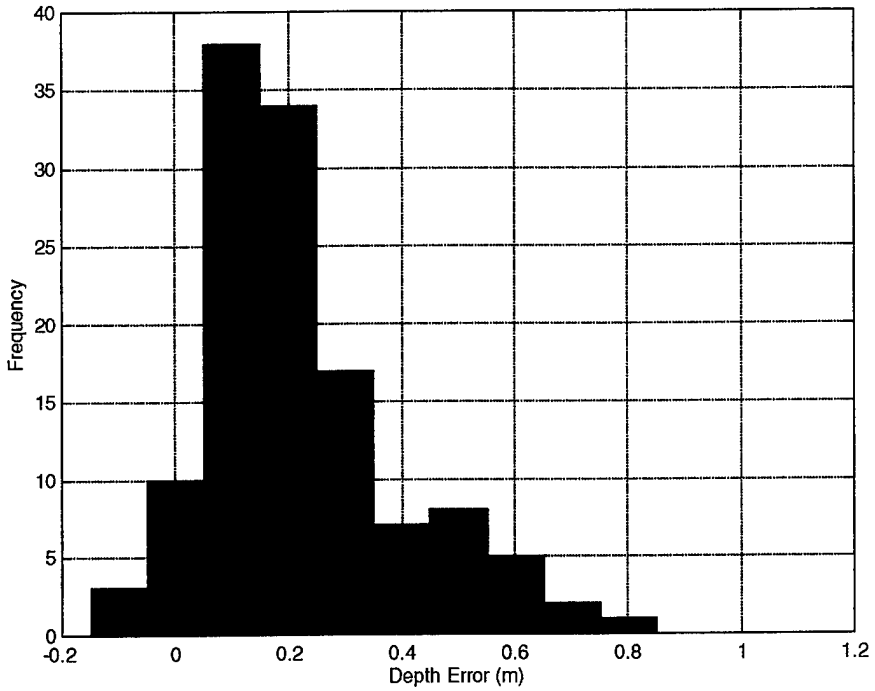

Figure II-49. Magnetometer Depth Error

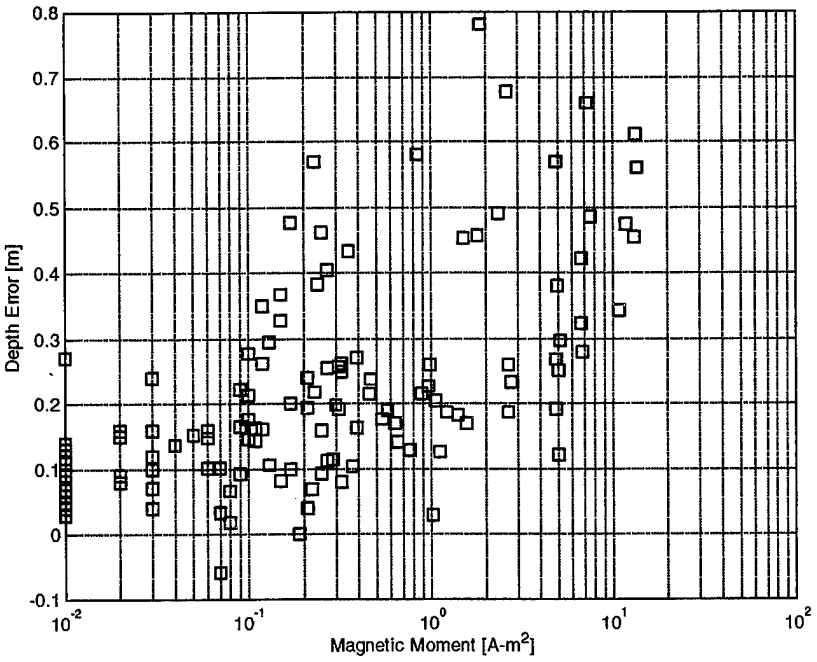

Figure 50. Magnetometer Depth Error vs. Magnetic Moment

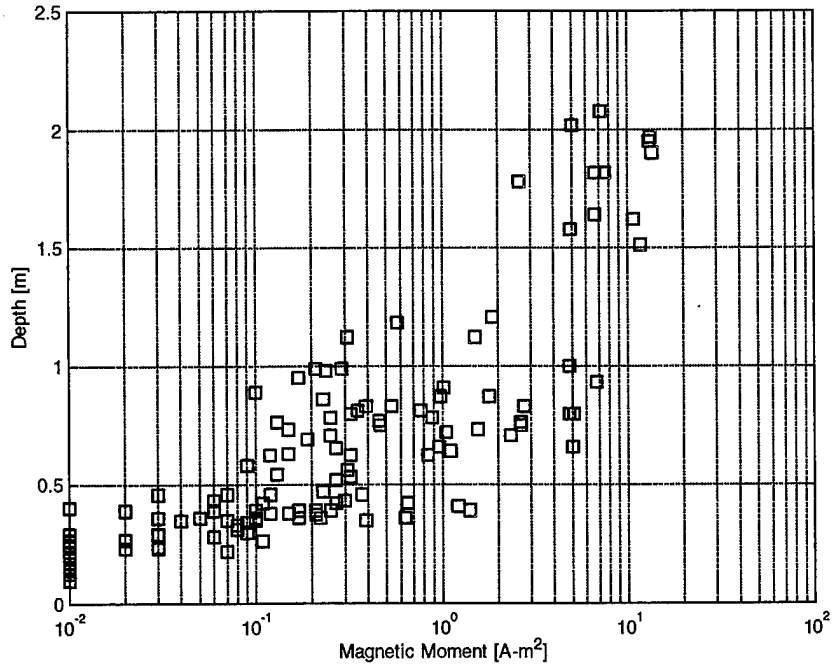

Figure II-51. Magnetometer Depth vs. Magnetic Moment

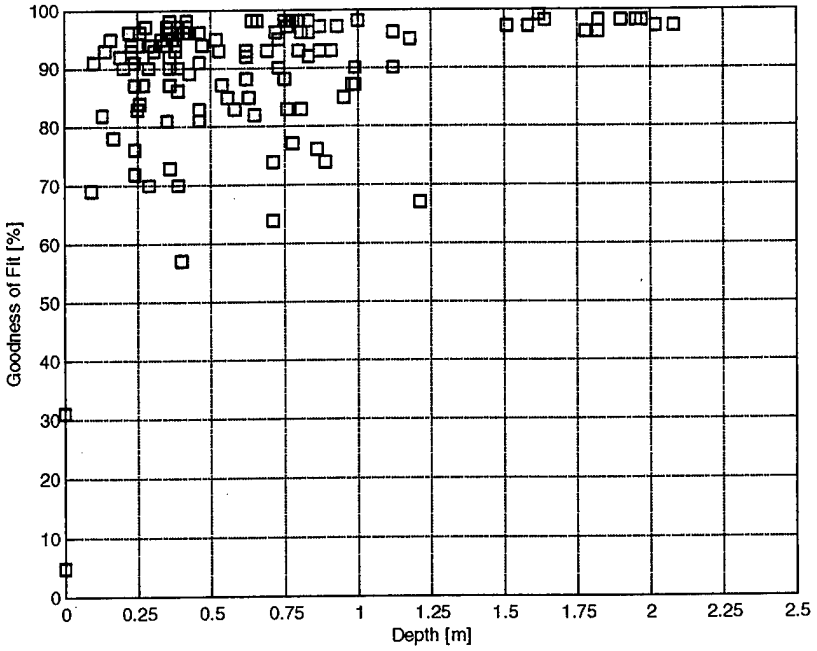

Figure II-52. Magnetometer GoF vs. Depth

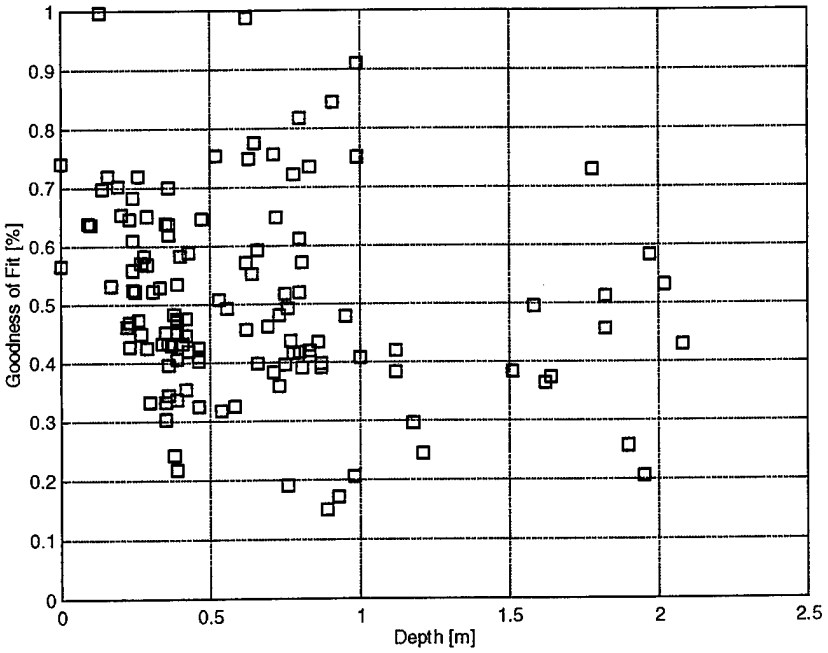

Figure II-53. Magnetometer GoF vs. Depth

4. Declarations Common to Magnetometer and EMI

We analyzed COM declarations to understand the general trends associated with detection by multiple systems. This section contains a comparison of the MTADS-DAS fit parameters for this sensor pair. Detections are common when they both match to the same piece of ordnance. False alarms are common when they are within 1.0 m of each other.

a. Common Detections

All declarations within a 1.0-m R_{crit} of a baseline ordnance item are considered to determine a common detection. Thus, the distance between common declarations can be as great as 2.0 m. The different fit parameters are considered to establish trends that might be exploitable for combining or fusing the two data sets.

b. Detection Radial Location Offset

The location offset is the difference between the fitted location of each detected baseline item (on the plane of Earth's surface) for the EMI system and the magnetometer.

One hundred twenty baseline items have detections in common. The mean radial distance between declarations for each baseline ordnance item detected by both sensors is 0.21 m, with a standard deviation of 0.16 m. The detections are highly clustered within an area of radius 0.5 m surrounding the baseline item (see Figure II-54). Figure II-55 indicates that there is some correlation (correlation coefficient of 0.37) between the EMI and MAG radial errors.

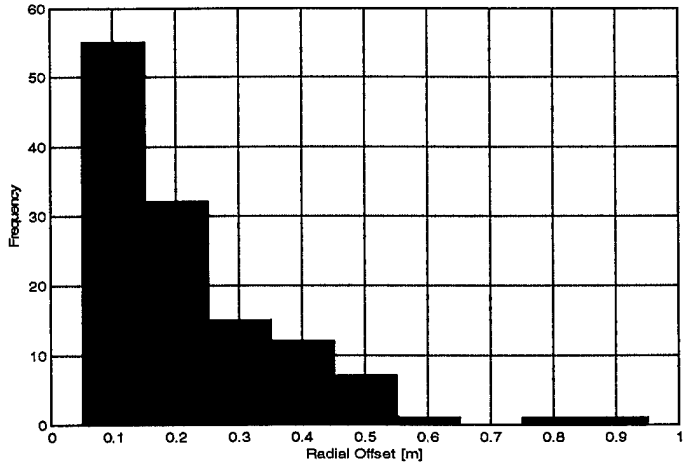

Figure II-54. Common Detection Radial Location Offset

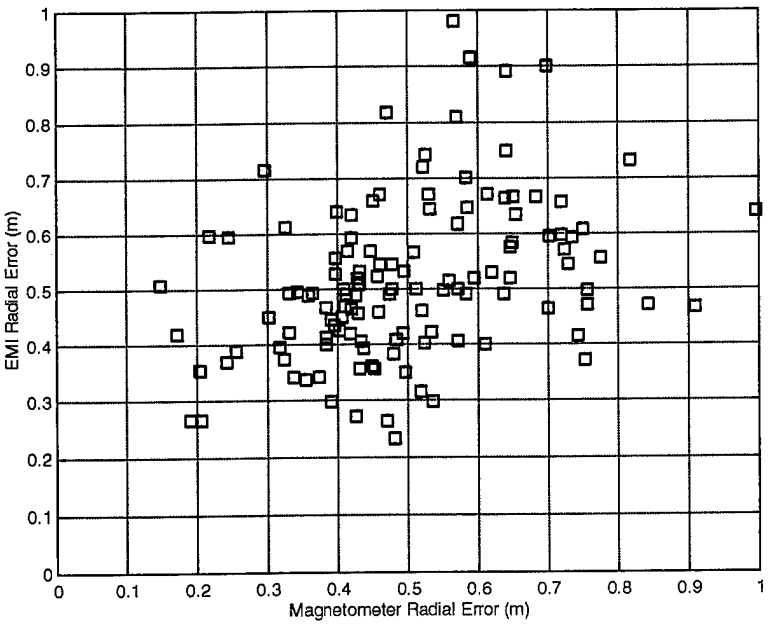

Figure II-55. EMI Radial Error vs. Magnetometer Radial Error for Common Detections

c. Detection Depth Offset

The depth offset is the difference between the fitted depth of each detected baseline item (in the plane of Earth's surface) for the two sensors; that is, the target depth estimated from the EMI data subtracted from that estimated from the magnetometer data. The depth offset can be positive or negative. The trend of the sign indicates whether one sensor consistently estimates the depth of the baseline item to be greater than the fitted depth from the other sensor.

Figure II-56 gives the common detection depth offsets. Note that the depth offsets are for locations already known to be within $2 \times R_{crit}$ of each other.

Figure II-57 shows the relationship between depth errors from the two sensors, with correlation coefficient 0.37. Figure II-58 shows the relationship between depths from the two sensors. These have a high correlation coefficient of 0.89.

d. Detection Goodness-of-Fit Comparison

Each time the MTADS-DAS attempts to fit a designated anomaly with the appropriate model, a measure of the relative fit of the model to the actual data is established. Because of the fit methodology, fits with GoF less than 0.90 are quite poor.

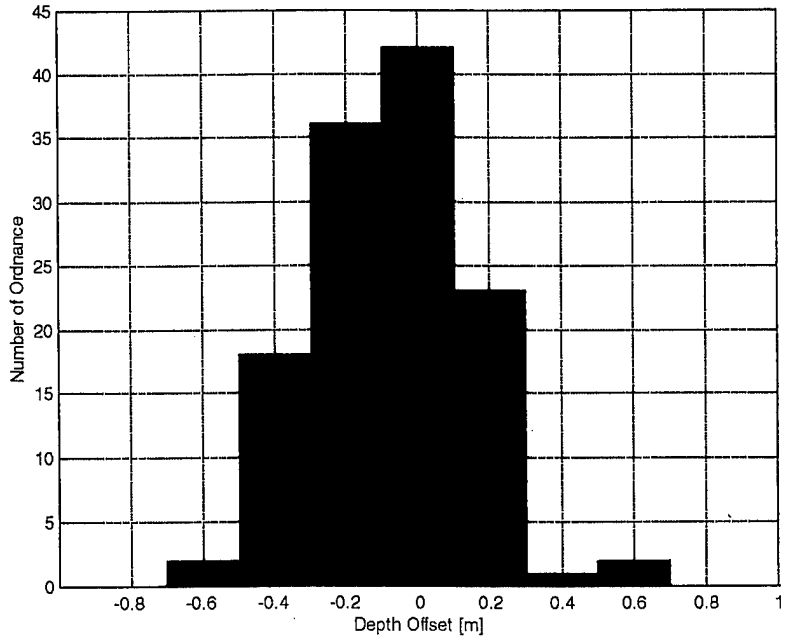

Figure II-56. EMI-MAG Depth Offset for Detected Ordnance

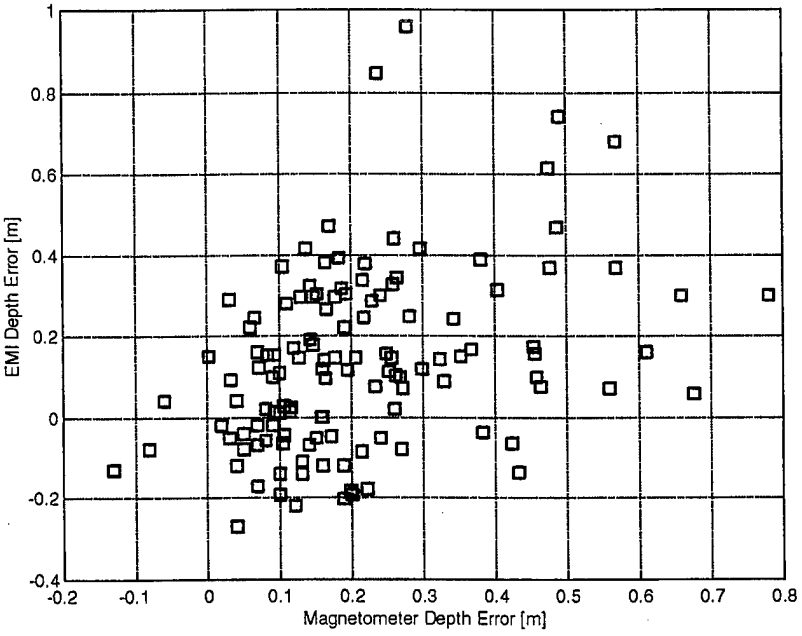

Figure II-57. EMI Depth Error vs. Magnetometer Depth Error for Detected Ordnance

These poor fits are generally associated with a very noisy background or with atypical objects in the ground. As shown in Figure II-59, common detections for the magnetometer and EMI exhibit some correlation between their GoFs. The correlation coefficient is 0.31.

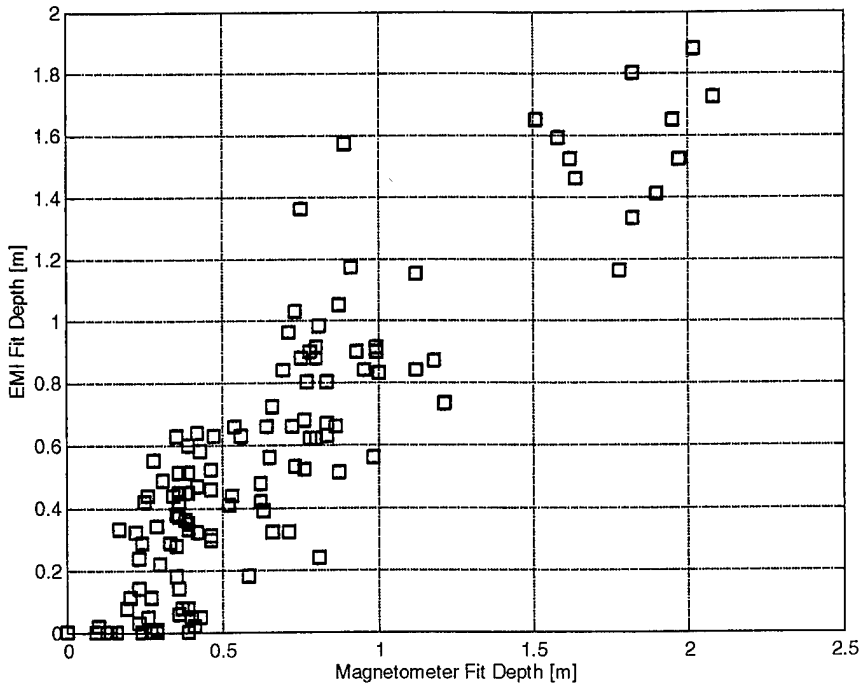

Figure II-58. EMI Depth vs. Magnetometer Depth for Detected Ordnance

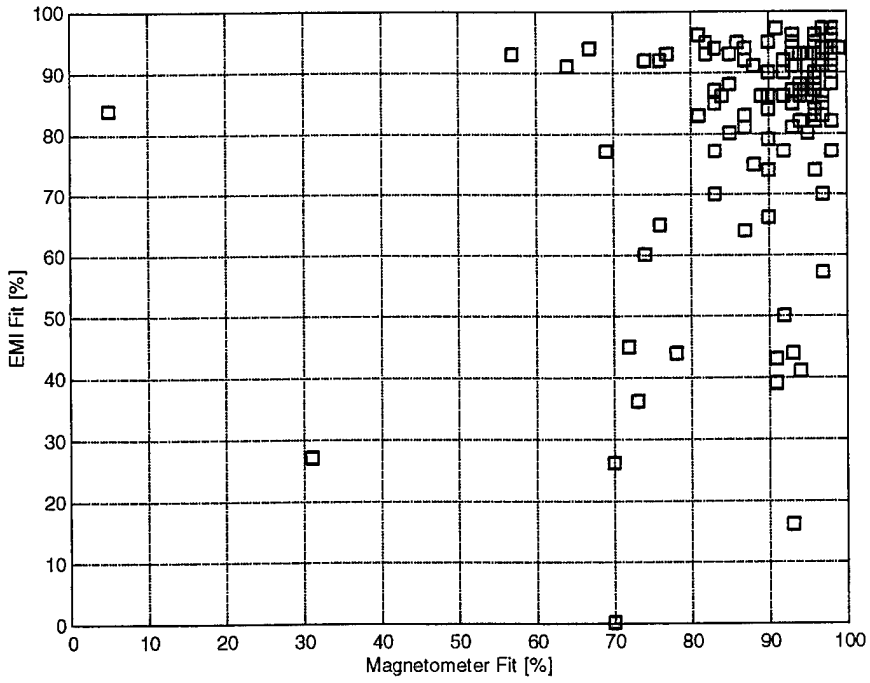

Figure II-59. EMI GoF vs. MAG GoF for Detected Ordnance

5. False Alarms Common to Magnetometer and EMI

This is an effort to understand false alarms by examining the declarations that correspond to nonordnance items in the baseline. The weak link in this exercise is the assumption that the nonordnance baseline items are representative of sources of false alarms in real-world employment of the MTADS. We first examine this assumption. Then, we present the false-alarm analysis proper.

a. Separation of Nonordnance and Nonbaseline Items

There are two sources of false alarms in the test of MTADS at JPG: the nonordnance items in the baseline and the items that are not in the baseline, called "nonbaseline" items. We examine the similarity of these two false-alarm sources by doing a discriminant analysis as done for the scenario-specific false-alarm mitigation. The purpose here is different; we want to gauge the validity of taking the nonordnance items as representative of the nonbaseline items in the following analysis of false alarms. We examine the degree to which nonordnance and nonbaseline items differ by doing a Kolmogorov-Smirnov comparison test on the most important discriminant.

Since three classes of declarations as ordnance are used in the discriminant analysis, two linear (Fisher) discriminants, or factors, are derived for each case examined. The three classes are ordnance, nonordnance, and nonbaseline.

Figures II-60 through II-63 show the graphical results of the discriminant analysis, together with definitions of the two discriminants, FACTOR(1) and FACTOR(2). Table II-19, the jackknifed percent of correct classification by the resultant discriminants, gives an indication of how good the discriminants are. Table II-20 shows how much of the dispersion in Figures II-60 through II-63 can be accounted for by the factors. By construction FACTOR(1) is the dominant factor, that is, it accounts for the most dispersion. Distributional characteristics for FACTOR(1) for declarations corresponding to ordnance, false alarm (just nonbaseline plus nonordnance), nonbaseline, and nonordnance items are also given in Table II-20.

Table II-21 shows the results of the Kolmogorov-Smirnov two-sample test. Notice that the nonordnance and nonbaseline classes differ strongly (significance level of 0.001 or less). This makes the exercise of using one as a surrogate for the other suspect,

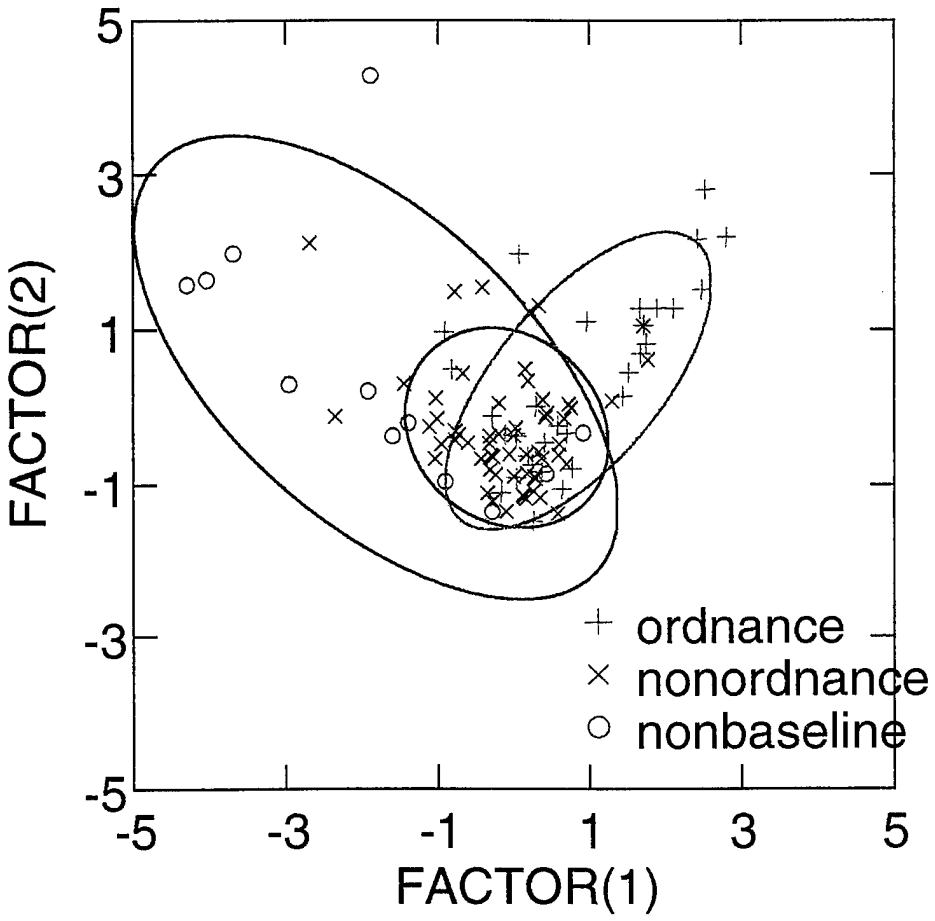

Figure II-60. Scenario 1 Ordnance, Nonordnance, and Nonbaseline Distributions as Functions of Factors from a Linear (Fisher) Discriminant Analysis.
FACTOR(1) = -13.513 + 7.751 RFE_EM + 0.113 GOF_MAG + 0.025 GOF_EM.
FACTOR(2) = 10.128 + 12.225 RFE_EM – 0.108 GOF_MAG – 0.020 GOF_EM.
50-percent ellipses are shown.

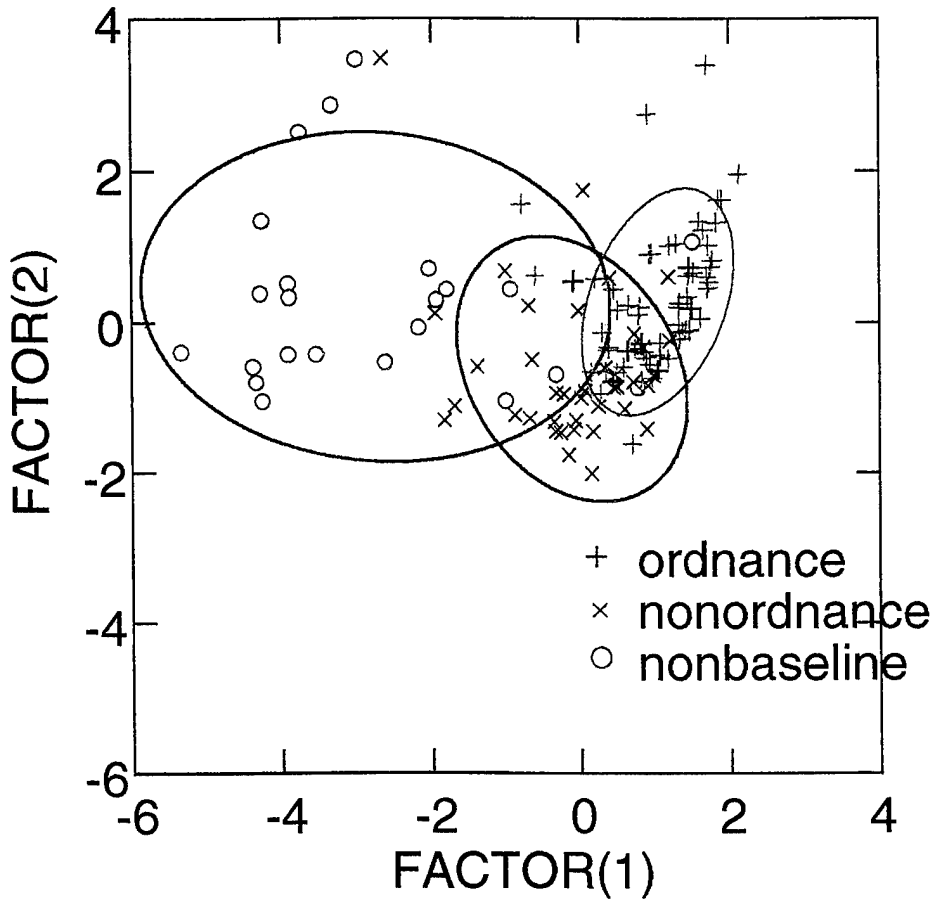

Figure II-61. Scenario 2 Ordnance, Nonordnance, and Nonbaseline Distributions as Functions of Factors from a Linear (Fisher) Discriminant Analysis.
FACTOR(1) = -6.605 + 0.482 ZMAG + 0.009 INCLIN + 0.076 GOF_EM.
FACTOR(2) = -0.892 + 1.636 ZMAG + 0.017 INCLIN – 0.011 GOF_EM.
50-percent ellipses are shown.

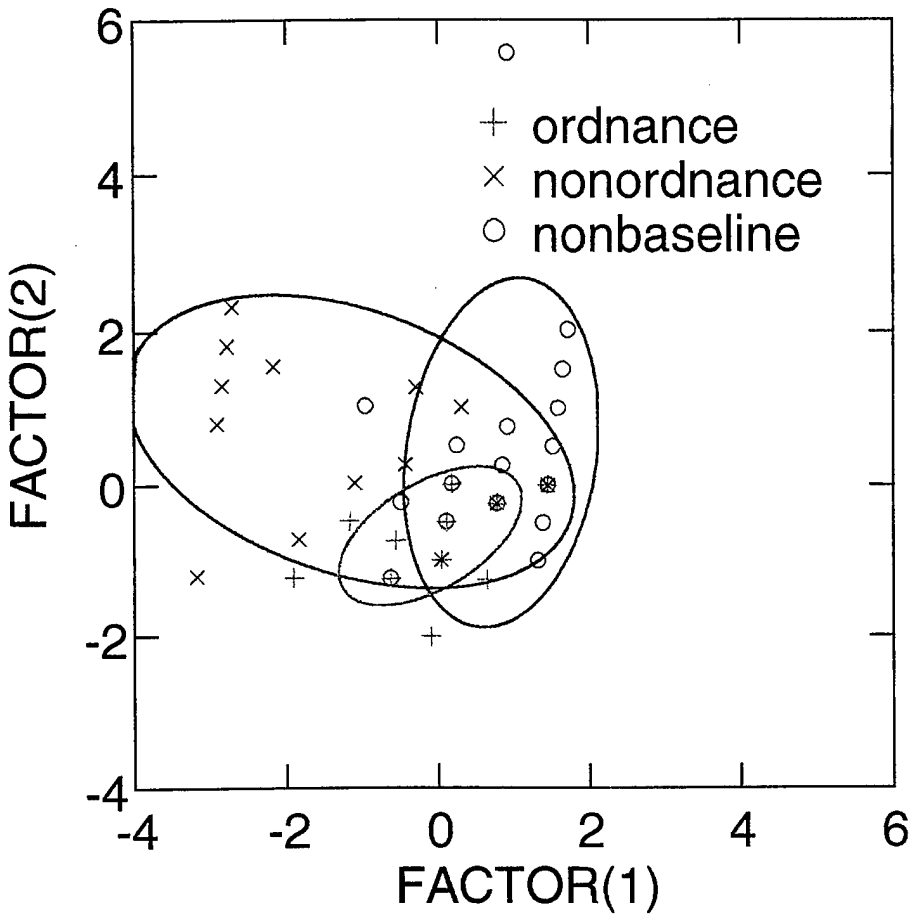

Figure II-62. Scenario 3 Ordnance, Nonordnance, and Nonbaseline Distributions as Functions of Factors from a Linear (Fisher) Discriminant Analysis.
FACTOR(1) = 1.919 + 6.748 RMAG – 66.979 RFE_EM.
FACTOR(2) = -1.276 + 50.503 RMAG – 24.513 RFE_EM.
50-percent ellipses are shown.

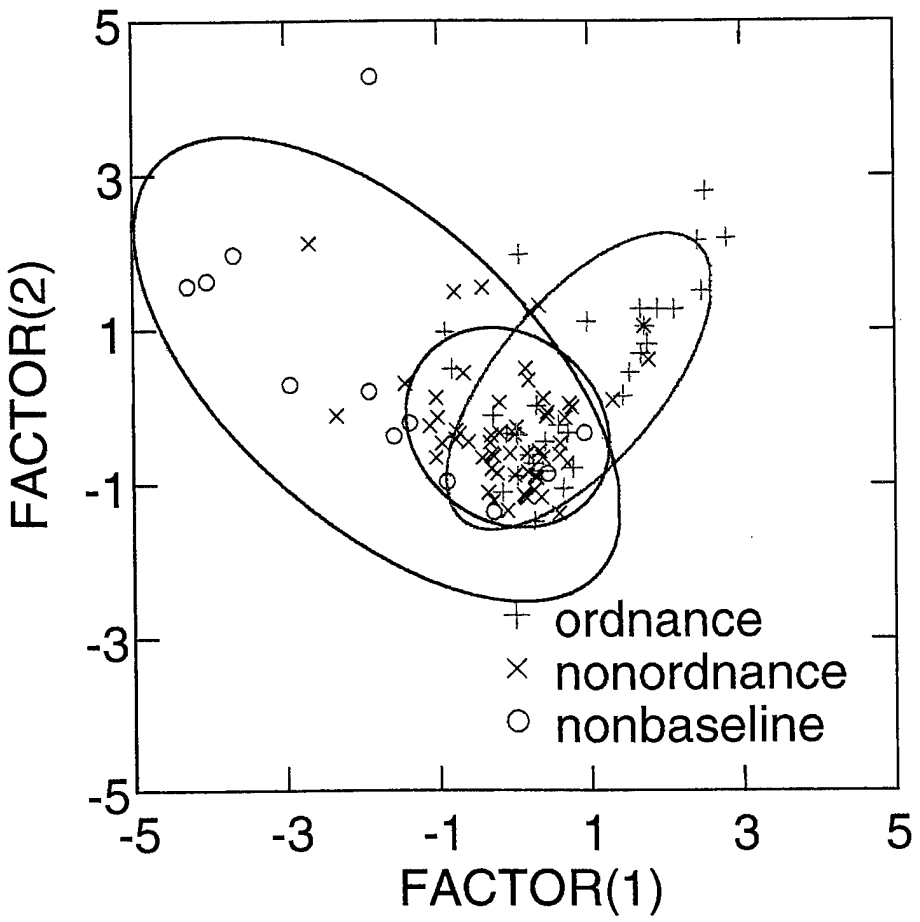

Figure II-63. Combined Scenarios' Ordnance, Nonordnance, and Nonbaseline Distributions as Functions of Factors from a Linear (Fisher) Discriminant Analysis.
FACTOR(1) = -3.802 + 0.006 INCLIN + 0.049 GOF_EM.
FACTOR(2) = -0.459 + 0.026 INCLIN – 0.010 GOF_EM
50-percent ellipses are shown.

Table II-19. Jackknifed Correct Classification by Linear Discriminants

Scenario	Percent Correct			
	Ordnance	Nonordnance	Nonbaseline	All
1	50	68	67	62
2	78	72	78	76
3	63	69	72	68
All	62	54	72	61

at least in so far as the variables making up the discriminants are concerned. It is thus, on the variables that do not figure in the discriminants, shown in Figures II-60 through II-63, given again in Table II-22 for emphasis, that the following analysis is more persuasive.

Table II-20. Separation Statistics for the Dominant Discriminant, FACTOR(1). The definitions of FACTOR(1) and FACTOR(2) are different for each scenario.

Scenario	Dispersion [%]		Values of FACTOR(1)											
	FACTOR(1)	FACTOR(2)	Ordnance			False Alarms			Nonordnance			Nonbaseline		
			Number of Data	Mean	Standard Deviation	Number of Data	Mean	Standard Deviation	Number of Data	Mean	Standard Deviation	Number of Data	Mean	Standard Deviation
1	85.5	14.5	32	0.9	1	71	-0.4	1.2	59	-0.1	0.8	12	-1.8	1.7
2	91.7	8.3	65	1	0.6	62	-1.1	1.8	39	-0.1	0.9	23	-2.7	1.8
3	64.9	35.1	27	-0.1	0.7	41	0.1	1.5	16	-1.1	1.6	25	0.8	0.7
All	88.6	11.4	124	0.6	0.9	174	-0.4	1.3	114	0.2	1	60	-1.5	1.2

Table II-21. Kolmogorov-Smirnov Two-Sample Test for Ordnance, Nonordnance, and Nonbaseline Items. The two samples indicated are tested as a function of FACTOR(1). The effective number of data is $N_e = N_1 \times N_2 / (N_1 + N_2)$, where N_1 is the number of data from the first sample and N_2 is the number of data from the second sample.

Scenario	Ordnance - False Alarms			Ordnance - Nonordnance			Ordnance - Nonbaseline			Nonordnance - Nonbaseline		
	Effective Number of Data	Kolmogorov D statistic	2-sided significance level	Effective Number of Data	Kolmogorov D statistic	2-sided significance level	Effective Number of Data	Kolmogorov D statistic	2-sided significance level	Effective Number of Data	Kolmogorov D statistic	2-sided significance level
1	22.1	0.419	0.001	20.7	0.391	0.003	8.7	0.722	<0.001	10	0.594	0.001
2	31.7	0.665	<0.001	24.4	0.581	<0.001	17	0.873	<0.001	14.5	0.71	<0.001
3	16.3	0.422	0.004	10	0.48	0.012	13	0.616	<0.001	9.8	0.623	0.001
All	72.4	0.415	<0.001	59.4	0.299	<0.001	40.4	0.718	<0.001	39.3	0.619	<0.001

Table II-22. Definitions of FACTOR(1)s for Three-Way Discrimination

Scenario	Definition of FACTOR(1)
1	–13.513 + 7.751 RFE_EM + 0.113 GOF_MAG + 0.025 GOF_EM
2	–6.605 + 0.482 ZMAG + 0.009 INCLIN + 0.076 GOF_EM
3	1.919 + 6.748 RMAG – 66.979 RFE_EM
All	–3.802 + 0.006 INCLIN + 0.049 GOF_EM

b. Radial Location Accuracy

An analysis of the radial location accuracy of the false alarms (detected non-ordnance items present in the baseline) reveals that both sensors localize most of the nonordnance items within 0.5-m halo. In the submunitions and grenades scenario, the nonordnance are emplaced at more shallow depths, where nonanthropic clutter is most dense. This causes the mean radial error for this scenario to increase 10 cm for both the magnetometer and the EMI. However, since the nonordnance baseline items were composed of metal, it is not surprising that the fit confidences were quite high in all scenarios.

Table II-23. Radial Location Accuracy

Sensor	Scenario	*FAR*	Mean Radial Error (m)	Standard Deviation	Fit	Standard Deviation
EMI	Aerial Gunnery	0.62	0.53	0.17	80	17
EMI	Artillery and Mortar	0.36	0.48	0.14	83	10
EMI	Submuni-tions and Grenade	0.39	0.61	0.23	54	33
Magnetometer	Aerial Gunnery	0.57	0.50	0.17	94	4
Magnetometer	Artillery and Mortar	0.40	0.48	0.10	92	6
Magnetometer	Submuni-tions and Grenade	0.21	0.63	0.10	82	21

c. Depth Location Accuracy

As Table II-24 shows, the mean depth error for the EMI and magnetometer ranges from 18 to 34 cm and from 9 to 18 cm, respectively. In each scenario, the magnetometer outperforms the EMI sensor in depth estimation by approximately 9 cm or more. This is most likely due to the MTADS fitting algorithm for the EMI sensor, which does not provide precision depth fittings. The depth error for these near-surface, metallic, non-ordnance items is in accordance with previous analyses of MTADS system performance. Individually, the MTADS fitting parameters are not useful to discriminate between nonordnance and ordnance in these scenarios.

Table II-24. Depth Accuracy

Sensor	Scenario	*FAR*	Mean Depth Error (m)	Standard Deviation	Depth (m)	Standard Deviation
EMI	Aerial Gunnery	0.62	0.27	0.21	0.60	0.46
EMI	Artillery and Mortar	0.36	0.34	0.25	0.50	0.28
EMI	Submuni-tions and Grenade	0.39	0.18	0.11	0.18	0.23
Magnetometer	Aerial Gunnery	0.57	0.18	0.12	0.70	0.36
Magnetometer	Artillery and Mortar	0.4	0.11	0.10	0.29	0.14
Magnetometer	Submuni-tions and Grenade	0.21	0.09	0.1	0.26	0.09

III. CONCLUSIONS

This document analyzed the results of a test of MTADS at Jefferson Proving Ground (JPG) from 14 to 24 January 1997. The probability of detection, P_D, is shown in Table III-1.

Table III-1. Detection

Scenario	Number of Baseline Ordnance	Number of Ordnance Declarations	Number of Correct Ordnance Declarations	P_D (%)
1—Aerial Gunnery	47	185	45	95.7
2—Artillery and Mortars	73	216	70	95.9
3—Submunitions and Grenades	86	215	80	93

The number of false alarms (FAs) is defined as the number of declarations as ordnance that did not correspond to baseline ordnance. The false alarm rate is shown in Table III-2.

Table III-2. False Alarm Rates

Scenario	Area Surveyed (Square Meters)	Number of False Alarms	False Alarm Rate (per Hectare)*
1—Aerial Gunnery	33,445 (8.265 acres)	140	41.9
2—Artillery and Mortars	39,391 (9.735 acres	146	37.6
3—Submunitions and Grenades	29,729 (7.347 acres)	135	45.4

* A hectare is 10,000 square meters or 2.47 acres.

The addition of EMI sensor information was crucial for reducing the *FAR*, particularly in scenarios 1 and 3, where it took part in every good detection. In scenario 1 it was not, by itself, responsible for any false alarms.[1] Table III-3 shows the discriminants that were derived in each case, and the potential *FAR* reduction.

---

1 This assumes that those declarations for which there were both EMI and MAG data were not more difficult (in some sense) than those for which only MAG or only EMI data were available. That is, no essential synergy is assumed between MAG and EMI.

Table III-3. Potential *FAR* Reduction by Using Linear Discriminants

Scenario	Declaration Type	Proportion of FAs	Discriminant	Possible *FAR* Reduction	Total *FAR* Reduction
1	Common and EMI-only	58% (81/140)	RFE_EM	16%	51.4%
	MAG-only	42% (59/140)	Not Applicable	100%	
2	Common	42.5% (62/146)	Function of ZMAG, INCLIN, GOF_EM	60%	25.5%
	MAG-only	45.2 (66/146)	None	0%	
	EMI-only	12.3% (18/146)	None	0%	
3	Common (excluding 3)	30.4% (41/135)	RMAG	41%	44%
	MAG-only	31.9% (49/135)	Not Applicable	100%	
	EMI-only (including 1 common)	36.3 (49/135)	None	0%	
	No Information (excluded from common)	1.5% (2/135)	None	0%	

The obvious implications are that between 25- and 50-percent reduction in false alarms should be achievable with fairly rudimentary discrimination algorithms. An important caveat to this finding is that it is essential to know what kind of scenario one is in. No useful discriminant was found that was good in all three scenarios. Also, it should be emphasized that Table III-3 accurately shows the *FAR* reduction that would have been achieved in the JPG MTADS test, it is not necessarily indicative of performance in other tests. Specifically, the discriminant thresholds chosen were such as to allow *zero* missed detections on account of the false alarm mitigation. The real population distribution may have tails that would imply some number of missed detections as the tradeoff for reducing the *FAR*.

Tests and surveys are needed to determine real population distributions for UXO. The implications of these distributions for realistic false alarm mitigation also depends on better understanding of the detection physics. These areas need to be further studied if the indicated false alarms mitigation is to be achieved in practice. Indeed, since the statistical discrimination approach taken in this report is essentially conservative (using only statistically significant factors, with only linear discriminants), there is reason to believe physics-based approaches could do *better* than the analysis of Table III-3 indicates.

REFERENCES

I-1. Technology Demonstration Plan "MTADS Demonstration at the Jefferson Proving Ground, January 13–24, 1997," The Naval Research Laboratory, 2 December 1996.

I-2. "MTADS Demonstration at the Jefferson Proving Ground," Memorandum from Jim McDonald, NRL, to PRC, undated (circa 1997).

II-1. *Evaluation of the Multi-Sensor Towed Array Detection System (MTADS) Performance at the Marine Corps Air Ground Combat Center (MCAGCC), Twentynine Palms, CA*, IDA Document D-2161, forthcoming.

II-2. *Pattern Recognition and Neural Networks* by Brian D. Ripley (Cambridge University Press, 1996).

II-3. *Applied Multivariate Statistical Analysis*, Third Edition, by Richard A. Johnson and Dean W. Wichern (Prentice Hall, 1992).

ACRONYMS

AZIM	Azimuthal Angle
CART	Classification and Regression Trees
COM	Common Detections
EMI	Electromagnetic Induction
ESTCP	Environmental Security Test Certification Program
FA	False Alarms
FAR	False-Alarm Rate
GoF	Goodness of Fit
GOF_EM	Goodness of Fit, EMI
GOF_MAG	Goodness of Fit, Magnetometer
IDL	Interactive Data Language
INCLIN	Fitted Inclination
JPG	Jefferson Proving Ground
MAG	Magnetometer
MAGMOM	Magnetic Moment
MOE	Measure of Effectiveness
MTADS	Multi-Sensor Towed Array Detection System
MTADS-DAQ	Multi-Sensor Towed Array Detection Systems-Data Analysis
MTADS-DAS	Multi-Sensor Towed Array Detection Systems-Data Analysis System
MTR	Magnetic Test Range
NRL	Naval Research Laboratory
RAL_EM	Nonferrous Radial Size, EMI
RFE_EM	Ferrous Radial Size, EMI
RMAG	Fitted Radius, Magnetometer
TDP	Technology Demonstration Plan
TECHEVAL	Technical Evaluation
UXO	Unexploded Ordnance
ZEM	Fitted Depth

REPORT DOCUMENTATION PAGE

Form Approved
OMB No. 0704-0188

Public Reporting burden for this collection of information is estimated to average 1 hour per response, including the time for reviewing instructions, searching existing data sources, gathering and maintaining the data needed, and completing and reviewing the collection of information. Send comments regarding this burden estimate or any other aspect of this collection of information, including suggestions for reducing this burden, to Washington Headquarters Services, Directorate for Information Operations and Reports, 1215 Jefferson Davis Highway, Suite 1204, Arlington, VA 22202-4302, and to the Office of Management and Budget, Paperwork Reduction Project (0704-0188), Washington, DC 20503.

1. AGENCY USE ONLY *(Leave blank)*	2. REPORT DATE	3. REPORT TYPE AND DATES COVERED
	February 1999	Final—February 1998 – February 1999

4. TITLE AND SUBTITLE
Evaluation of the Multi-Sensor Towed Array Detection Systems (*MTADS*) Performance at Jefferson Proving Ground, January 14–24, 1997

5. FUNDING NUMBERS
DASW01 94 C 0054
T-AM2-1528

6. AUTHOR(S)
Samuel L. Park, Marc Mander

7. PERFORMING ORGANIZATION NAME(S) AND ADDRESS(ES)
Institute for Defense Analyses
1801 N. Beauregard St.
Alexandria, VA 22311-1772

8. PERFORMING ORGANIZATION REPORT NUMBER
IDA Document D-2174

9. SPONSORING/MONITORING AGENCY NAME(S) AND ADDRESS(ES)
ESTCP Program Office
901 N. Stuart Street, Suite 303
Arlington, VA 22203

10. SPONSORING/MONITORING AGENCY REPORT NUMBER

11. SUPPLEMENTARY NOTES

12a. DISTRIBUTION/AVAILABILITY STATEMENT
Approved for public release; distribution unlimited.

12b. DISTRIBUTION CODE

13. ABSTRACT ***(Maximum 180 words)***

This document provides an analysis of the results of a test of the Multi-sensor Towed Array Detection System (MTADS) conducted from 14 to 24 January 1997 at the Jefferson Proving Ground in Indiana. MTADS was tested in three scenarios of roughly 10 acres each. For scenario 1, with aerial gunnery unexploded ordnance (UXO), MTADS achieved a 95.7% probability of detection (P_D) with a false-alarm rate (FAR) of 41.9 per hectare (10,000 square meters). For scenario 2, with artillery and mortar UXO, MTADS achieved a 95.9% P_D with a FAR of 37.6 per hectare. For scenario 3, with submunitions and grenade UXO, MTADS achieved a 93% P_D with a FAR of 45.4 per hectare. An examination of the FAR with classical linear discriminants showed that reduction of the FAR of 51.4%, 25.5%, and 44%, for the respective scenarios, would have been achieved in the JPG test. Further study is needed to determine if comparable FAR reduction could be achieved in other situations. The discriminants that achieved these FAR reductions were particular to the individual scenario. No general (i.e., useful in all scenarios) discriminant was found.

14. SUBJECT TERMS
Jefferson Proving Ground, JPG, Multi-Sensor Towed Array Detection System, MTADS, unexploded ordnance, UXO

15. NUMBER OF PAGES
94

16. PRICE CODE

17. SECURITY CLASSIFICATION OF REPORT	18. SECURITY CLASSIFICATION OF THIS PAGE	19. SECURITY CLASSIFICATION OF ABSTRACT	20. LIMITATION OF ABSTRACT
UNCLASSIFIED	UNCLASSIFIED	UNCLASSIFIED	SAR